TINIAN AAV LANDING SITE ENGINEERING INVESTIGATIONS

Sea Engineering, Inc.
November 10, 2014

1. AAV LANDING ZONE ALTERNATIVES

1.1 Dredge Only Approach and Ramp

This concept uses only dredging into the solid reef mass to construct a ramp of natural reefal material and limestone, up to the reef shelf elevation at roughly -1.0 m (-3.3 ft) mean lower low water (MLLW). To achieve this requires a horizontal bench cut at -4 m (-13.1 ft) MLLW extending inshore of any depressions or channels that would otherwise require fill, followed by a 15° slope approximately 12 m long, ramping up from -4 to -1 m elevation (MLLW). All dredged surfaces of the ramp are left exposed with no surface treatment. The horizontal bench varies in width, averaging approximately 35 m wide at Babui and 50 m wide at Chulu. Required dredge volumes are 15,200 m^3 and 21,300 m^3 at Babui and Chulu, respectively. Refer to attached figures for general schematic of ramp.

The advantage of this option is that it does not involve construction of an armored ramp surface, and will therefore be substantially less expensive to construct. A significant downside to this alternative is that the longevity of the unprotected surface is uncertain. Continual wave action may cause rapid erosion that may result in depressions and holes that are hazardous to AAV operations.

1.2 Pile Armored Ramp

The pile protected ramp option consists of a dredge-only ramp approach and ramp slope (e.g., no fill used to develop ramp shape). All dredged surfaces of the ramp are left exposed with no surface treatment, except for the 15 degree primary ramp slope. The bottom of the armored ramp is at -4.0 m (-13.1 ft) MLLW and the top of the ramp is at approximately -1.0 m (-3.3 ft).

Wave force modeling results indicated that typical launch ramp designs consisting of interlocked concrete panels laid across the slope could be subject to extreme lift and drag forces, and substantial failure, during design wave conditions. These results suggested use of a contiguous armor unit from top to bottom of the slope, such as a pile, that would not be subject to wave induced lift and drag forces. This ramp armoring option consists of 24 inch square piles, installed side by side in an up-down slope configuration (as opposed to horizontally across the ramp). The piles would be pre-cast on Guam and transported by barge to Tinian. A key construction requirement is dredging or preparation of an even, smooth slope such that the placed piles terminate evenly at the top, approximately at -1 m elevation on the reef flat. Two design options are provided for this: 1) the ramp slope may slightly overcut and may be irregular, and a layer of bedding material (processed dredge spoils) will be utilized to fill depressions and

dress the slope to desired grade prior to pile installation; 2) the ramp slope is a straight line cut with no bedding, but could have gaps, holes or depressions up to 1.5 m (5 ft) in span width.

The piles would be 15 m (50 ft) long, and placed on the slope using a crane or excavator. To stabilized the base of the ramp, the piles will extend into an excavated trench 1.5 m (5 ft) deep and 2.5 m (8 ft) wide. The trench will be filled with tremie concrete. To stabilize the top of the ramp, the piles will terminate in a trench 1.8 m (6 ft) deep and 1.2 m (4 ft) wide. The trench will be filled with tremie concrete, and dowels extending from the end of the piles will lock the piles to the tremie concrete block. The toe and crest trenches would require about 1,300 m^3 of additional dredging at each site. The surface of the piles will contain grooves 1 inch deep, spaced 7 inches apart, to provide traction for the AAVs.

The advantage of this alternative is that it should provide a long term, durable surface for AAV operations. The pile surface should be stable under severe, design wave conditions. The disadvantages of this option include the possibility for some unevenness at the top of the slope, and the substantial costs required to fabricate, transport and install the piles at the project site on Tinian.

Refer to attached figures for general schematic of ramp and conceptual plans.

1.3 Tribar Armored Ramp

The tribar protected ramp option consists of a dredge-only ramp approach and ramp slope (e.g., no fill used to develop ramp shape). All dredged surfaces of the ramp are left exposed with no surface treatment, except for the 15 degree primary ramp slope. The bottom of the armored ramp is at -4.0 m (-13.1 ft) MLLW and the top of the ramp is at approximately -1.0 m (-3.3 ft) MLLW.

The ramp slope is armored with a single layer of armor units known as ‘tribars’, which are man-made concrete armor units that have been developed for use in constructing wave protection structures in high design wave height environments. These units have higher stability coefficients than traditional stone construction, and are typically used where adequately sized stone is not available or the required stone size is not practical. Tribar units have been used with considerable success for over 50 years, in sizes ranging from 1 to 50 tons. Their shape and placement pattern yields a relatively smooth “waffle” pattern on the structure surface. While primarily used on structures such as harbor breakwaters and shoreline revetments, with typical side slopes of about 35º, the design guidance for tribars indicates that their stability coefficients are applicable to slopes as flat as 12º. Thus the design ramp slope of 15º is within the current design guidelines for tribar use.

The required stable weight at this site on a ramp slope of 15º would be 3 tons. As with virtually all armor units their stability is primarily achieved through interlocking and proper placement. The tribar units will be uniformly placed in a single layer, with tight interlocking and maximum

possible contact between adjacent units and minimal gaps between units. The dimensions of the tribar units will result in a layer thickness of 3.7 feet. Approximately 1,400 individual tribar units would be required to cover each 200m wide ramp surface.

A tribar toe trench will be excavated below the elevation of the dredged approach area to a depth of 5 feet to key the tribars into the reef material. The trench will be filled with tremie concrete to the level of the adjacent dredged approach area following placement of the tribars. Concrete filled geotextile bags shall be filled in place at the ramp crest to buttress the tribar units. The bags shall firmly abut the top of the dredge cut and wrap around the top row of tribar units to lock them into place. The geotextile bags shall have approximate filled dimensions of 6 feet in length and 4 feet wide and high, and be placed to span a minimum of two tribar units. Construction of the toe trench and crest configuration would again require additional dredging of about 1,300 m^3 at each site. If large voids or cavities are encountered during dredging of the ramp they can be filled with 100 to 400 pound stone prior to placing the tribars.

The advantage of the tribar alternative is that tribars were designed for the express purpose of protecting surfaces or areas from wave attack. They have been used for shore protection and for harbor breakwaters all over the world. There is an extensive body of information from both field and research studies showing their stability during extreme waves. The proposed design is within published application guidelines, thus, there is high confidence in the stability of the tribar armored ramp slope for the exposed conditions at the proposed project sites. A disadvantage of tribars is the irregular surface - it is not know if this surface is desirable for AAV operations. Another possible issue is the long term durability of the tribars to continual AAV operations. While the tribars would be constructed of high strength concrete, they typically would not have steel reinforcement, and if breakage occurred their stability could be compromised. It is recommended that prior to selection or construction, additional hydraulic tests be conducted, and a prototype tribar surface be field tested on land to determine suitability for AAV operations.

Refer to attached figures for general schematic of ramp and conceptual plans.

2. DREDGING AND CONSTRUCTION METHODOLOGY

2.1 Logistics

Construction of the ramp will require some staging, as well as resources to be transported from the island of Guam. Concrete casting of the tribar and concrete pile armor units will occur on Guam. The construction site is located approximately 200 km (124 miles) away on the island of Tinian. The actual project site is another 14 km (9 miles) by land from Tinian Harbor, with no existing heavy vehicle access at either of the proposed sites from the main roadway. The limited access varies from ½ to 2 miles in length. A staging area of 1 to 2 acres will be required.

Several potential on-site staging areas were identified, however, it is expected that significant clearing of thick vegetation would still be required. A potential alternative for larger staging sites exists at nearby runways Able, Baker, Charlie, or Delta, which would provide excellent paved areas for heavy equipment servicing and stockpiles, if available for use. Distance from the proposed landing sites to these runway areas is approximately 1 km (0.6 miles).

Prrimary resources necessary for this construction effort are expected to include at a minimum the following major items: a large crawler crane; a large, long-reach excavator; bulldozer; front end loader; dump truck; forklift; flat bed trucks and trailers; and, several crew trucks for small hauls and crew transport to and from the site. A tug and barge will be required for shipping heavy equipment from Apra Harbor, Guam.

2.2 Dredging and Construction

The close proximity to shore, relatively shallow water, and persistent wave action makes the use of waterborne dredging equipment impractical and unsafe. Dredging and construction of the armored ramp slope would be accomplished using a land-based crawler crane and excavator. Use of a 150 ton crawler crane is anticipated for dredging of the flat -4m ramp approach zone, which does not require dredging a smooth surface, and for lifting and placing heavy material, and a long reach excavator would be used for dredging the 15º ramp which requires more precise excavation to achieve a relatively smooth slope. A typical excavator would be a Komatsu Long Reach Hydraulic Excavator, which is designed for use in dredging and has the power and reach to efficiently do the work. At Unai Babui the 1m depth contour is about 130 feet from shore, and the 4m depth seaward end of the dredge cut is about 400 feet from shore. At Unai Chulu the 1m depth ranges from about 230 feet to 400 feet from shore, and the 4m depth is 650 feet offshore.

Access to the areas to be dredged would be provided by a causeway, constructed of a combination steel sheet pile cell with fill out to the approximate 1m depth landward of the surf zone, and a pile supported trestle through the surf zone and out to the 4m depth. The fill causeway would be constructed by driving two steel sheet pile walls 30 feet apart to contain the fill, and then filling between them with rock and/or dredged material. The sheet piles would be tied together for stability and thus would only need to penetrate several feet into the reef flat. The trestle would be constructed of steel pipe piles supporting a steel bent, steel stringers running parallel to the long axis of the trestle, and wooden crane mats placed on top of the stringers for an equipment driving surface. Both the fill causeway and the trestle would be 30 feet wide for safe equipment operation. The steel sheet pile and the steel pipe piles would be primarily vibrated into place, with some use of an impact hammer in harder reef material.

The excavator reach is about 60 feet from the equipment center, or 45 feet from the causeway, for an effective dredging diameter of 120 feet (36m) around the causeway. Thus approximately six causeway installations would be required to dredge and construct the 200m wide approach

zones at each landing location. It is assumed that up to two causeways would be utilized simultaneously to maximize efficiency. Assumed dredging methodology would be as follows:

- Construct the first causeway seaward to the -4m depth and start dredging with the crawler crane.
- Move landward dredging a 100 to 120 ft (30 to 36 m) wide swath, removing the causeway as the dredging around the end is completed.
- When the location of the ramp slope toe is reached, replace the crane with the excavator and continue landward with ramp dredging and causeway removal. Dredge toe and top anchor trenches as necessary to secure armor units.
- Construct the second causeway and commence dredging at the 4m depth with the crane.
- When the ramp slope and trench dredging is complete, begin placing Tribar or concrete pile armor using the crane or excavator.
- Pour tremie concrete into top and toe anchor trenches to stabilize armor units.
- Remove the remaining portion of the causeway.
- Repeat this sequence until dredging and construction is complete.

Typical causeway sheet pile cell and trestle plan and sections are shown on the attached drawing.

PACIFIC OCEAN

40 20 0 40

GRAPHIC SCALE IN METERS

N

- MODIFIED SCALE -
PRINTED AT 1:1,000

40

30

20

10

0

4 METER CONTOUR

APPROXIMATE SHORELINE

ISLAND OF TINIAN

UNAI BABUI BEACH

APPROXIMATE LIMITS OF MODIFICATIONS

Sea Engineering, Inc.
MAKAI RESEARCH PIER
WAIMANALO, HI 96795
PH 808.259.7966
FAX 808.259.8143

NOTES:

Contours and elevations given in meters.

Contour interval is 1 m.

Highlighted contour every 10 m.

Elevations referenced to mean lower low water (MLLW).

Map based on provided LiDAR survey data.

KEY MAP

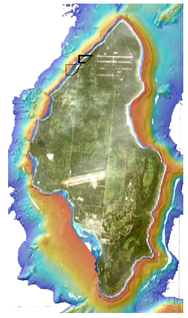

Sheet Name

**Figure X-X.
Existing Site
Conditions:
Unai Babui Contours**

Project Name

**Tinian AAV
Landing Sites
Investigation**

Project No. 25445	Sheet C-1
Date 04 SEP 2014	
Scale 1 : 2,,000	

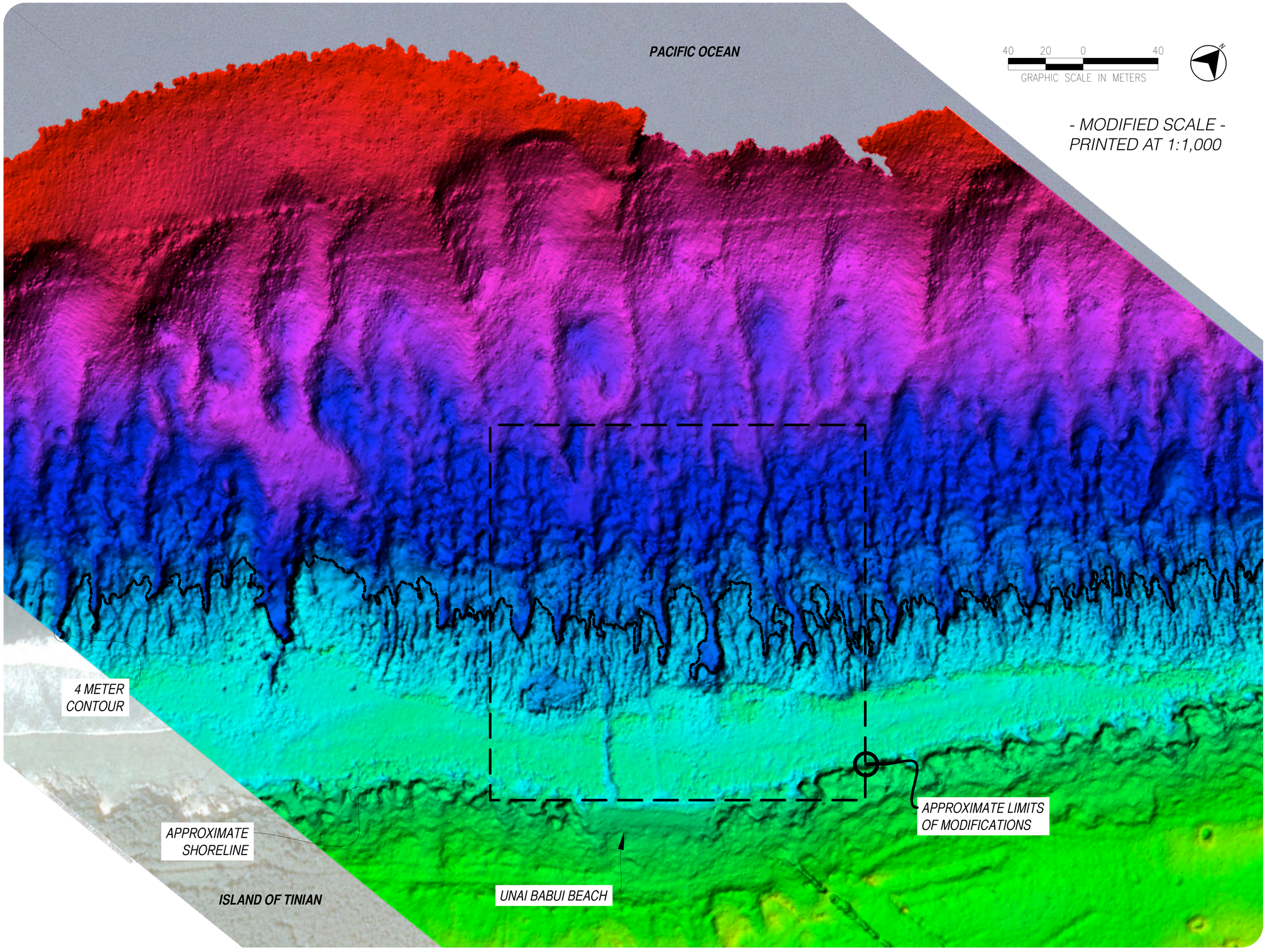

Sea Engineering, Inc.
MAKAI RESEARCH PIER
WAIMANALO, HI 96795
PH 808.259.7966
FAX 808.259.8143

NOTES:

Color Scale Legend for Digital Terrain Model (elevations in meters):

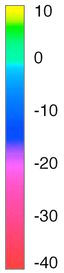

Contours and elevations given in meters.

Elevations referenced to mean lower low water (MLLW).

Map based on provided LiDAR survey data.

Sheet Name
Figure X-X. Existing Site Conditions: Unai Babui DTM

Project Name
Tinian AAV Landing Sites Investigation

Project No.	Sheet
25445	C-2
Date: 04 SEP 2014	
Scale: 1 : 2,000	

PACIFIC OCEAN

40 20 0 40

GRAPHIC SCALE IN METERS

- MODIFIED SCALE -
PRINTED AT 1:1,000

-40

-30

-20

HORIZONTAL LANDING
GRADED TO -4.0 MLLW

4 METER
CONTOUR

200 METER WIDE RAMP
15° SLOPE

0

APPROXIMATE
SHORELINE

ISLAND OF TINIAN

UNAI BABUI BEACH

Sea Engineering, Inc.
MAKAI RESEARCH PIER
WAIMANALO, HI 96795
PH 808.259.7966
FAX 808.259.8143

NOTES:

Contours and elevations given in meters.

Contour interval is 1 m.

Highlighted contour every 10 m.

Elevations referenced to mean lower low water (MLLW).

Map based on provided LiDAR survey data.

KEY MAP

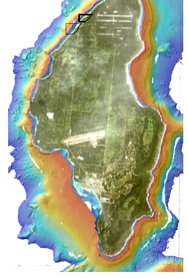

Sheet Name

**Figure X-X.
Babui Conceptual
Ramp Placement**

Project Name

**Tinian AAV
Landing Sites
Investigation**

Project No. 25445	Sheet C-3
Date 04 SEP 2014	
Scale 1 : 2,,000	

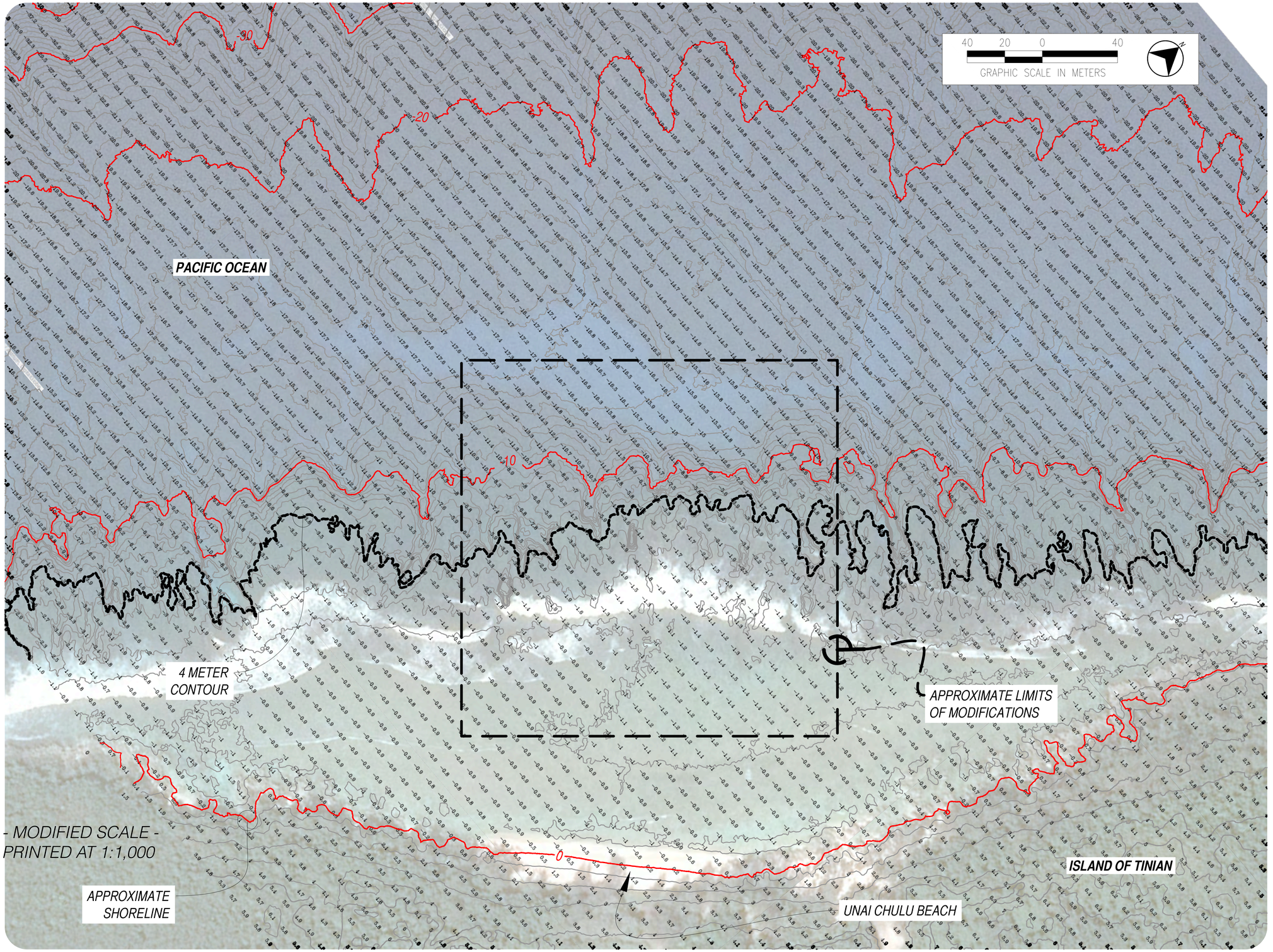

Sea Engineering, Inc.

MAKAI RESEARCH PIER
WAIMANALO, HI 96795
PH 808.259.7966
FAX 808.259.8143

NOTES:

Contours and elevations given in meters.

Contour interval is 1 m.

Highlighted contour every 10 m.

Elevations referenced to mean lower low water (MLLW).

Map based on provided LiDAR survey data.

KEY MAP

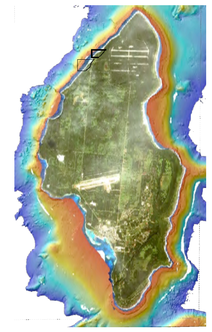

Sheet Name

Figure X-X. Existing Site Conditions: Unai Chulu Contours

Project Name

Tinian AAV Landing Sites Investigation

Project No. 25445	Sheet C-4
Date 04 SEP 2014	
Scale 1 : 2,000	

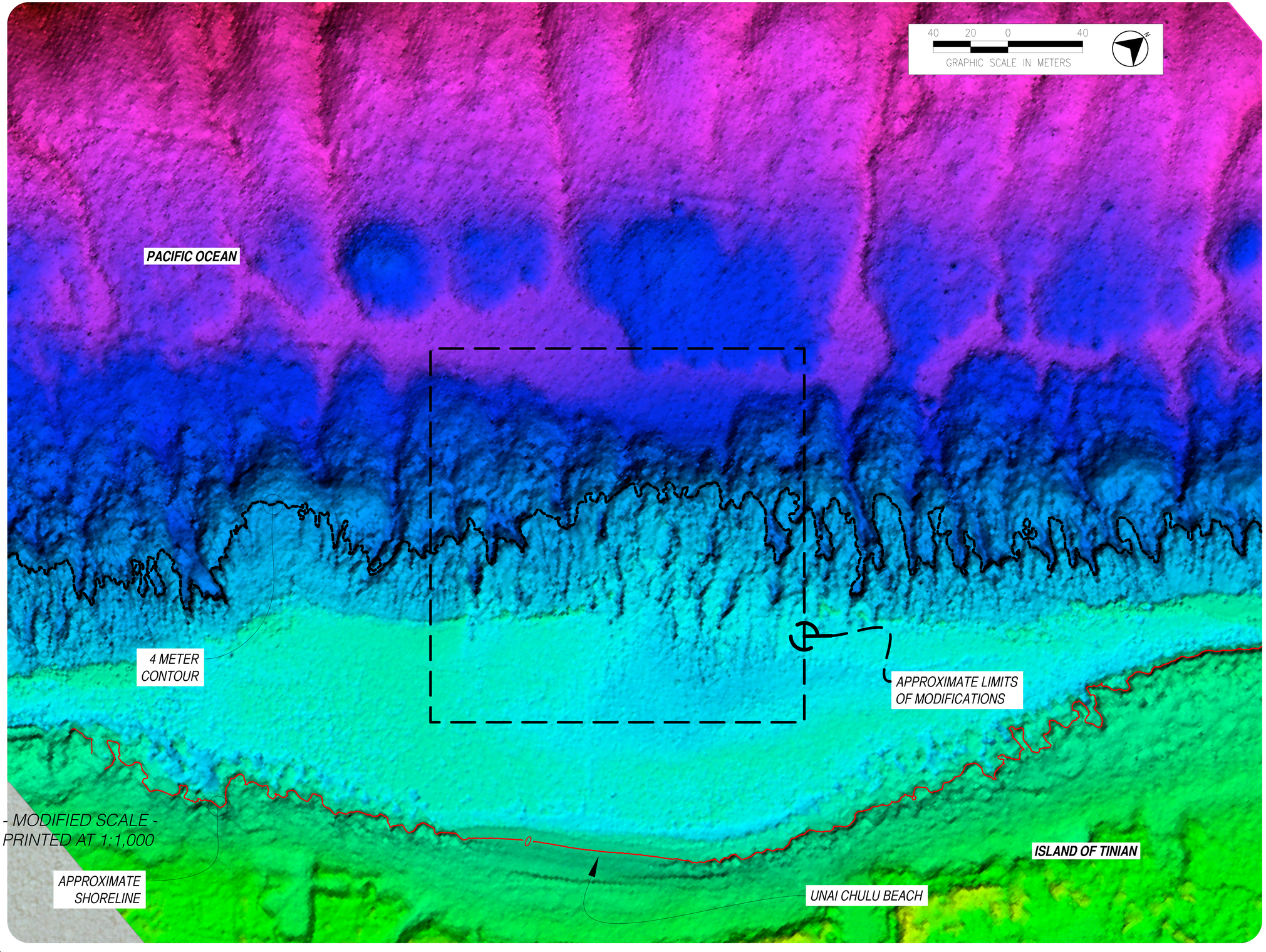

Sea Engineering, Inc.
MAKAI RESEARCH PIER
WAIMANALO, HI 96795
PH 808.259.7966
FAX 808.259.8143

NOTES:

Color Scale Legend for Digital Terrain Model (elevations in meters):

10
0
-10
-20
-30
-40

Contours and elevations given in meters.

Elevations referenced to mean lower low water (MLLW).

Map based on provided LiDAR survey data.

Sheet Name

Figure X-X. Existing Site Conditions: Unai Chulu DTM

Project Name

Tinian AAV Landing Sites Investigation

Project No. 25445	Sheet C-5
Date 04 SEP 2014	
Scale 1 : 2,,000	

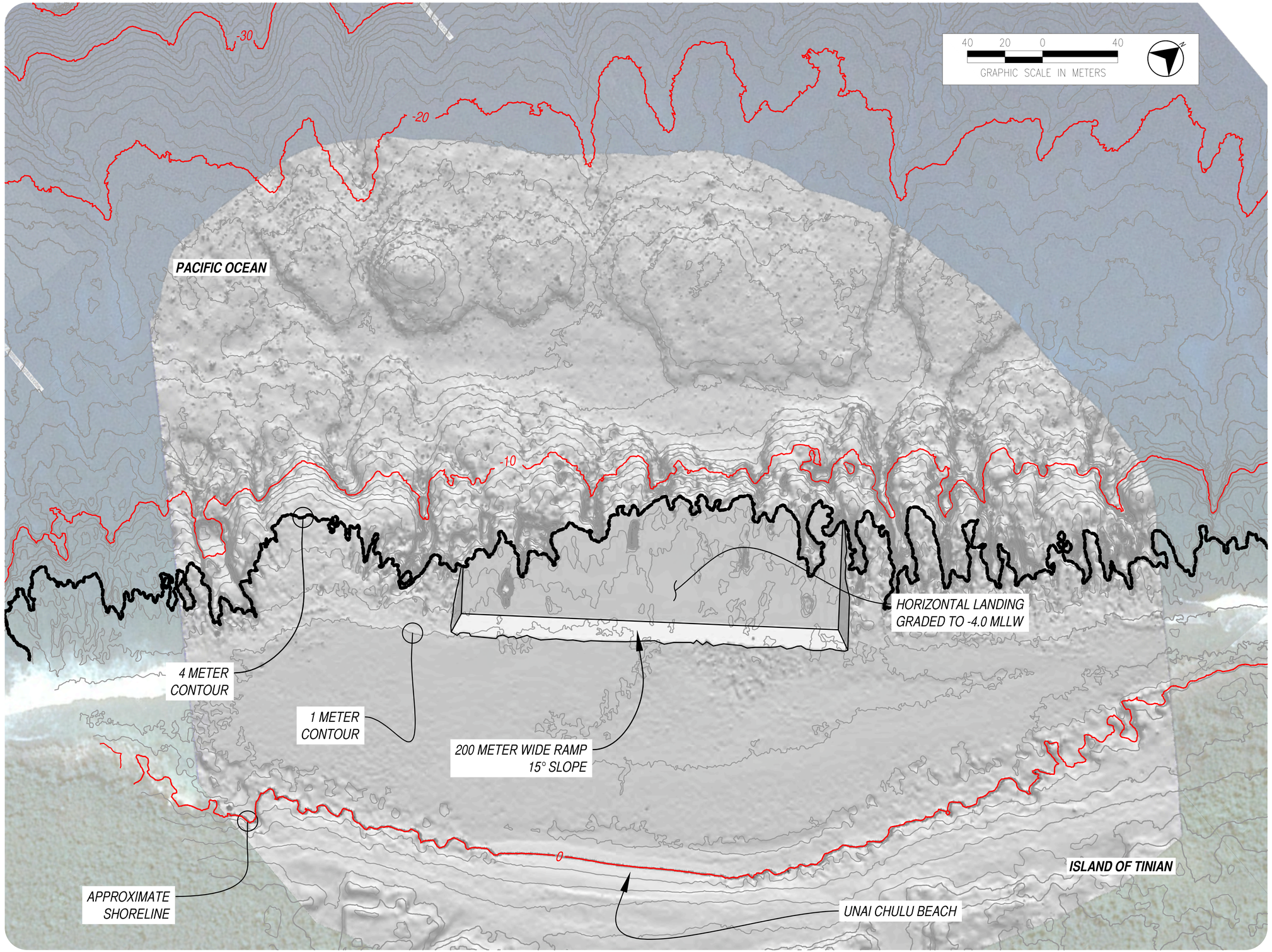

Sea Engineering, Inc.

MAKAI RESEARCH PIER
WAIMANALO, HI 96795
PH 808.259.7966
FAX 808.259.8143

NOTES:

Contours and elevations given in meters.

Contour interval is 1 m.

Highlighted contour every 10 m.

Elevations referenced to mean lower low water (MLLW).

Map based on provided LiDAR survey data.

KEY MAP

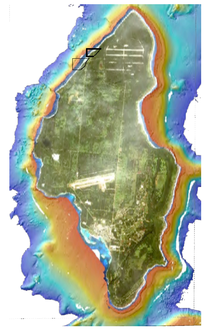

Sheet Name

Figure X-X. Chulu Conceptual Ramp Placement

Project Name

Tinian AAV Landing Sites Investigation

Project No. 25445	Sheet C-6
Date 04 SEP 2014	
Scale 1 : 2,000	

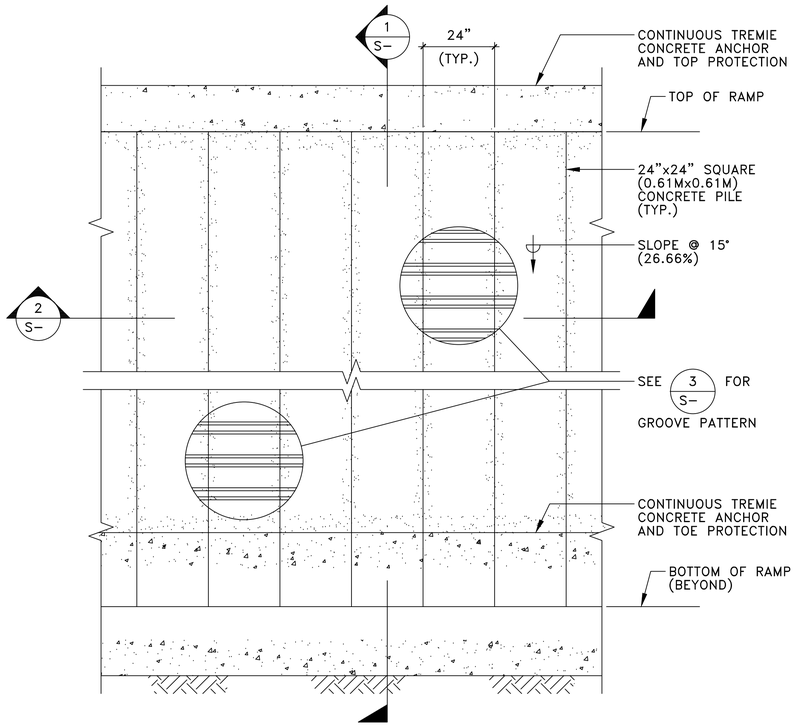

A S– RAMP PLAN
SCALE: 1/2" = 1'–0"

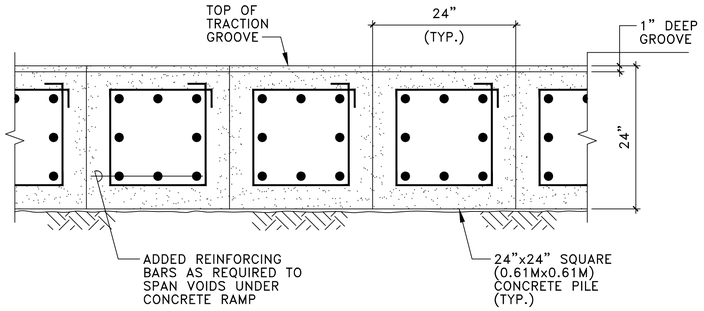

2 S– SECTION
SCALE: 1" = 1'–0"

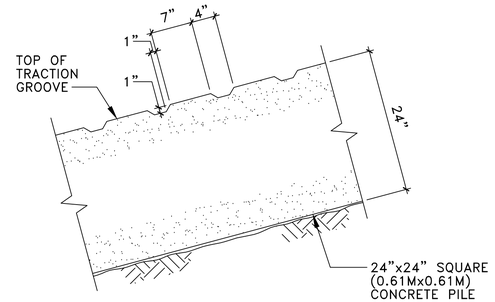

3 S– TYPICAL GROOVE DETAIL
SCALE: 1" = 1'–0"

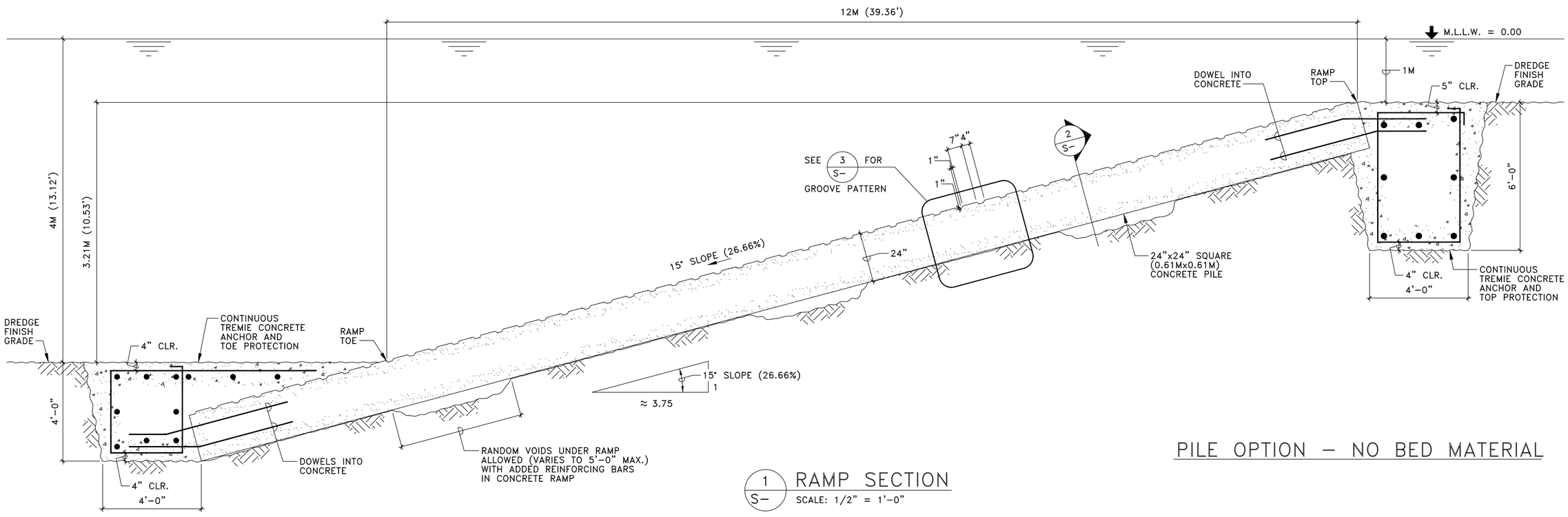

1 S– RAMP SECTION
SCALE: 1/2" = 1'–0"

PILE OPTION – NO BED MATERIAL

REVISIONS	BY

TINIAN AAV STUDY

RAMP PLAN & SECTIONS

Date: 10/28/2014
Scale: AS SHOWN
Drawn:
Job:
Sheet
of Sheets

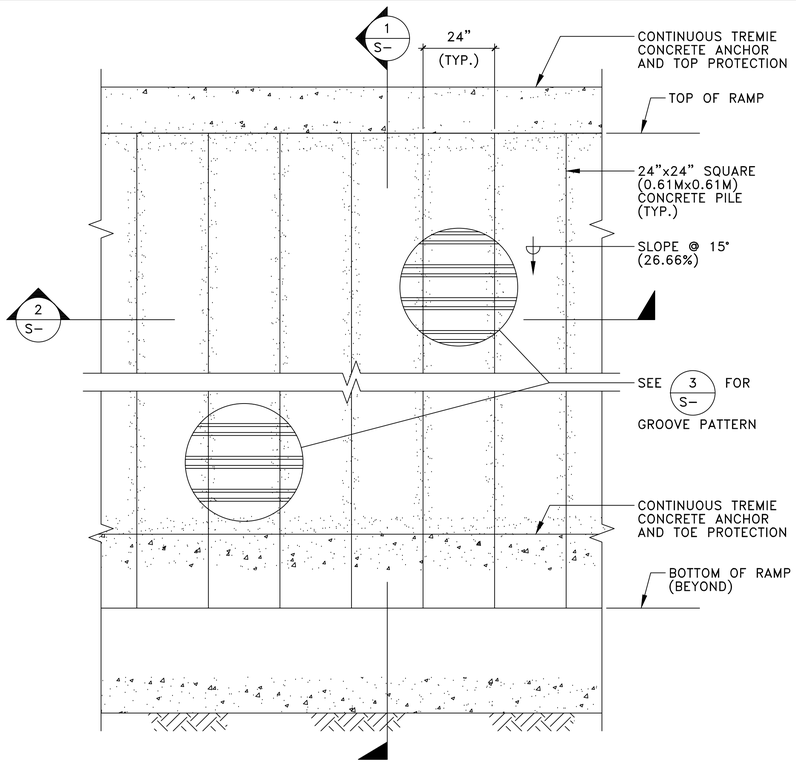

A S– RAMP PLAN
SCALE: 1/2" = 1'–0"

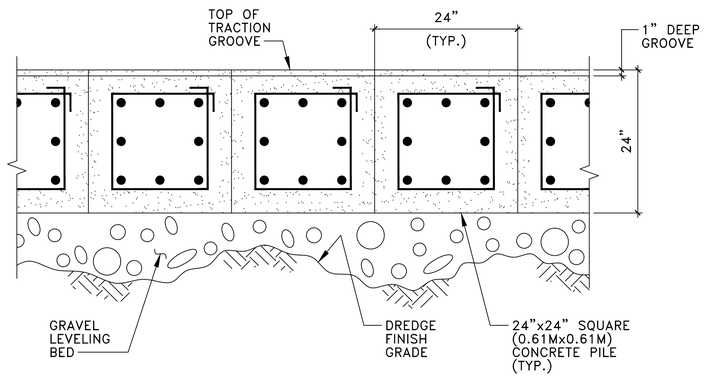

2 S– SECTION
SCALE: 1" = 1'–0"

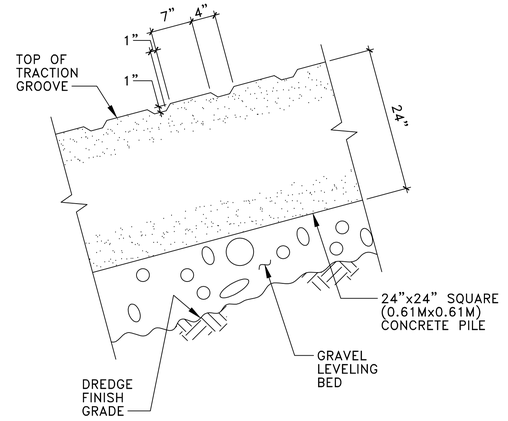

3 S– TYPICAL GROOVE DETAIL
SCALE: 1" = 1'–0"

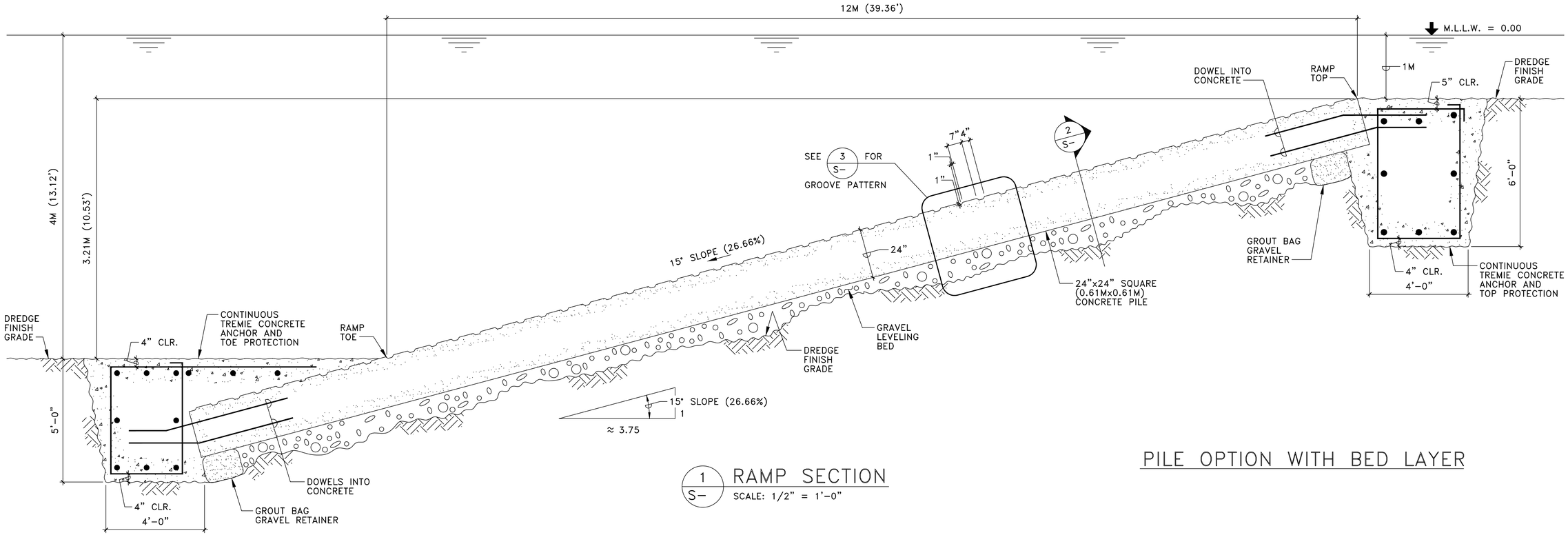

1 S– RAMP SECTION
SCALE: 1/2" = 1'–0"

PILE OPTION WITH BED LAYER

REVISIONS	BY

TINIAN AAV STUDY

RAMP PLAN & SECTIONS

Date: 10/28/2014
Scale: AS SHOWN
Drawn:
Job:
Sheet
of Sheets

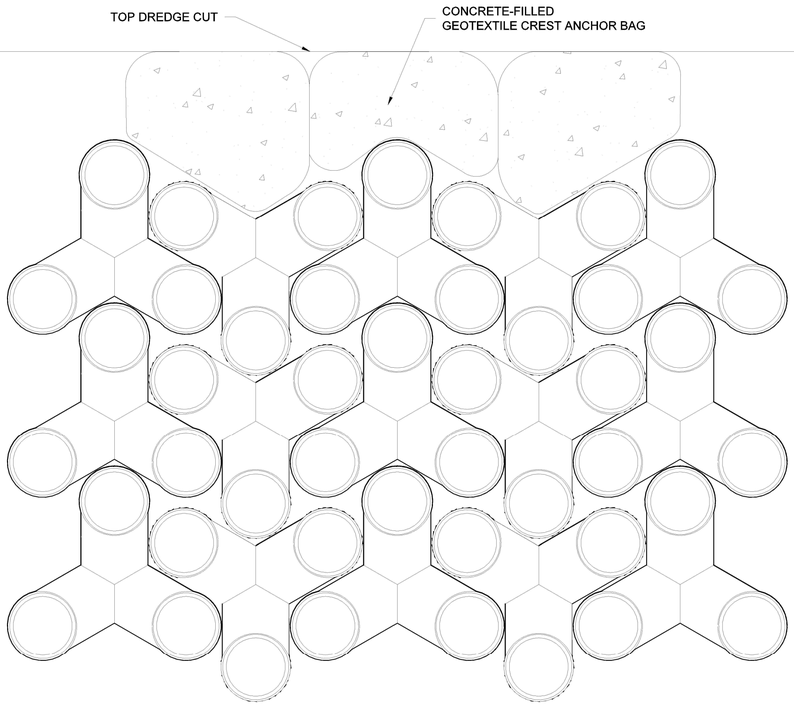

RAMP CREST PLAN

SCALE: 1/2" = 1'-0"

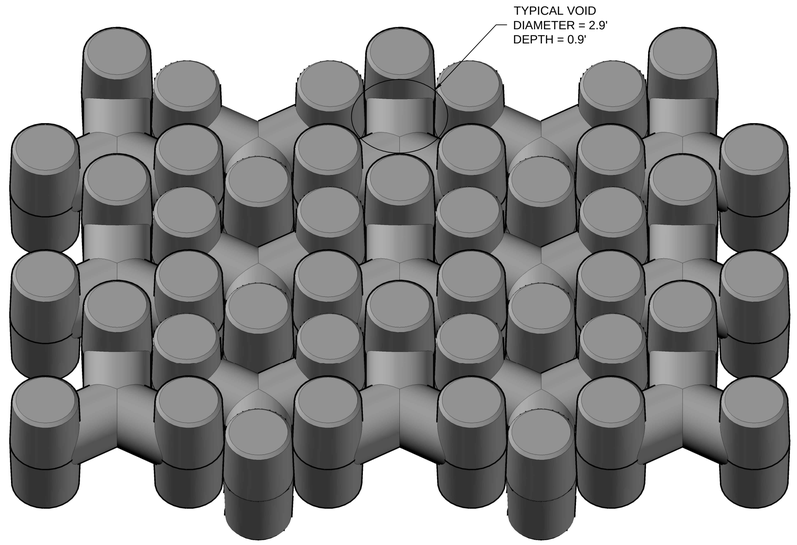

TYPICAL TRIBAR PATTERN

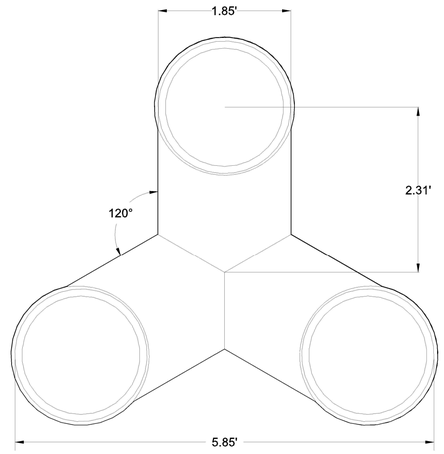

3-TON TRIBAR DETAIL (PLAN)

SCALE: 1" = 1'-0"

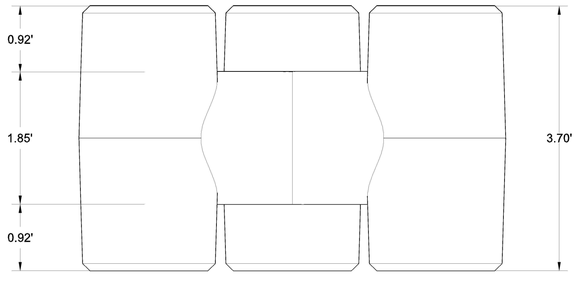

3-TON TRIBAR DETAIL (ELEVATION)

SCALE: 1" = 1'-0"

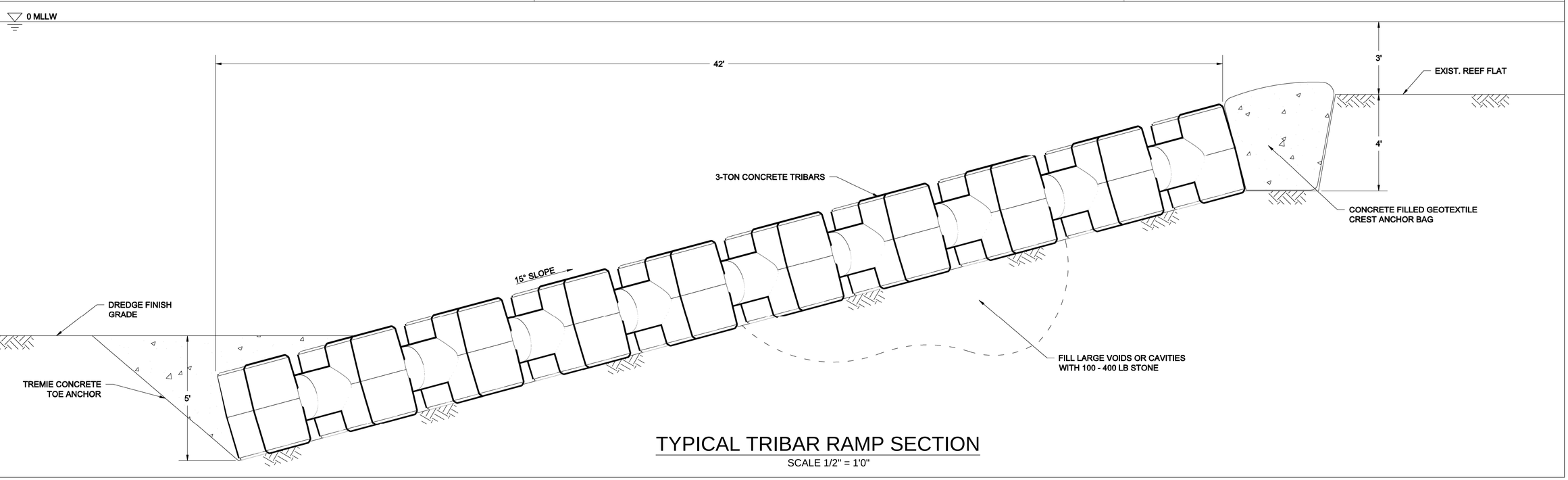

TYPICAL TRIBAR RAMP SECTION

SCALE 1/2" = 1'0"

TINIAN AAV STUDY

TRIBAR RAMP PLAN & DETAILS

Engineering Analysis Evaluation (11-14-14)

Assumptions

- 3 options for construction of ramp area: 1 unarmored, 2 armored.
- Each involves causeways to facilitate land-based construction; construction from offshore barges is not feasible due to safety and stability issues.

Common Components

- Amphibious landing ramp specifications:
  - Width: 20-68 m, average 50 m @ Chulu, 10-58 m, average 35 m @ Babui.
  - Length: 200 m.
  - Slope: 15 degrees.
- Transport: construction supply/materials would be transported from Guam, fill material from onsite on Tinian
- Staging: need 1-2 acres, potentially North Field. Some laydown area(s) on or adjacent to each beach.
- Equipment:
  - large crawler crane
  - large long-reach excavator (either a drag line or a clam shell could be used from the excavator)
  - bulldozer
  - front end loader
  - 6 dump trucks (10 cubic yard capacity)
  - forklift
  - flat bed trucks and trailers
  - several crew trucks for small hauls and crew transport to and from the site
  - a tug and barge would be required for shipping heavy equipment and construction materials from Apra Harbor, Guam to Tinian Harbor
- Causeways
  - Combination steel sheet pile cell with fill from shore out to approx. 1-m depth and a pile-supported trestle through the surf zone and out to 4-m depth.
  - Driving two steel sheet pile walls 30 feet apart to contain the fill, and then filling between them with rock and/or dredged material.
  - Causeway pipe piles are 24 inch diameter. There would be 3 piles for every 15 feet (4.6 m) of trestle. Average of 33 piles per trestle at Chulu, and 24 piles per trestle at Babui.
  - Sheet piles and pipe piles would be removed with crane or excavator, using vibratory hammer as necessary.
  - The sheet piles would be tied together for stability and thus would only need to penetrate several feet into the reef flat.
  - The sheet piles would rise to an elevation of 2 m above MLLW. The trestle would be constructed of steel pipe piles supporting a steel bent, steel stringers running parallel to

the long axis of the trestle, and wooden crane mats placed on top of the stringers for an equipment driving surface.

  - The steel sheet pile and the steel pipe piles would be primarily vibrated into place, with some use of an impact hammer in harder reef material and for proofing of the pipe piles. The amount of impact pile driving will be dictated by substrate conditions at the time of pile installation.
  - Causeway is the only viable construction method. Accessing the sites from the ocean using barges and tugs is not feasible due to the shallow water, irregular reef edge and breaking waves in the required dredge areas. A jackup barge is fitted with moveable legs that can raise the barge/platform above the sea surface. Tugs or other means are required to reposition and move the barges. A jackup barge with the capacity to support the crane and excavator required for the work would draft as much as 1.8 m. Use of a jackup barge is not feasible at Chulu and Babui because the barge draft exceeds water depths on the reef flat, the bottom at the reef edge is too irregular for stable placement of legs, and deployment at the seaward edge of the reef flat would be too hazardous due to breaking waves and surge. Constructing access causeways from shore is therefore considered the only feasible construction method at Chulu and Babui.

- Onshore components:
  - Staging – North Field, beach, and adjacent area (size and location TBD)
  - Regular activity over beach
  - Road along beach for access of construction vehicles to/from causeway
- Construction steps:
  - Construct the first causeway seaward to the -4-m depth and start dredging with the crawler crane.
  - Move landward dredging a 100 to 120 ft (30 to 36 m) wide swath, removing the causeway as the dredging around the end is completed.
  - When the location of the ramp slope toe is reached, replace the crane with the excavator and continue landward with ramp dredging and causeway removal. Under Options 2 and 3, dredge toe and top anchor trenches as necessary to secure armor units.
  - Construct the second causeway and commence dredging at the -4-m depth with the crane.
  - When the ramp slope and trench dredging is complete, begin placing Tribar or concrete pile armor using the crane or excavator.
  - Pour tremie concrete into top and toe anchor trenches to stabilize armor units.
  - Remove the remaining portion of the causeway.
  - Repeat this sequence until dredging and construction is complete.

Comparison of Options

Element	Option 1 (Dredge Only)	Option 2 (Pile Armored)	Option 3 (Tribar)
Key Components			
Surface Treatment	• None	• Grooves 1 inch deep, spaced 7 inches apart	• Tribar (man-made concrete armor units) • 3.7 feet • Sizes ranging from 1 to 50 tons • Approximately 1,400 units
Fill	• None	• Tremie concrete to fill toe anchor trench	• Tremie concrete to fill toe anchor trench • Geotextile bags 6 by 4 feet, placed to span a minimum of two tribar units • If large voids or cavities are encountered during dredging of the ramp they can be filled with 100 to 400 pound stone prior to placing the tribars
Volume	• Chulu: 21,300 m^3 • Babui: 15,200 m^3	• Chulu: 21,300 m^3 + 1,300 m^3 (toe/top slopes) • Babui: 15,200 m^3 + 1,300 m^3	• Chulu: 21,300 m^3 + 1,300 m^3 (toe/top slopes) • Babui: 15,200 m^3 + 1,300 m^3 • Tribar toe trench will be excavated below the elevation of the dredged approach area to a depth of 5 feet to key the tribars into the reef material
Piles	• Yes for construction causeways. • No for ramp.	• Yes for construction causeways. • 24-inch piles • 15 m long, placed on the slope using a crane or excavator, extend into an excavated trench 1.5 m deep and 2.5 m wide (base) and 1.8 m deep and 1.2 m wide (top)	• Yes for construction causeways. • No for ramp.
Wave Design/Strength (long term)	• Low, could deteriorate during continual training/currents	• Higher than Dredge Only	• Higher than Dredge Only
Other	• Fill gaps, holes or depressions up to 1.5 m in span width	--	--

Element	Option 1 (Dredge Only)	Option 2 (Pile Armored)	Option 3 (Tribar)
Construction			
Causeway	• Yes • 6 or 7 per beach, each constructed and then removed before constructing next one • Dredged material will be used as fill for the sheet pile causeway portion; the first causeway consists only of trestle. Material excavated from first causeway provides fill for subsequent sheet pile segments. • What is fate of fill material for causeway after completion of causeways?	Same as Option 1	Same as Option 1
Pile Driving/Vibration	• Each causeway has: o Steel sheet pile walls, vibrated into place o X steel pipe piles vibrated into place, use of impact hammer in harder reef material	Same as Option 1	Same as Option 1
ROM Cost	• Lower construction • Higher maintenance	• Higher construction • Lower maintenance	• Higher construction • Lower maintenance
Duration	• 31 weeks: o Onsite mobilization - 3 weeks o Dredging and construction - 21 weeks o Weather downtime (20%) - 4 weeks o Onsite demobilization and cleanup - 3 weeks •	• 36 weeks o Onsite mobilization - 4 weeks o Dredging and construction - 24 weeks o Weather downtime (20%) - 4 weeks o Onsite demobilization and cleanup - 4 weeks	• Same as 2
Longevity	• Short term	• Long term	• Long term
Maintenance	• requires more maintenance	• Requires less maintenance	• Requires less maintenance
Impacts			

Element	Option 1 (Dredge Only)	Option 2 (Pile Armored)	Option 3 (Tribar)
Marine Biology	• Loss of reef flat and deeper reefs during construction • Potential for mobile rubble: High • Recolonization potential (coral, algae, invertebrates, turtles, fish): Medium • Potential impacts to sea turtles and marine mammals from underwater noise from pile driving	• Loss of reef flat and deeper reefsx during construction • Potential for mobile rubble: Medium • Recolonization potential (coral, algae, invertebrates, turtles, fish): Lowest • Potential impacts to sea turtles and marine mammals from underwater noise from pile driving	• Loss of reef flat and deeper reefs during construction • Potential for mobile rubble: Low • Recolonization potential (coral, algae, invertebrates, turtles, fish): Highest • Potential impacts to sea turtles and marine mammals from underwater noise from pile driving
Terrestrial Biology	• Sea turtle nesting activity would be precluded during construction – loss of turtle nesting habitat on entire beach for full length of construction period (approx. 31 weeks) • Future turtle nesting activity affected by future maintenance activities or need to rebuild: Highest • Pile driving effects minimal • Potential impacts from laydown areas: low • In all cases, impacts to nesting turtles could be minimized by constructing outside of the April-July peak nesting period.	• Slightly greater effects due to longer construction period (approx. 35 weeks) • Future turtle nesting activity affected by future maintenance activities or need to rebuild: Lowest	• Slightly greater effects due to longer construction period (approx. 35 weeks) • Future turtle nesting activity affected by future maintenance activities or need to rebuild: Medium

Element	Option 1 (Dredge Only)	Option 2 (Pile Armored)	Option 3 (Tribar)
Cultural Resources	• Direct adverse effects to NHL, site deposits/latte sets during construction from heavy equipment usage or from road construction. • Possible direct effects from ground disturbance due to AAV use; impacts to fishing grounds of a TCP at Chulu. • Direct effects to potential underwater objects due to construction. • Indirect impacts due to erosion of the beach with change in setting of a TCP and possible deterioration of archaeological features.	Slightly greater effects due to longer construction period	Slightly greater effects due to longer construction period
Other	• Potential visual, recreation, tourism impacts during construction	Slightly greater effects due to longer construction period	Slightly greater effects due to longer construction period
Pro's (engineering)	• No armored ramp surface, therefore substantially less expensive to construct	• Long term, durable surface for AAV operations • Pile surface should be stable under severe, design wave conditions	• Designed for protecting surfaces or areas from wave attack • Used for shore protection and for harbor breakwaters all over the world • Extensive body of information from both field and research studies showing their stability during extreme waves • proposed design is within published application guidelines

Element	Option 1 (Dredge Only)	Option 2 (Pile Armored)	Option 3 (Tribar)
Con's (engineering)	• Longevity of the unprotected surface is uncertain • Continual wave action may cause rapid erosion that may result in depressions and holes that are hazardous to AAV operations	• Possibility for some unevenness at the top of the slope • Substantial costs required to fabricate, transport and install the piles	• It is not known if this surface is desirable for AAV operations • Long term durability of the tribars to continual AAV operations • Typically would not have steel reinforcement, and if breakage occurred their stability could be compromised • Substantial costs required to fabricate, transport, and install tribars

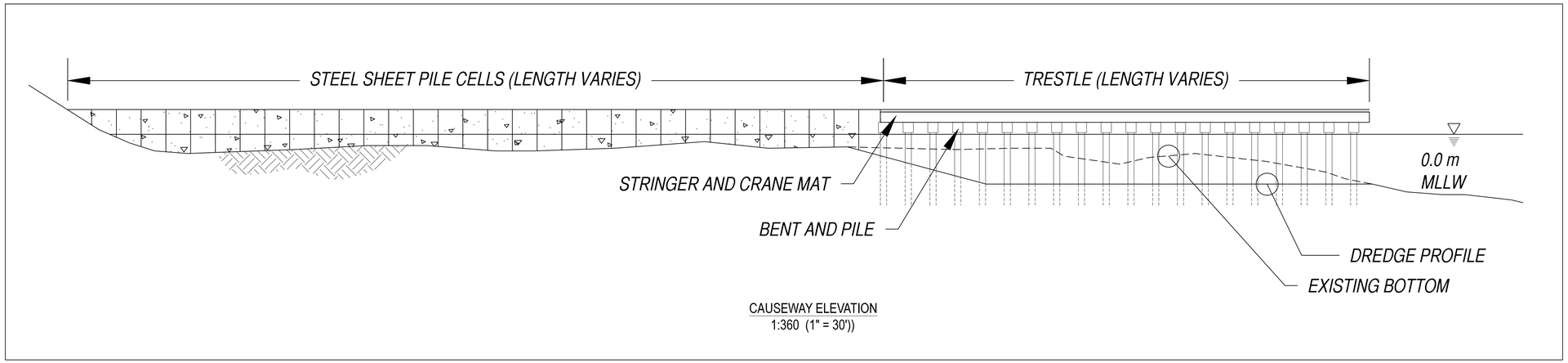

CAUSEWAY ELEVATION
1:360 (1" = 30'))

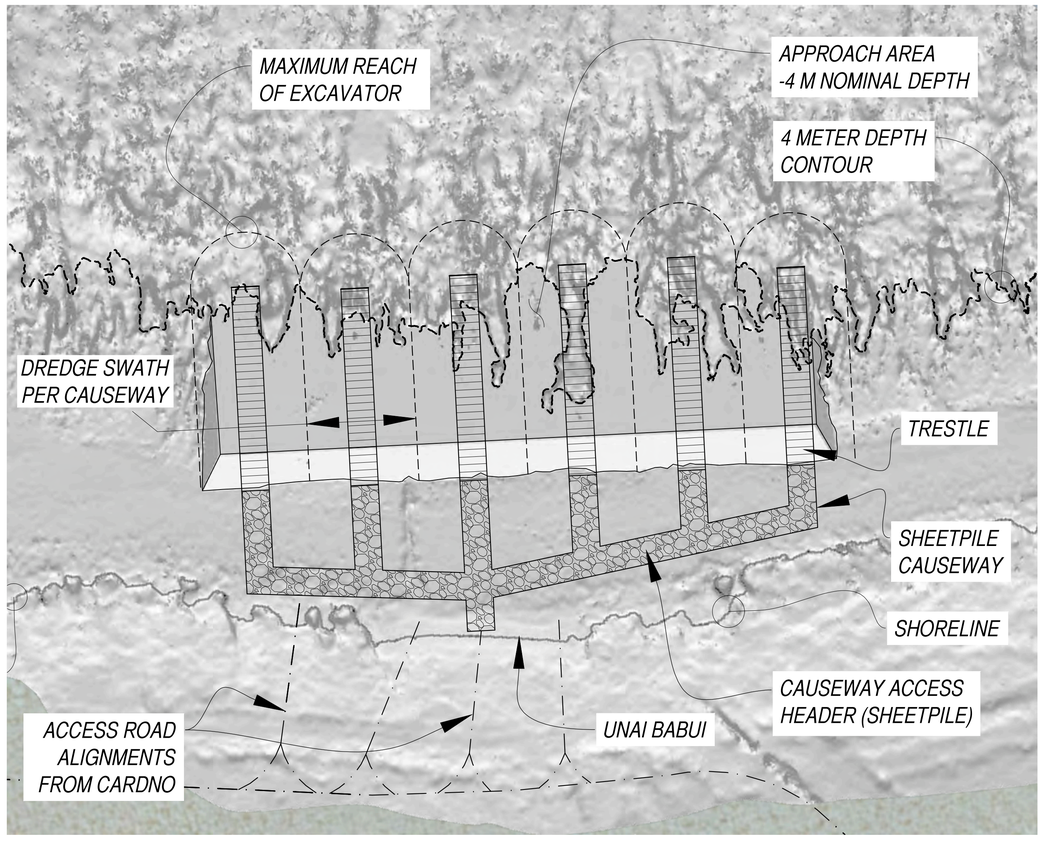

DREDGE PLAN
1:1,000 (D SIZE SHEET)

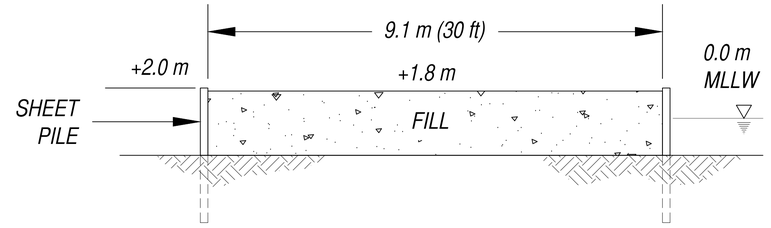

SHEET PILE CAUSEWAY SECTION
1:120 (1" = 10'))

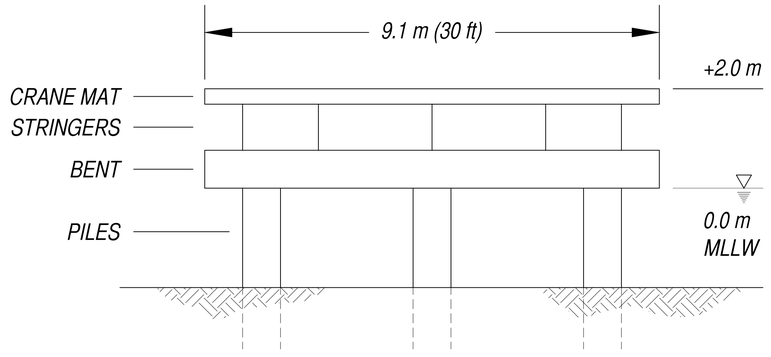

TRESTLE CAUSEWAY SECTION
1:120 (1" = 10'))

Sea Engineering, Inc.
MAKAI RESEARCH PIER
WAIMANALO, HI 96795
PH 808.259.7966
FAX 808.259.8143

NOTES:

Contours and elevations given in meters.

Contour interval is 1 m.

Highlighted contour every 10 m.

Elevations referenced to mean lower low water (MLLW).

Map based on provided LiDAR survey data.

KEY MAP

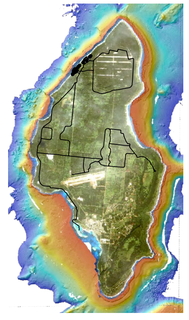

Sheet Name

Figure X-X.
Typical Dredge Plan:
Unai Babui

Project Name

Tinian AAV
Landing Sites
Investigation

Project No.	Sheet
25445	C-7
Date: 04 SEP 2014	
Scale: VARIES	

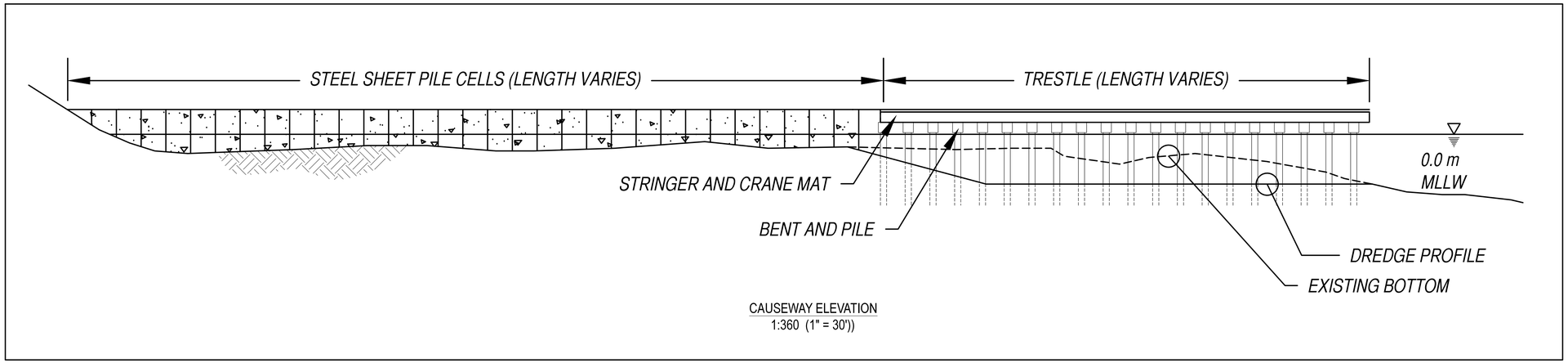

CAUSEWAY ELEVATION
1:360 (1" = 30'))

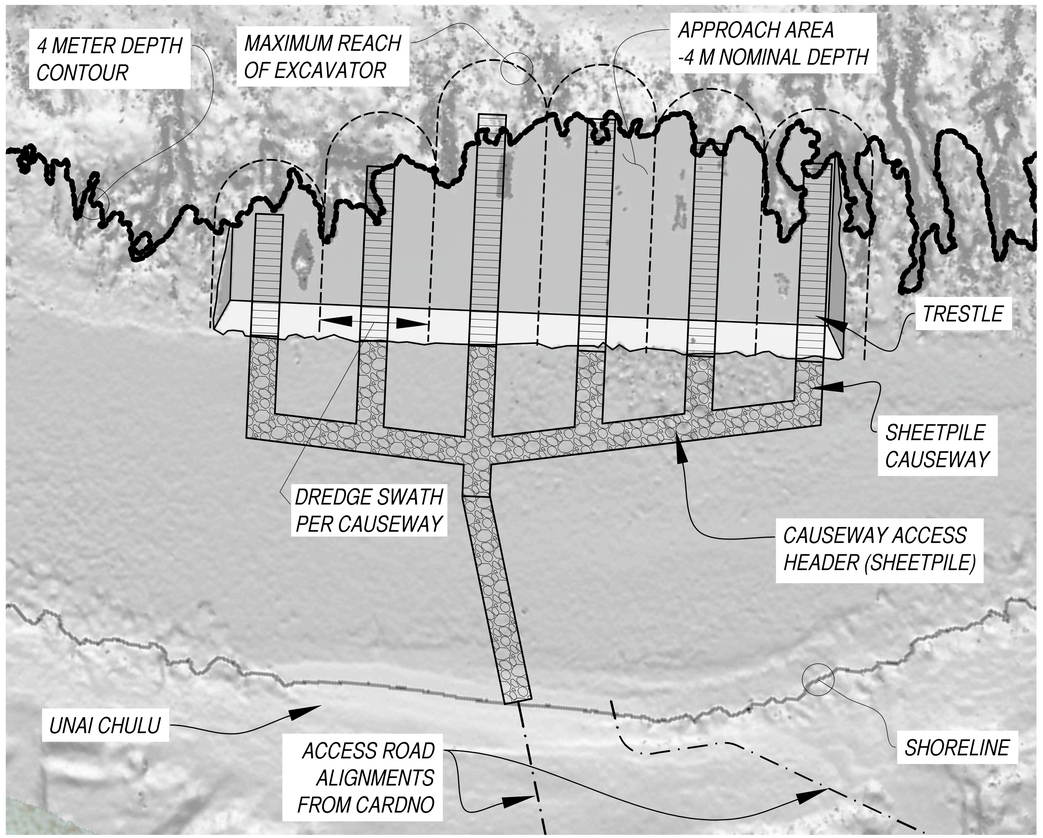

DREDGE PLAN
1:1,000 (D SIZE SHEET)

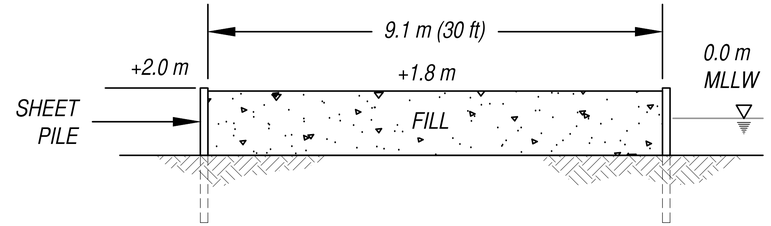

SHEET PILE CAUSEWAY SECTION
1:120 (1" = 10'))

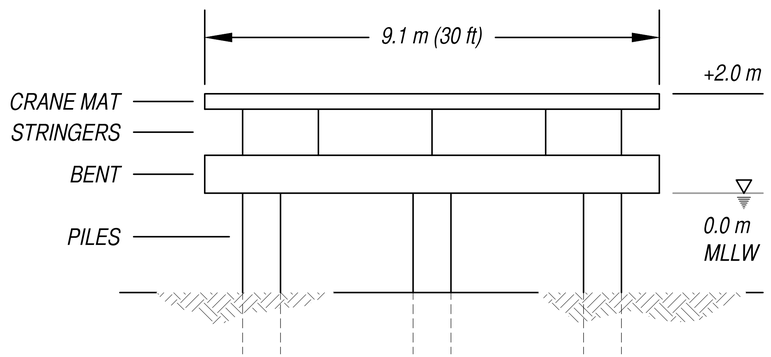

TRESTLE CAUSEWAY SECTION
1:120 (1" = 10'))

Sea Engineering, Inc.
MAKAI RESEARCH PIER
WAIMANALO, HI 96795
PH 808.259.7966
FAX 808.259.8143

NOTES:

Contours and elevations given in meters.

Contour interval is 1 m.

Highlighted contour every 10 m.

Elevations referenced to mean lower low water (MLLW).

Map based on provided LiDAR survey data.

KEY MAP

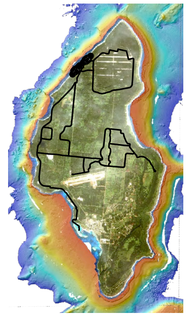

Sheet Name
Figure X-X.
Typical Dredge Plan: Unai Chulu

Project Name
Tinian AAV Landing Sites Investigation

Project No.	Sheet
25445	C-8
Date: 04 SEP 2014	
Scale: VARIES	

FINAL (V2)

COASTAL PROCESSES REPORT

Unai Babui & Unai Chulu, Tinian
Commonwealth of the Northern Mariana Islands

Department of the Navy
Naval Facilities Engineering Command, Pacific
258 Makalapa Drive, Suite 100
JBPHH HI 96860-3134

December 2014

This page is intentionally left blank.

FINAL
(VERSION 2)
COMMONWEALTH OF THE NORTHERN MARIANA ISLANDS JOINT MILITARY TRAINING COASTAL PROCESSES REPORT

Department of the Navy
Naval Facilities Engineering Command, Pacific
258 Makalapa Drive, Suite 100
JBPHH HI 96860-3134

Prepared by:

Sea Engineering, Inc.
Makai Research Pier
Waimanalo, HI 96795

DECEMBER 2014

N62742-11-D-1801 AMD 01 CONTRACT TASK ORDER 02

This page is intentionally left blank.

Final (V2)
Coastal Engineering Report
Unai Babui & Unai Chulu, Tinian
Commonwealth of the Northern Mariana Islands

TABLE OF CONTENTS

LIST OF FIGURES

LIST OF TABLES

List of Acronyms and Abbreviations

AAV	Amphibious Assault Vehicle
AR4	Fourth Assessment Report
BOUSS-2D	Boussinesq
CJMT	Commonwealth Joint Military Training
CMS	Coastal Modeling System
CNMI	Commonwealth of the Northern Mariana Islands
deg	degree
ft	foot or feet
Hs or Hmo	Significant Wave Height
km	kilometers
LVT	amphibious tractor
m	meter
mm	millimeter
MHW	Mean High Water
MHHW	Mean Higher High Water
MLLW	Mean Lower Low Water
MSL	mean sea level
NOAA	National Oceanic and Atmospheric Administration
NW	Northwest
RTA	Range and Training Area
s	seconds
SWAN	Simulating Waves Near-shore
Tp	Peak Wave Period
U.S.	United States
USCS	Unified Soil Classification System
WIS	Wave Information Study
yrs	years

This page intentionally left blank.

CHAPTER 1
INTRODUCTION

1.1 BACKGROUND

The purpose of this report is to assess the impact to coastal processes and existing sand beaches associated with a proposed action to establish a series of live-fire and maneuver ranges, and training areas and supporting facilities within the Commonwealth of the Northern Mariana Islands (CNMI) to address the United States (U.S.) Pacific Command Service Components' unfilled training requirements in the Western Pacific. These live-fire ranges, training courses, and maneuver areas collectively constitute a Range and Training Area (RTA). Under the proposed action, a unit level RTA is proposed for Tinian and a combined level RTA is proposed on Pagan. The proposed action includes construction, range management, expanded training and operations (to include combined-arms, live-fire, and maneuver training at the unit and combined levels), establishment of danger zones, designation of Special Use Airspace, and acquisition and/or lease of land to support simultaneous and integrated training. Figure 1-1 provides an overview of the CNMI and shows the project location for this report on Tinian.

The separate engineering analysis involved review of existing information about the proposed landing sites, preparation of site topographic and bathymetric maps; development of landing site layout alternatives; and, creation of landing site conceptual designs including general construction methodology.

The basic ramp concept entails dredging into the solid reef mass to construct a ramp of natural reef and limestone material, up to the reef shelf elevation at roughly -3.3 feet (ft) (-1.0 meters [m]) mean lower low water (MLLW). To achieve this requires a horizontal bench cut at -13.1 ft (-4 m) MLLW extending inshore of any depressions or channels that would otherwise require fill, followed by a 15° slope approximately 39.6 ft (12 m) long, ramping up from -13.2 to -3.3 ft (-4 to -1 m) elevation MLLW. The horizontal bench varies in width, averaging approximately 115 ft (35 m) wide at Babui and 165 ft (50 m) wide at Chulu. Estimated dredge volumes are 19,800 $yard^3$ (15,200 m^3) and 27,900 $yard^3$ (21,300 m^3) at Babui and Chulu, respectively. A conceptual drawing of the ramp for Unai Babui is illustrated in Figure 1-2, and for Unai Chulu in Figure 1-3.

This document reports on the findings of the coastal processes analysis task of the project, and how the dredged ramps may affect the existing nearshore conditions.

1.2 COASTAL PROCESSES ANALYSIS -- PROJECT SCOPE

1. *Site Visit*: A site visit was conducted between October 22 and 25, 2014, to assess existing shoreline conditions and characteristics at the project sites. An emphasis was placed on the gathering of qualitative observations on the physical characteristics and indicators of coastal processes on the shoreline at the landing sites. Beach profiles were surveyed and sand samples were collected and analyzed for grain size fraction.
2. *Existing Information Review:* Historical information on coastal processes and beach characteristics on Tinian and in the project vicinity were researched and reviewed. Recent and historical aerial or satellite images were acquired and analyzed to determine beach erosion trends.

3. *Deep Water Wave Analysis*: Typical prevailing deep water wave conditions offshore of the project sites were determined utilizing existing wave data developed by the U.S. Army Corps of Engineers Wave Information Study (WIS).
4. *Wave Transformation Modeling:* Numerical wave models were used to propagate and transform the deep water wave conditions to resulting nearshore wave conditions, as well as to quantify the resulting nearshore wave-generated currents. Models were developed for representative conditions at each site, including the existing condition and the proposed ramp condition.
5. *Coastal Impacts Assessment:* Results of the numerical modeling, historical shoreline analysis, and site visit were used to assess possible changes in coastal processes and potential impacts to the beaches as a result of the proposed reef alterations.

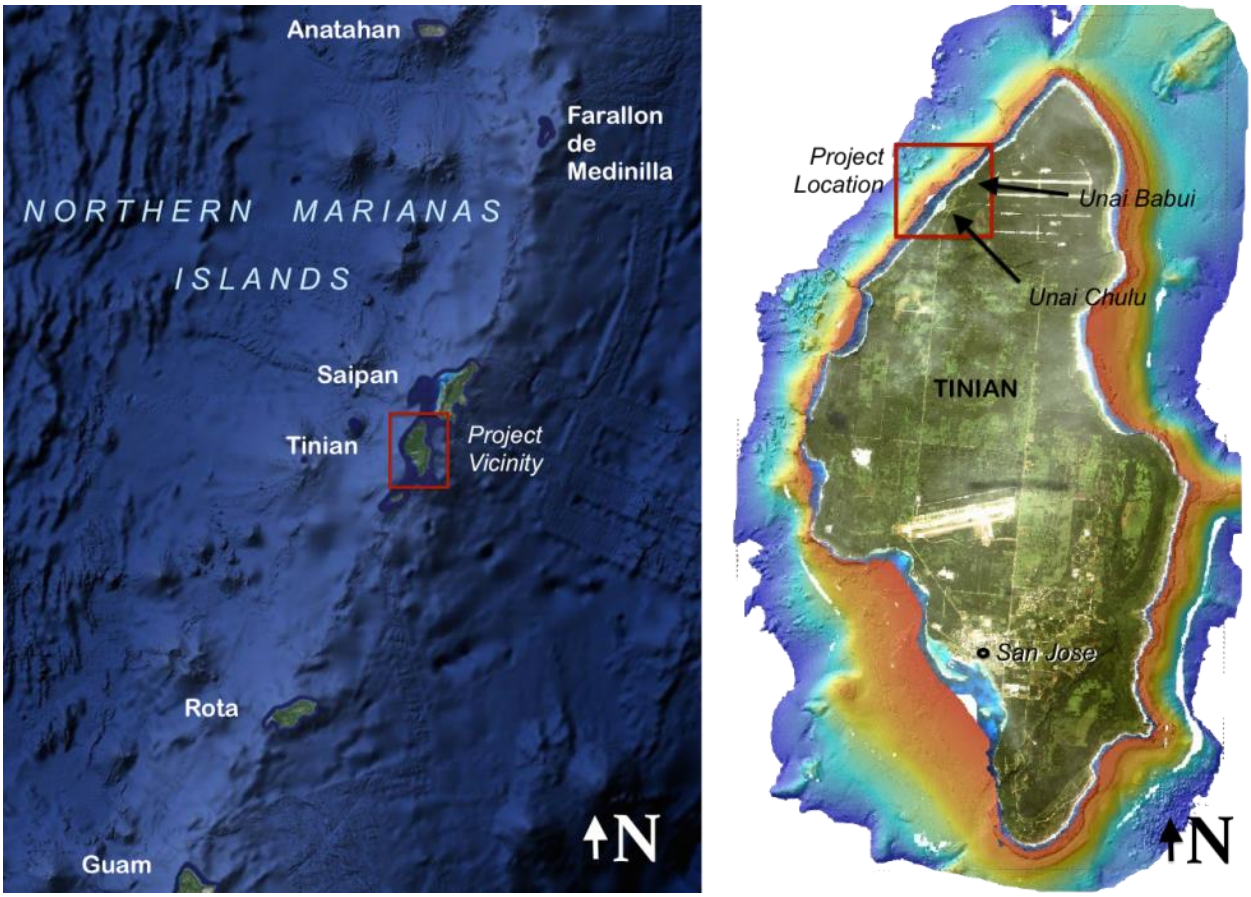

Figure 1-1 Project location and vicinity maps. Credit: Base imagery extracted from Google Maps (left) and University of Hawaii SOEST's Pacific Island Benthic Habitat Mapping Center (right)

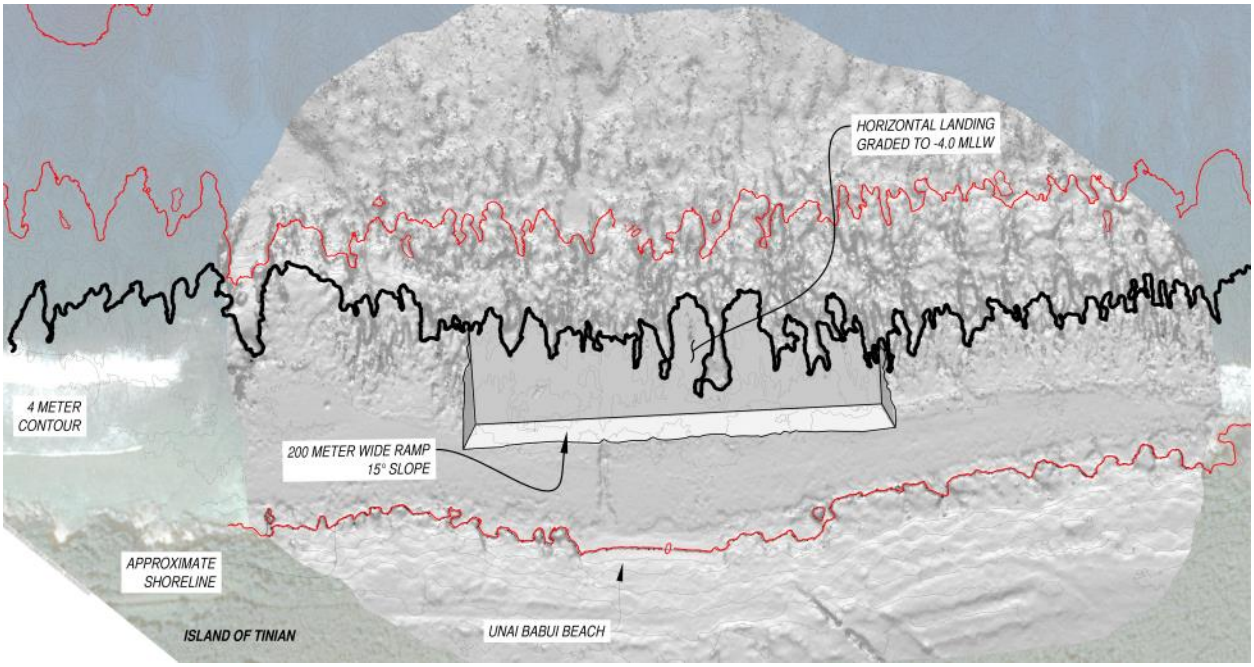

Figure 1-2 Conceptual ramp placement at Unai Babui

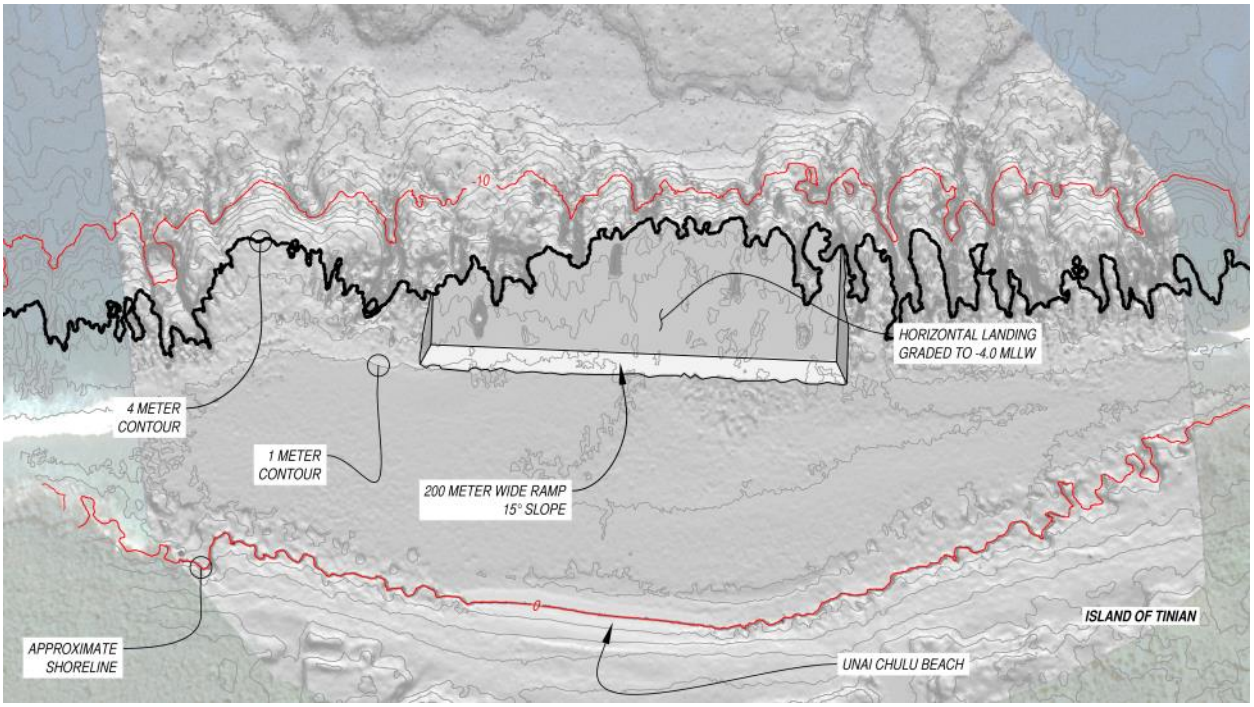

Figure 1-3 Conceptual ramp placement at Unai Chulu

This page intentionally left blank.

CHAPTER 2
SITE CONDITIONS

2.1 REGIONAL SETTING

The project sites at Unai Babui and Unai Chulu are located along the northwest shoreline of Tinian, within the Northern Mariana Islands, as shown in Figure 1-1 and Figure 2-1. The shoreline of Tinian is typical in structure to the southern islands in the chain (which include Guam, Rota, Tinian and Saipan), which are a part of the frontal arc of the Mariana arc-trench system that formed roughly 15 – 20 million years ago. The islands' geomorphology is volcanic in origin, however they are nearly all covered with uplifted limestone from ancient coral reefs. The fossilized reef layer is episodically uplifted by plate tectonics as the Pacific Plate is subducted beneath the Philippine Sea Plate, resulting in the limestone terraces that form a flat "wedding-cake" topography riddled with caves, both on land and underwater.

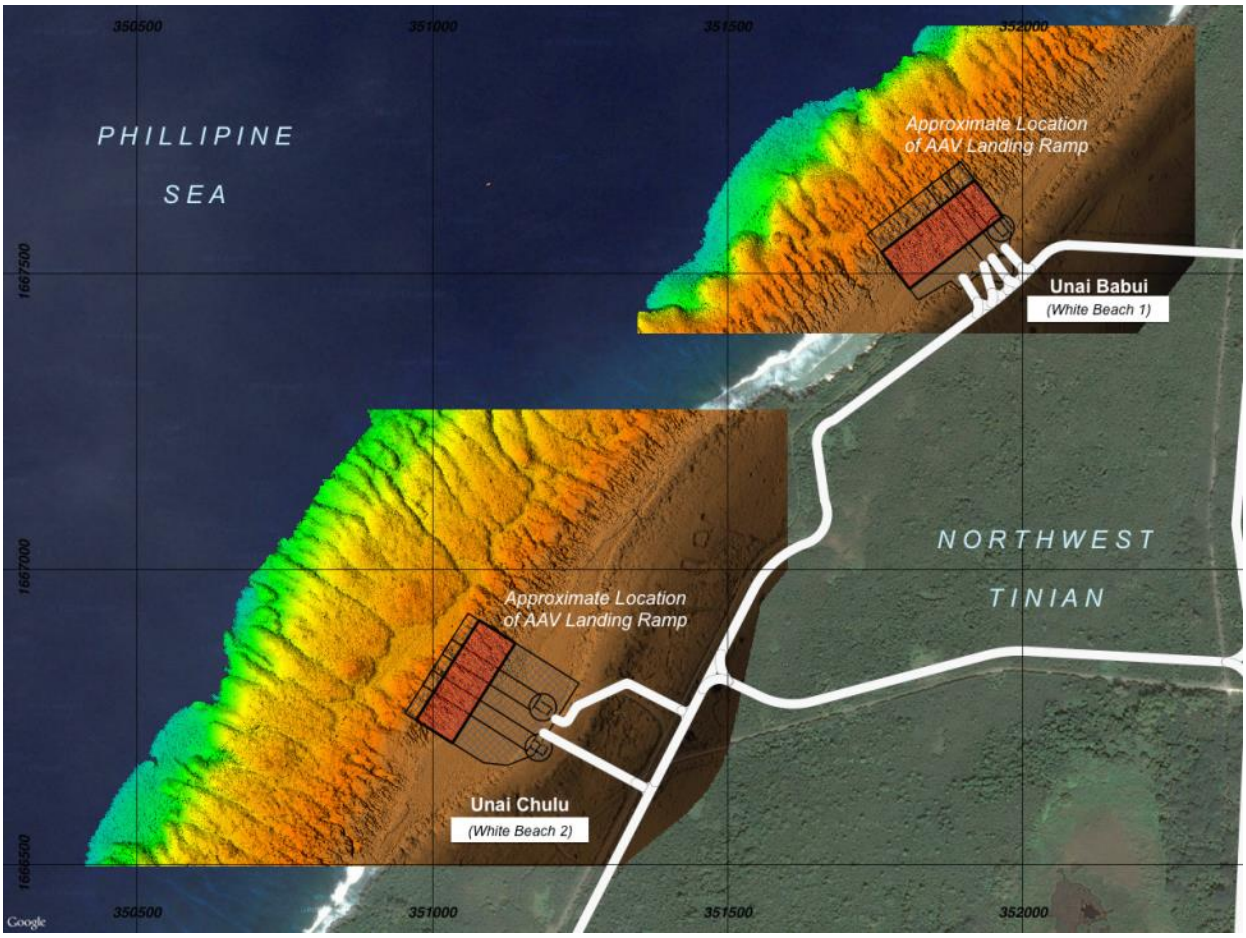

Figure 2-1 Project site map, with approximate location of Amphibious Assault Vehicle Landings and access roadways. Grid lines in UTM 55 N, 500 m interval. (Aerial photo courtesy of Google Maps)

The northwestern coast, like much of the rest of Tinian's coastline, is characterized by jagged, undercut rocky bluffs, which form the shoreline. A reef shelf of varying width extends from the shoreline some distance offshore before descending rapidly to greater depths. The coastline is unsheltered and directly exposed to North Pacific winter swells and typhoon swells, and potentially exposed to southern monsoonal swells. The location is well sheltered from persistent northeast tradewind waves.

Atypical of Tinian's coastline, are the presence of small pocket beaches at Unai Chulu, Unai Babui, and further to the north, Unai Lam Lam. This investigation focuses on Unai Chulu and Unai Babui, which were proposed landing sites for amphibious assault vehicles and potentially other amphibious craft.

The beaches at these locations were the site of a major US amphibious landing known as "Jig-Day" by the 25th and later 23rd Marines during World War II. The landing sites were given the identifiers 'White Beach 1' for Unai Babui to the north and 'White Beach 2' for Unai Chulu to the south. The beaches saw significant military action during the July 24, 1944 invasion, and were used extensively for a time afterwards for resupply efforts from sea (Figure 2-2). The red arrow in the figure indicates the location of a dozer-ploughed path through the beach rock for vehicular access further inland.

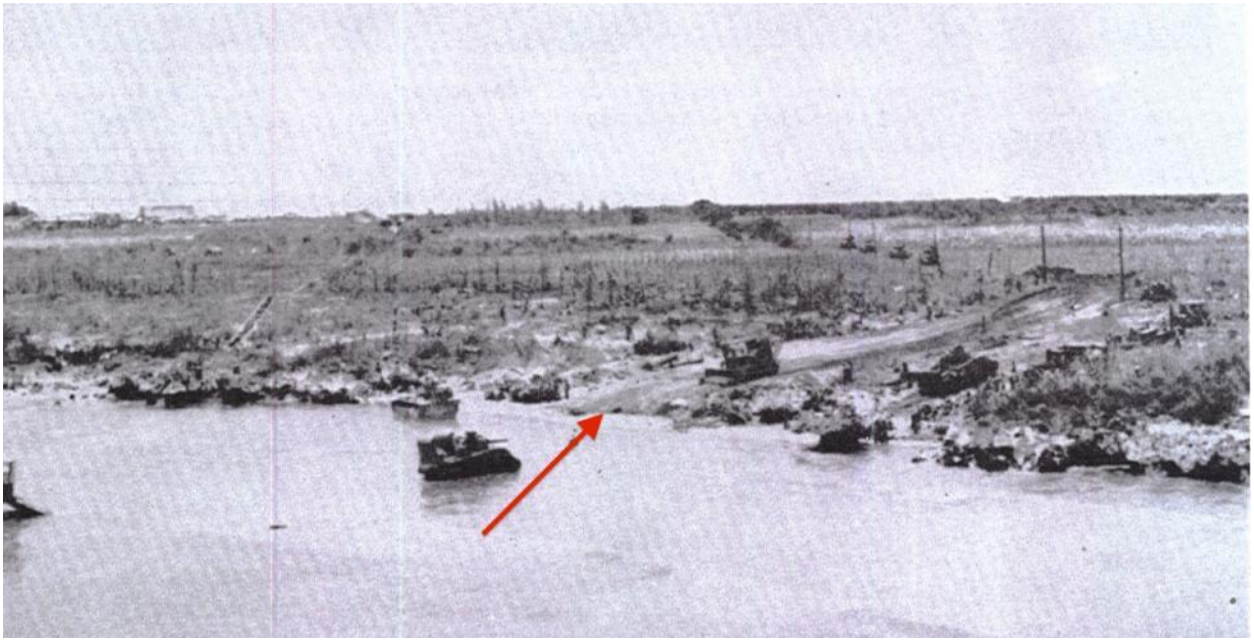

Figure 2-2 Unai Babui (White Beach 1) July 1944, with a medium tank making its way ashore from LCM at reef's edge. (Hoffman 1951)

2.2 EXISTING SHORELINE CONDITIONS AND COASTAL PROCESSES

In general, the NW Tinian shoreline is naturally hardened against erosion due to the craggy limestone bluff from which it is formed. The limited areas of sandy beach which are found at Unai Babui and Unai Chulu (and in very limited areas between the two beaches) are trapped *pocket beaches*, which are contained by rocky boundaries at either end of the beach. It is these beaches which are the focus of this investigation. A site visit for this report was done from October 24-25, 2014.

2.2.1 Unai Babui Shoreline

The beach at Babui was found to be relatively small, with a maximum length of approximately 207 ft (63 m) and width of 33 ft (10 m). The beach is composed of discontinuous, medium-to-fine grained calcareous sand, perched on a craggy, extensive limestone bench. Slight promontories of rock appear to bound the beach to the north and south. The basement limestone rock complex appears to extend under the entire stretch of beach, and protrudes through the sand over approximately 50% of the beach area, as illustrated in Figure 2-3 and Figure 2-4. The only segment of continuous beach (indicated by the red arrow in Figure 2-3) exists at the location of the dozer path created during World War II. Based on surrounding rock features to the north and south of the beach, and assuming these features remain relatively consistent as they proceed under the beach, it is estimated that the maximum thickness of the sand layer may range up to 6.6 ft (2 m), but it is likely much less than that for most of the beach.

Figure 2-3 The sparse sandy beach at Unai Babui (White Beach 1) as seen from offshore

A shallow reef shelf extends roughly 164 ft (50 m) offshore from the beach, with limited sand deposits of less than 1 ft (0.3 m) in thickness found in various pockets over the reef top. Sand from these deposits likely migrates to and from the beach, depending on wave conditions. A pronounced cross-shore fissure in the reef, roughly 7 ft by 130 ft (2 m by 40 m) was observed at the southern end of the beach (Figure 2-5), which appeared to be extensive enough to present issues for tracked or wheeled vehicle attempting to transit over it.

Ocean conditions at Unai Babui during the site visit were relatively quiescent, with 2 to 3 ft (0.6 to 1 m) breakers on the outer reef edge from a northwest groundswell and smooth water from the offshore winds. Waves along the beach were approximately 0.5 ft (0.15 m), with negligible currents. Further out from the shore, a slight current was observed running offshore through the previously identified fissure shown in Figure 2-5.

Figure 2-4 Numerous rock outcroppings stud the beach at Unai Babui

Figure 2-5 Large fissure dissecting the reef off southern Babui beach

2.2.2 Unai Chulu Shoreline

The beach at Unai Chulu is a continuous, relatively large, crescent-shaped beach composed of fine-to-medium grained calcareous sands. The 425 ft (130 m) long beach is bounded on both ends by the weathered limestone bluff, which appears to extend in a sweeping arc underneath the entire length of Unai Chulu, as shown in Figure 2-6 and Figure 2-7. A broad, shallow reef shelf extends roughly 650 ft (200 m) offshore from the beach, forming a convex arc of reef with the widest point roughly centered on the middle of Unai Chulu. Field observations suggest that the concave shape of the shoreline at this location in conjunction with the convex reef shelf running offshore act to form an area of convergence, driven by wave action. The accumulation of sand at this location is likely a result of this physical configuration.

Figure 2-6 The beach at Unai Chulu (White Beach 2), as seen from offshore

Figure 2-7 Limestone ledge running under the beach at Unai Chulu

Ocean conditions at the time of the site visit were relatively mild, with a small northwest swell producing 3 – 4 ft (0.9 – 1.2 m) breakers on the outer reef edge. Breaking wave heights were noticeably larger at Chulu as compared to Babui on the same day. Focusing of wave energy was observed at the peak of the convex curve in the reef, aligning approximately with the center of the beach. Wave crests propagating

over the inner reef generally mimic the convex curve of the reef, and result in wave crest alignments with respect to the shoreline that result in a convergence of wave energy and sand transport. This phenomenon was also seen in aerial imagery, as shown in Figure 2-8. Such areas of convergence along shorelines are typically associated with sand or sediment accretion, as occurs at this location.

Figure 2-8 Wave convergence at Unai Chulu (red line indicates approximate wave alignment)

Source: Photograph courtesy of Google Earth 2012

2.2.3 Typical Existing Shoreline Profiles

Representative shoreline transects were surveyed at both landing sites for comparison with the 2014 LiDAR survey data. Change in beach profile shape over time is often indicative of seasonal changes in wave energy or of existing erosional activity. Survey results are presented in Figure 2-9 through Figure 2-12, which show the relative locations of the profile transects as well as the profile plots, which include profiles extracted from the LiDAR data. In general, the comparison reveals only minor differences in beach shape between the two surveys, suggesting that the beaches at both Unai Babui and Unai Chulu have been stable over the 18 month period.

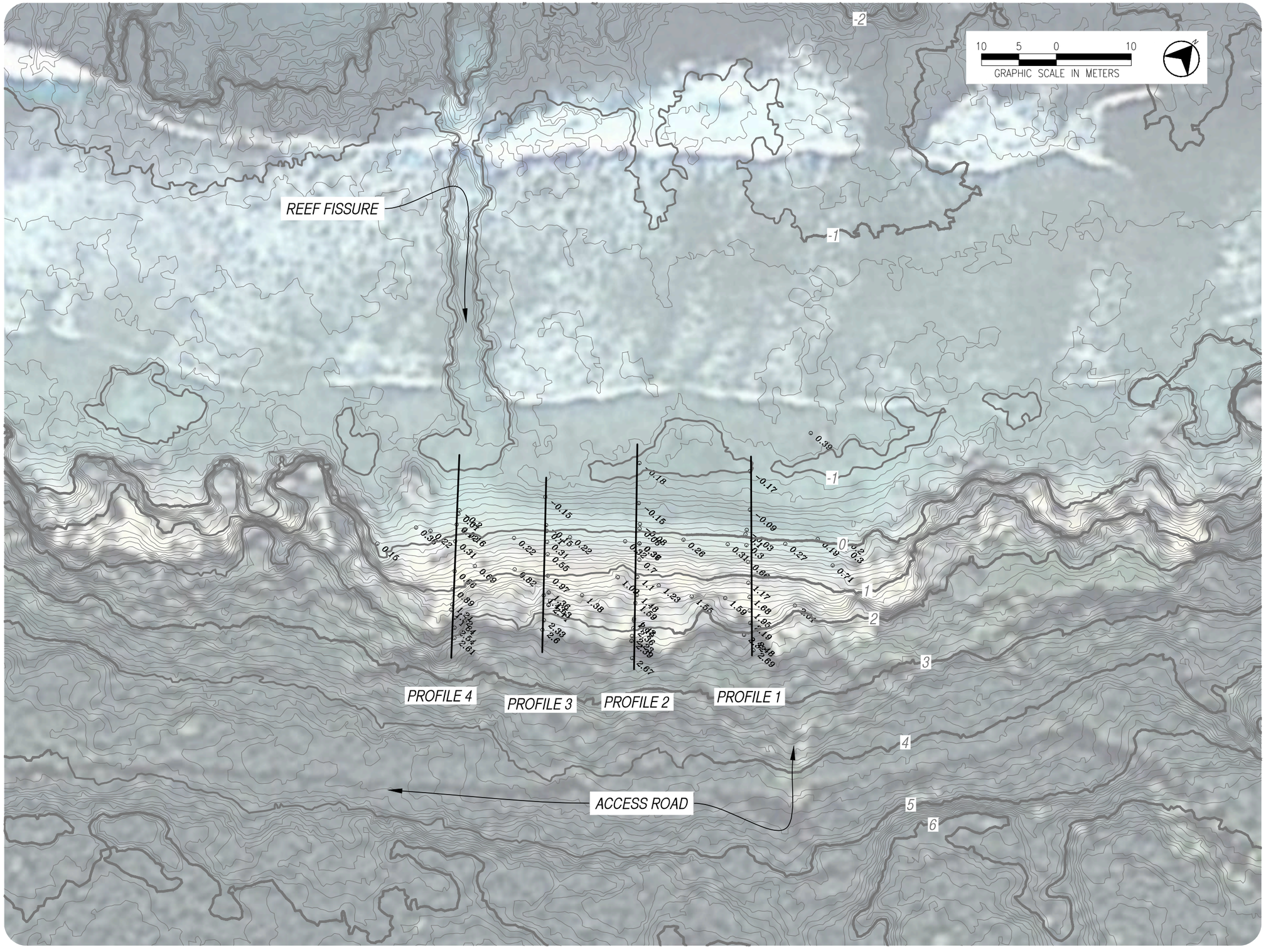

Sea Engineering, Inc.

MAKAI RESEARCH PIER
WAIMANALO, HI 96795
PH 808.259.7966
FAX 808.259.8143

NOTES:

Elevations and contours in meters referenced to mean lower low water (MLLW).

Contour interval is 0.1 m, highlighted contours every 1 m. Contours based on April 2013 LiDAR dataset.

Beach profiles and shoreline surveyed by SEI on 24 Oct 2014.

LEGEND:

Surveyed Point Elevations

⊙ 2.65

Figure 2-9.
Survey and Contour Map:
Unai Babui

Tinian AAV Landing Sites Investigation

Project: 25445	C-1
November 2014	
Scale 1 : 500	

This page intentionally left blank.

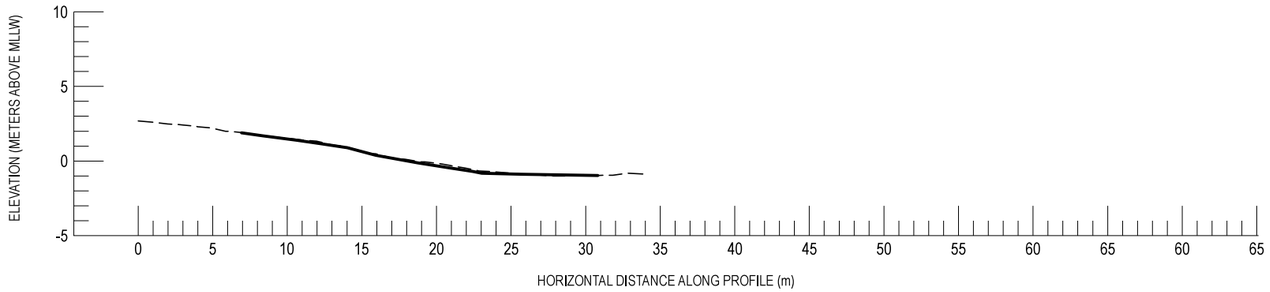

01 PROFILE NO. 1 – UNAI BABUI
1:400

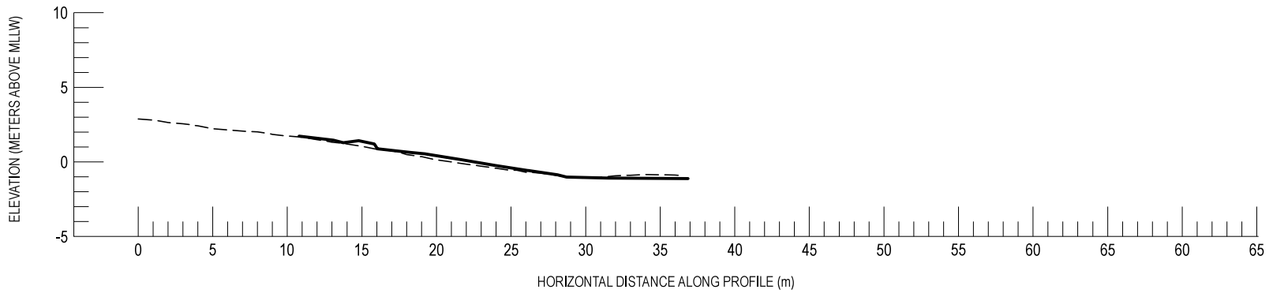

02 PROFILE NO. 2 – UNAI BABUI
1:400

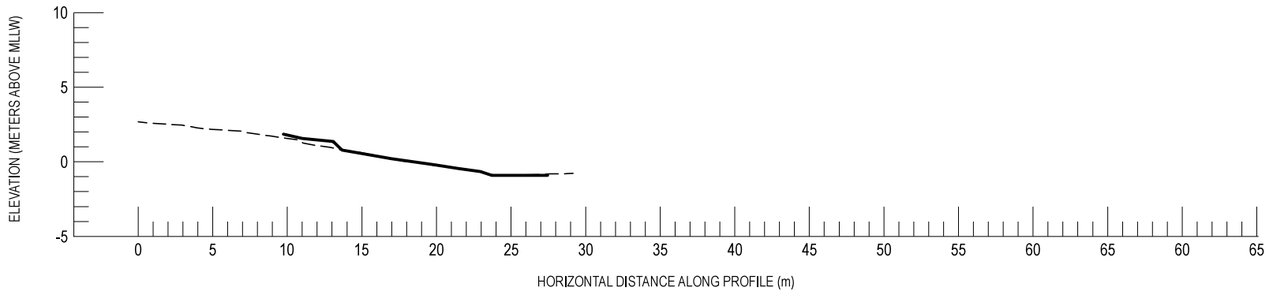

03 PROFILE NO. 3 – UNAI BABUI
1:400

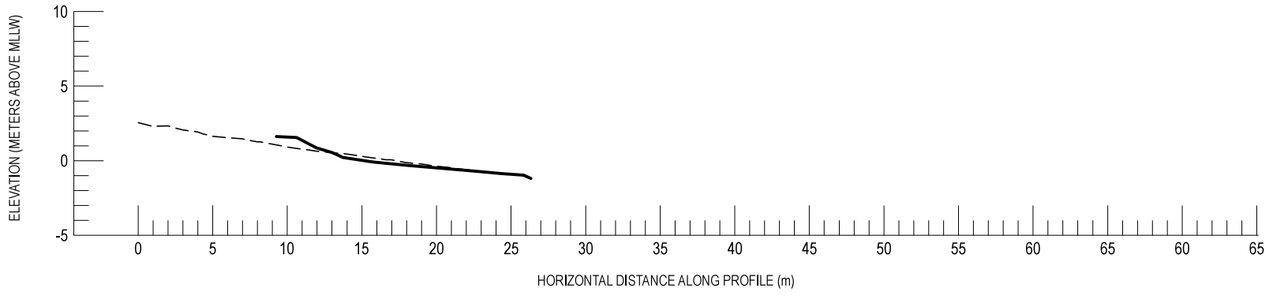

04 PROFILE NO. 4 – UNAI BABUI
1:400

Sea Engineering, Inc.
MAKAI RESEARCH PIER
WAIMANALO, HI 96795
PH 808.259.7966
FAX 808.259.8143

NOTES:

Elevations and distances given in meters.

LEGEND:

Profile based on April 2013 SHOALS LiDAR survey data:

Field measured profile, surveyed October 2014:

Figure 2-10.
Beach Profiles:
Unai Babui

Tinian AAV Landing Sites Investigation

Project: 25445
November 2014
Scale 1 : 400

C-2

This page intentionally left blank.

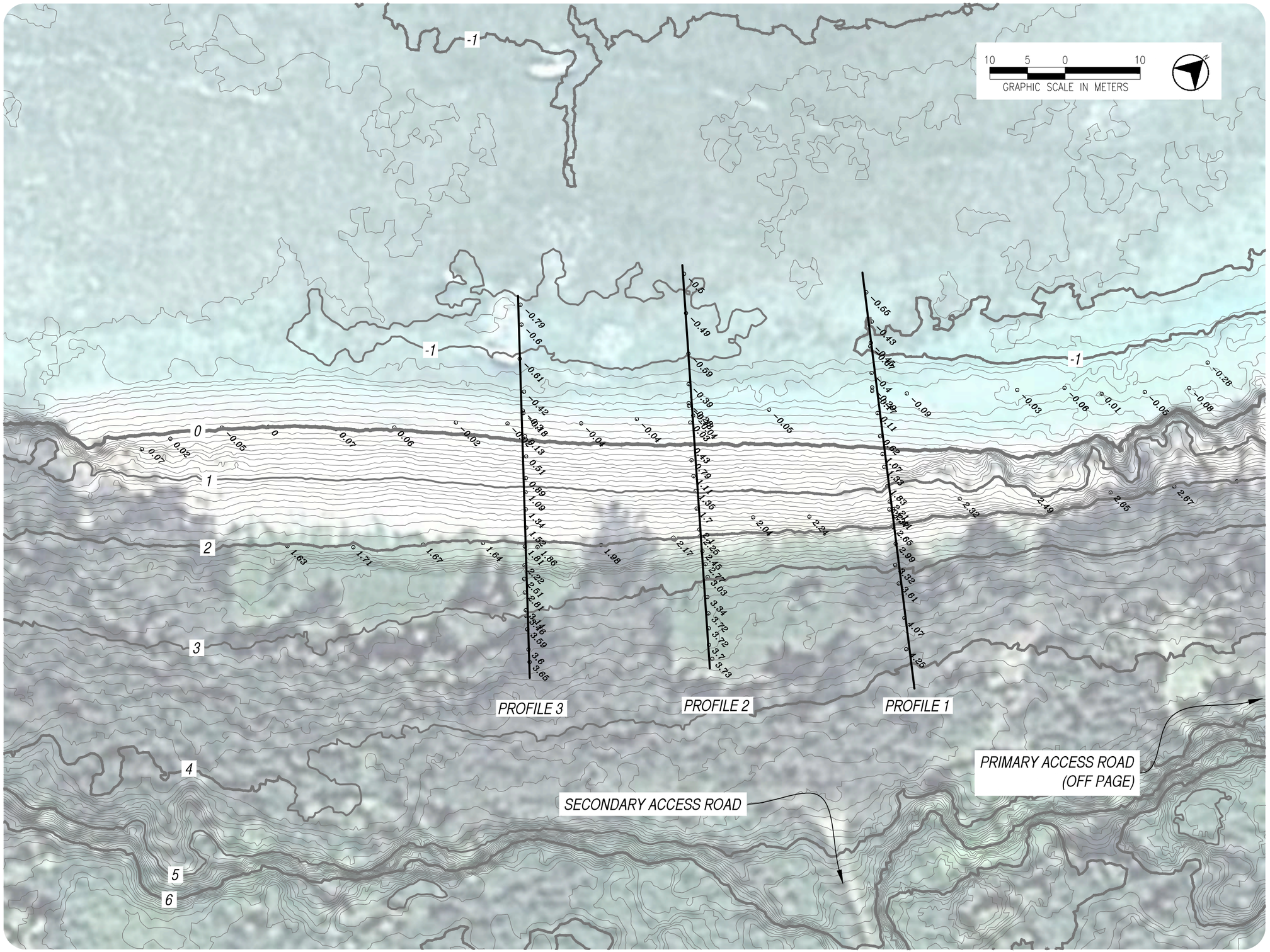

Sea Engineering, Inc.

MAKAI RESEARCH PIER
WAIMANALO, HI 96795
PH 808.259.7966
FAX 808.259.8143

NOTES:

Elevations and contours in meters referenced to mean lower low water (MLLW).

Contour interval is 0.1 m, highlighted contours every 1 m. Contours based on April 2013 LiDAR dataset.

Beach profiles and shoreline surveyed by SEI on 24 Oct 2014.

LEGEND:

Surveyed Point Elevations

⊙ 2.65

Figure 2-11.
Survey and Contour Map:
Unai Chulu

Tinian AAV Landing Sites Investigation

Project: 25445	C-3
November 2014	
Scale 1 : 500	

This page intentionally left blank.

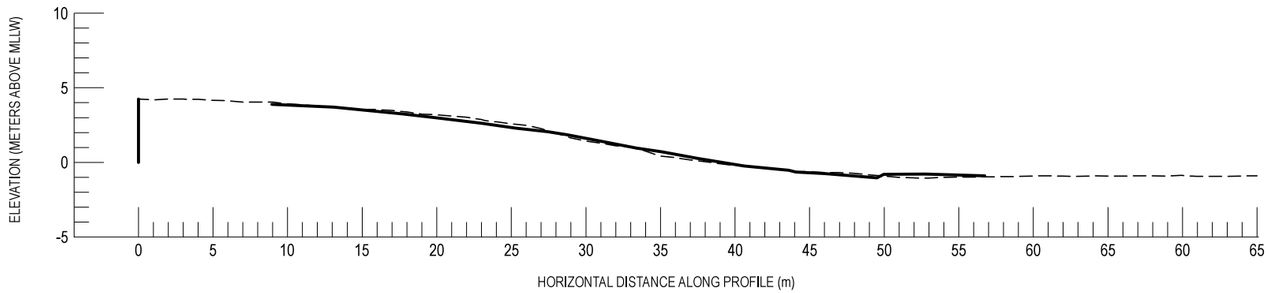

01 PROFILE NO. 1 – UNAI CHULU
1:400

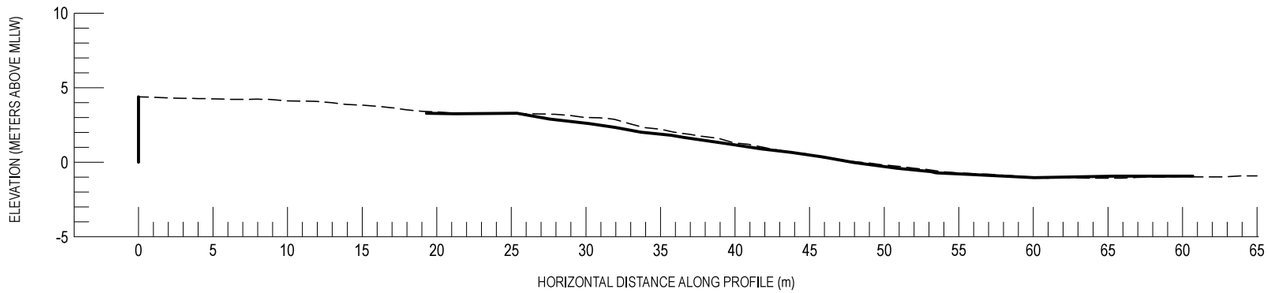

01 PROFILE NO. 2 – UNAI CHULU
1:400

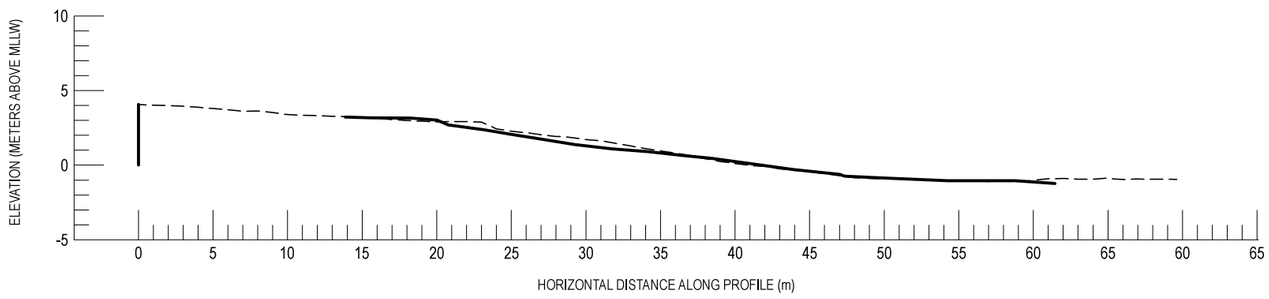

01 PROFILE NO. 3 – UNAI CHULU
1:400

Sea Engineering, Inc.
MAKAI RESEARCH PIER
WAIMANALO, HI 96795
PH 808.259.7966
FAX 808.259.8143

NOTES:

Elevations and distances given in meters.

LEGEND:

Profile based on April 2013 SHOALS LiDAR survey data:

Field measured profile, surveyed October 2014:

Figure 2-12.
Beach Profiles:
Unai Chulu

Tinian AAV Landing Sites Investigation

Project: 25445
November 2014
Scale 1 : 400

C-4

This page intentionally left blank.

The profiles at Unai Babui show the beach toe resting on hard reef at an average elevation of -3.3 ft (-1 m) and cresting among exposed rock clumps at an elevation of approximately +5 ft (+1.5 m), with an average active beach face slope of 1 on 6 vertical to horizontal. At Unai Chulu, profile data show the beach toe again at -3.3 ft (-1 m) while the beach crest is noticeably higher at an average +12 ft (+3.5 m), with an average active beach face slope of 1 on 7 vertical to horizontal.

2.2.4 Grain Size Analysis

Information on the size and composition of sands that comprise a beach can often lend insights into its geomorphology, or lifecycle. In general, beaches with steeper faces and coarser beach material such as cobbles have been shaped by extreme coastal processes. These beaches are subject to large waves, which have acted over time to strip away all fine sedimentary material, leaving only those that are just large enough to resist erosional forces. Conversely, beaches that are protected from large waves or strong currents are often comprised of a majority of fine-grained materials.

Sand samples were collected at a number of locations on both Unai Babui and Unai Chulu beaches, from which composite samples were then created for the north and south ends of each beach. Compositing was performed by blending the sand collected from various elevations on the beach face in order to develop a representative sample at each end of the beach. A total of four composite sand samples were then taken to a laboratory for a sieve (or size fraction) analysis, from which the grain size distribution curve shown in Figure 2-13 was created.

The plot in Figure 2-13 shows that the majority of sand from both beaches falls within the category of *medium sands*, as defined by the Unified Soil Classification System (USCS) classifications, indicated by dashed vertical lines and labels on the figure. Median grain size (D_{50}) for Unai Babui is approximately 0.55 millimeter (mm), while at Unai Chulu it is approximately 0.64 mm. Both the median grain sizes and classification are representative for tropical Pacific Ocean islands with fringing coral reefs and direct exposure to the open water.

The sands at both beaches appeared to be completely marine in origin (calcium carbonate), as implied by the light coloration and texture (Figure 2-14). This is as expected for this location, due to a lack of any significant terrestrial sediment sources such as rivers or streams. This is significant because it means that all sand production occurs on the nearby reef top, and changes to the reef could affect this sand source.

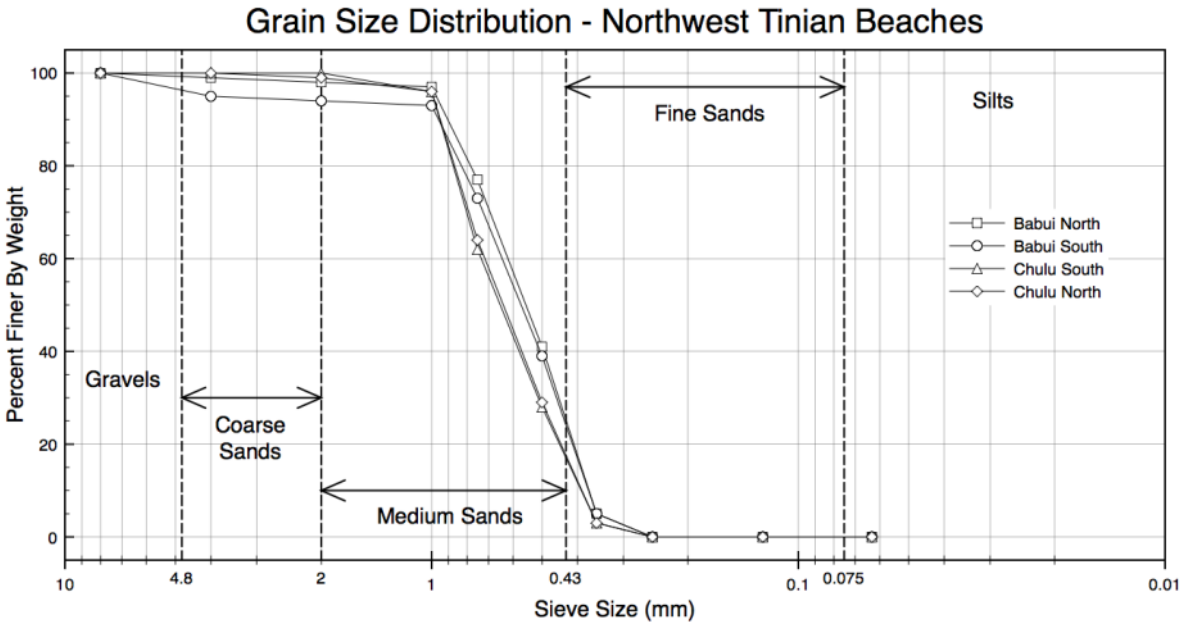

Figure 2-13 Beach sand grain size distributions for Unai Babui and Unai Chulu

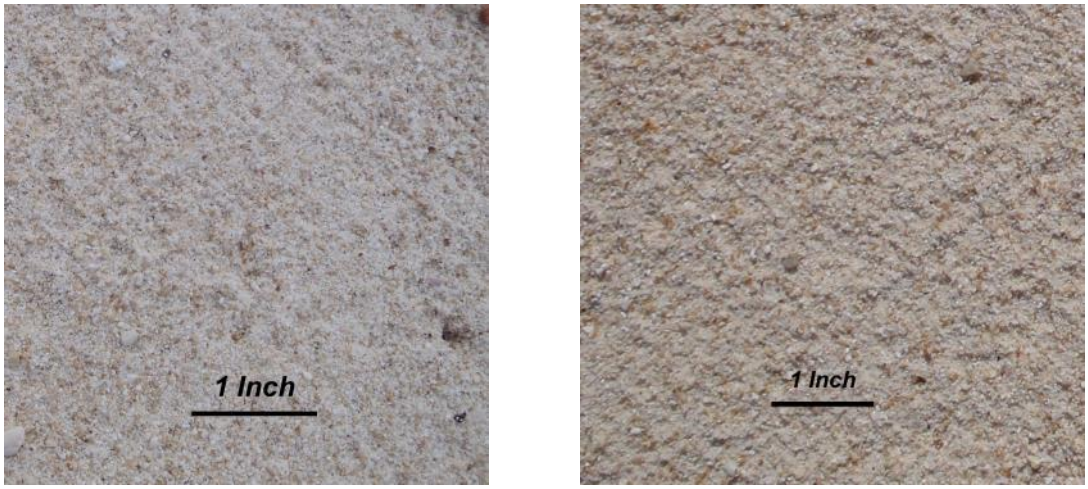

Figure 2-14 Sand color and texture at Unai Babui (left) and Unai Chulu (right)

2.3 HISTORIC SHORELINE DATA

Existing aerial and satellite imagery of northwest Tinian was reviewed for usable photographs of the beaches at Babui and Chulu. From existing repositories such as Google Earth, eight images were found, spanning a 10-year time frame from 2003 to 2013. The identified images were geo-rectified, inserted into a CAD-based map, and used to quantify beach change over time by digitizing the low water mark for each photograph. The subsequent collection of historic shorelines, plus the October 2014 survey yields information on past beach stability. The historical shoreline maps are presented in Figure 2-15 and Figure 2-16.

2.3.1 Unai Babui Aerial Photograph Analysis

Over the 11-year period since 2003, the beach at Babui averaged approximately 200 ft (60 m) in length, with numerous rock outcroppings visible throughout the beach in all photographs, indicating a limited volume of sand available to this littoral system, and a lesser degree of stability. Beach width has varied by 13 ft (4 m) at the north end and by 30 ft (9 m) at the south, as shown in Figure 2-15, signifying a significant amount of shoreline variation. The photographs indicate limited small pockets of sand in the rocky areas to the north and south of the beach, and it is likely that some sand transport occurs between these locations.

2.3.2 Unai Chulu Aerial Photograph Analysis

During the same period, Unai Chulu averaged 430 ft (130 m) in length, with the southern two-thirds consistently remaining continuous, while the northern third exhibited fluctuations with the beach retreating and exposing rocks and then advancing again to partially cover those rocky areas. The historic shorelines for Unai Chulu shown in Figure 2-16 indicate that the south end of the beach has varied in width by approximately 16 ft (5 m), while the north end has varied by 30 ft (9 m), indicating a wide degree of shoreline fluctuation.

This page intentionally left blank.

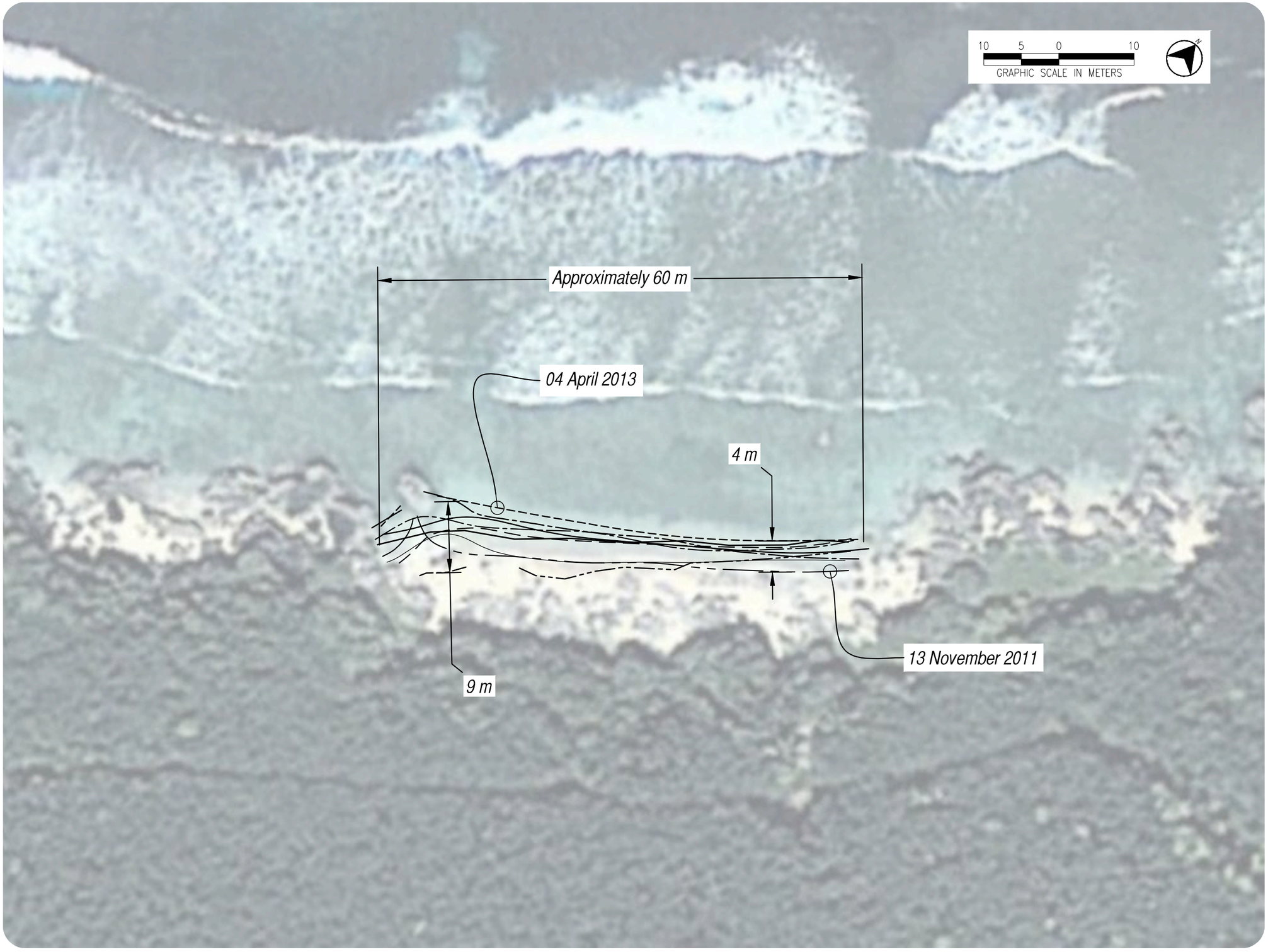

Sea Engineering, Inc.
MAKAI RESEARCH PIER
WAIMANALO, HI 96795
PH 808.259.7966
FAX 808.259.8143

NOTES:

Elevations in meters referenced to mean lower low water (MLLW).

Historic shorelines based on geo-referenced imagery from Google Earth.

Beach profiles and shoreline surveyed by SEI on 24 Oct 2014.

LEGEND:

Historic Shorelines

Date	Linetype
24 Oct 2014	————
26 Dec 2013	—·—·—
04 Apr 2013	- - - - -
26 Dec 2012	————
13 Nov 2011	— - - —
30 Sep 2009	- - - - -
29 Nov 2005	— - · —
22 Mar 2005	————
07 Jan 2003	—·—·—

Figure 2-15.
Unai Babui Historic Shorelines

Tinian AAV Landing Sites Investigation

Project: 25445	C-5
November 2014	
Scale 1 : 500	

This page intentionally left blank.

Sea Engineering, Inc.
MAKAI RESEARCH PIER
WAIMANALO, HI 96795
PH 808.259.7966
FAX 808.259.8143

NOTES:

Elevations in meters referenced to mean lower low water (MLLW).

Historic shorelines based on geo-referenced imagery from Google Earth.

Beach profiles and shoreline surveyed by SEI on 24 Oct 2014.

LEGEND:

Historic Shorelines

Date	Linetype
24 Oct 2014	———
26 Dec 2013	—·—·—
04 Apr 2013	----------
26 Dec 2012	———
13 Nov 2011	— - - —
30 Sep 2009	- - - - -
29 Nov 2005	— - · —
22 Mar 2005	———
07 Jan 2003	—·—·—

Figure 2-16.
Unai Chulu Historic Shorelines

Tinian AAV Landing Sites Investigation

Project: 25445
November 2014
Scale 1 : 500

C-6

This page intentionally left blank.

2.3.3 World War II Archival Photographs

A number of WORLD WAR II era photographs of the northwest Tinian coastline were found that show the proposed Amphibious Assault Vehicle (AAV) landing sites. The images, taken both before and after the amphibious invasions, show widely varying degrees of beach at the two sites. The photographs in Figure 2-17 and Figure 2-18 indicate a small, narrow beach with limited sand. The images in Figure 2-19 and Figure 2-20, taken during the invasion of Tinian (July 24, 1944, Jig-Day), show a minimal, to almost nonexistent beach at Unai Babui.

Figure 2-17 Unai Babui (White Beach 1) sometime during the Japanese administration of Tinian, prior to the July 1944 landing by the U.S. Marine Corps. (Farrell 2012)

Figure 2-18 Unai Babui leading up to the invasion, and before alteration by the landing effort. (Hoffman 1951)

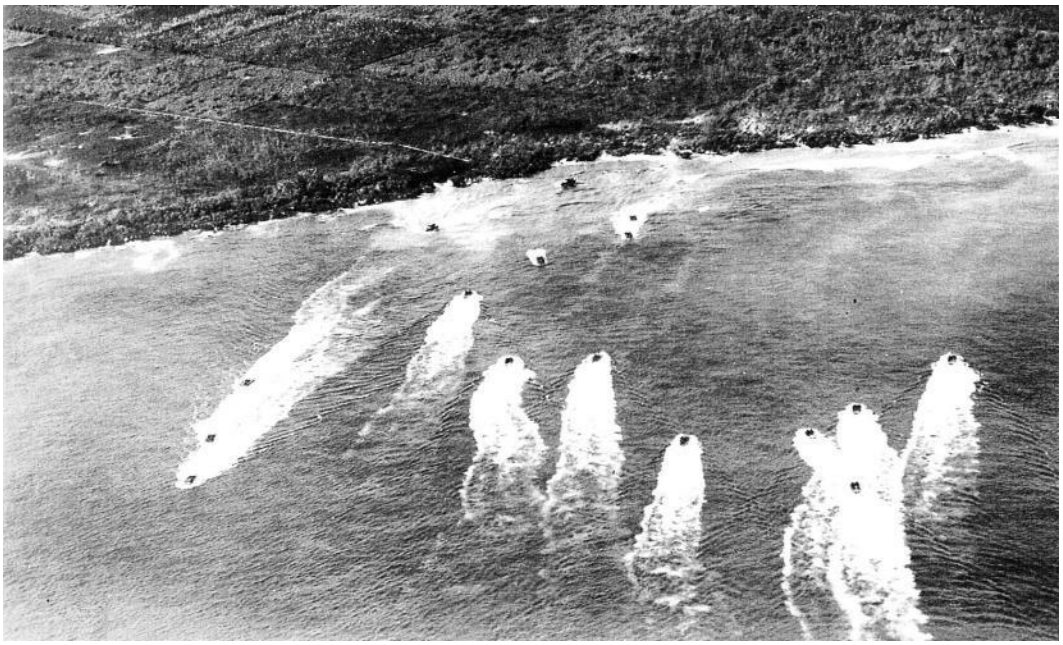

Figure 2-19 Unai Babui on Jig-Day, July 24, 1944. Initial landing by amphibious tractors (LVTs) of E Company, 2nd Battalion, 24th Marines. (Hoffman 1951)

Figure 2-20 Following the initial landing, some modifications were made to the shoreline at Unai Babui for access. Note the complete lack of a sandy beach in this image. (Hoffman 1951)

A pre-invasion photograph of Unai Chulu (White Beach 2) is shown in Figure 2-21, which reveals that the beach was, at times, nearly devoid of sandy material. The photograph shows a near continuous outcrop of rock at the shoreline. Figure 2-22 is a post-invasion picture of a temporary causeway constructed at Unai Chulu for the resupply effort. The picture illustrates wave action than occur at this location.

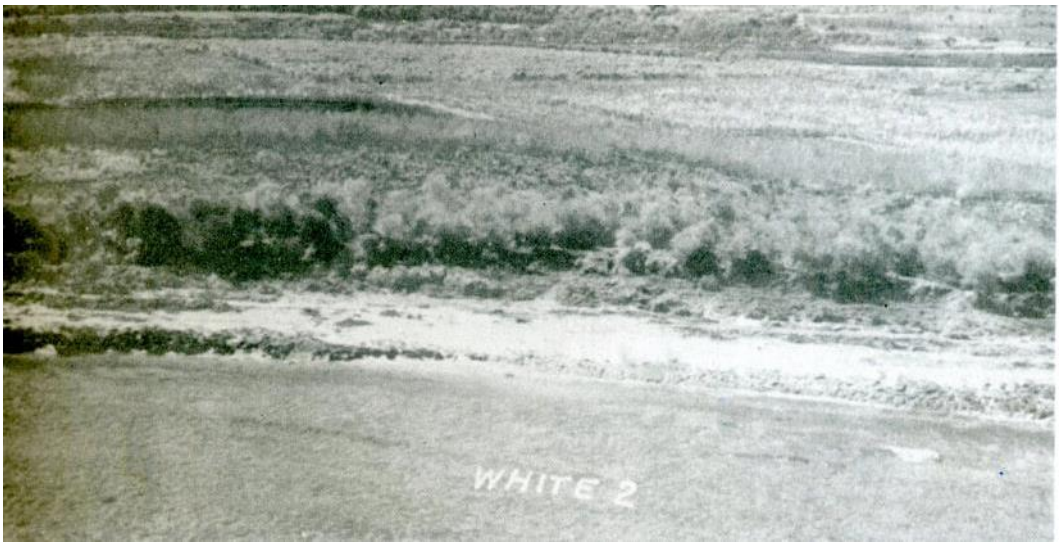

Figure 2-21 Unai Chulu (White Beach 2), prior to the July 1944 landing by the U.S. Marine Corps. (Hoffman 1951)

Figure 2-22 Resupply causeway, constructed by the US Navy's Seabees at Unai Chulu. (Hoffman 1951)

This page intentionally left blank.

CHAPTER 3
OCEANOGRAPHIC CONDITIONS

Existing wave and water level data were acquired and used to develop a basic oceanographic analysis of the NW Tinian shoreline vicinity. The following sections present the findings, organized by oceanographic topic.

3.1 NORTHERN MARIANAS REGIONAL WAVE CLIMATE

3.1.1 Wave Information Studies Data

Wave information is available in the form of hindcast data sets provided by the U.S. Army Corps of Engineers' WIS. WIS information generates records of wave conditions based on historical wind and wave conditions at numerous stations around the Marianas island chain. These hourly records of wave conditions are available for the 32-year period from 1980 through 2011.

3.1.2 Spectral Partitioning

Most available wave buoy data is reported as "parametric wave height", whereby the parameters of the most energetic (i.e., highest) peak are used to describe the entire wave field period and direction, and the wave height is calculated by summation of the energy density over the entire spectral surface. The parametric WIS data is available directly from the WIS website. What is called "spectral wave heights" in this study refers to partitioning the energy density spectrum to isolate distinct peaks in the spectral surface. These distinct peaks represent individual swells with their own characteristics. This process allows multiple waves to be reported for the same time period and better represents the sea state at sites like Unai Babui and Unai Chulu that are sheltered from the prevailing, energetic trade wind waves.

3.1.3 Deep Water Wave Climate

Hourly parametric and spectral deep water wave characteristics were determined for the 32-year period for WIS Station 81104, located 40 miles east of Tinian (Figure 3-1). This time series dataset was then filtered to include only waves from directions that could reasonably impact the landing sites - approximately 180° to 30°. Figure 3-2 is a rose diagram of deep water spectral wave height and direction, and Table 3-1 presents the accompanying data. Figure 3-3 and Table 3-2 are the spectral wave period rose diagram and data table, respectively. The percentages shown are the percent occurrence by time. With the spectral partitioning method it is possible to have multiple swell events every hour and therefore have a total percent greater than 100%. The diagrams show that waves predominantly have a significant wave height (Hs, or Hmo) less than 2 ft (0.6 m) and a peak period (Tp) less than 10 seconds. The most predominant wave directions are from 15°, 0° and 315°, occurring 48%, 47%, and 25% of the time, respectively.

Figure 3-4 is a rose diagram of deep water parametric wave height and direction, and Table 3-3 shows the accompanying data. Figure 3-5 and Table 3-4 are the parametric wave period rose diagram and data, respectively. Two differences are evident when comparing the spectral results with the parametric. First, the parametric results show waves that would reach the project site only occur 30.7% of the time whereas the spectral results show waves over 100% of the time. This is because on most days, the peak wave energy comes from prevailing easterly trade wind waves which are not within the 180° to 30° exposure window of the project site.

Second, the parametric results do not show any waves less than 2 ft (0.6 m). The reason for this is that the parametric results only show the dominant swell direction and combine all wave energy to a single peak. The typical wave climate in the area is dominated by easterly trade wind waves which usually masks smaller swell events. The dominant trade wind waves are not filtered out in this analysis, with wave events occurring from 180° to 30°. The spectral results therefore provide a better definition of the sea state affecting the site, while the parametric results help illustrate the major wave events impacting the vicinity of Tinian.

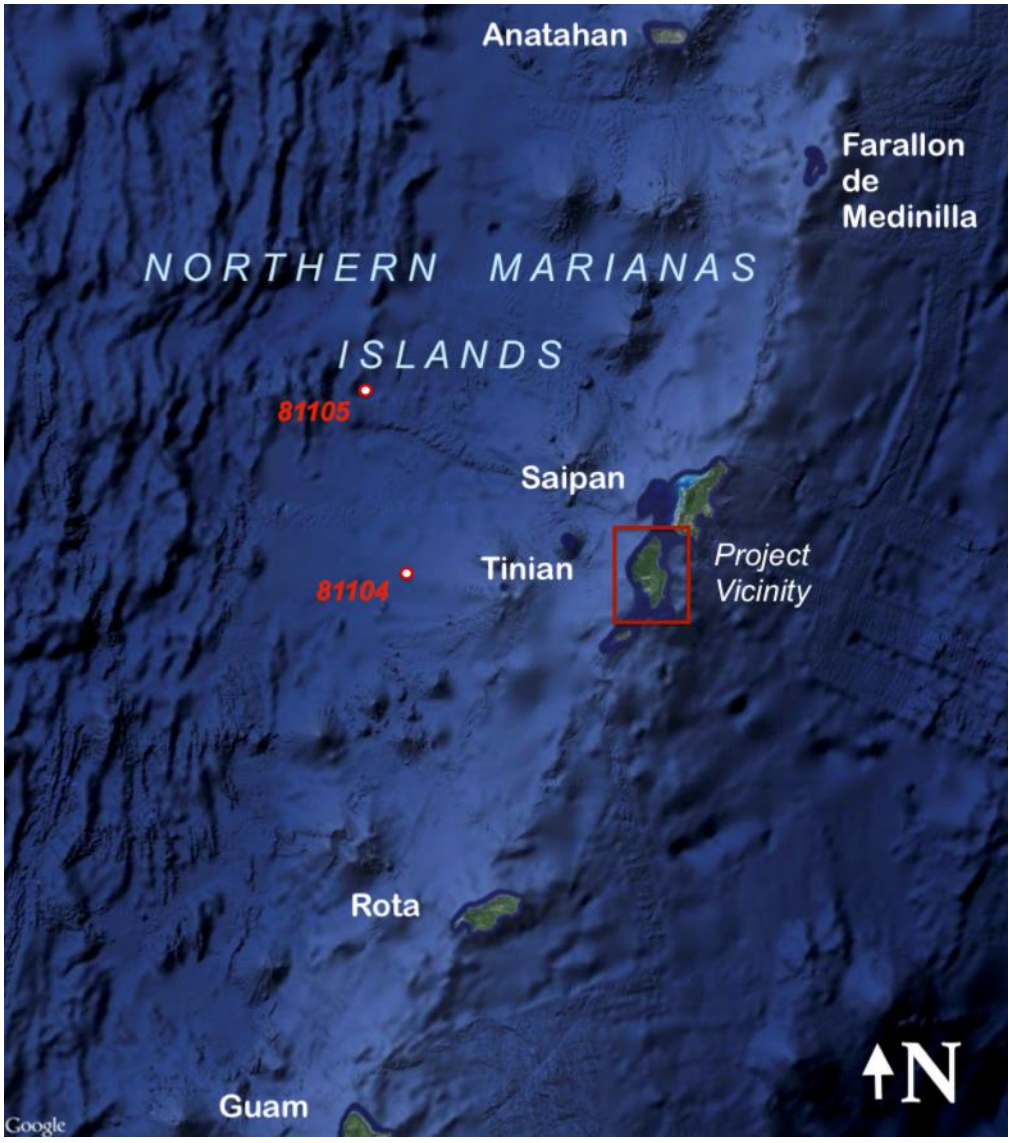

Figure 3-1 WIS station locations

Source: background image from Google Earth

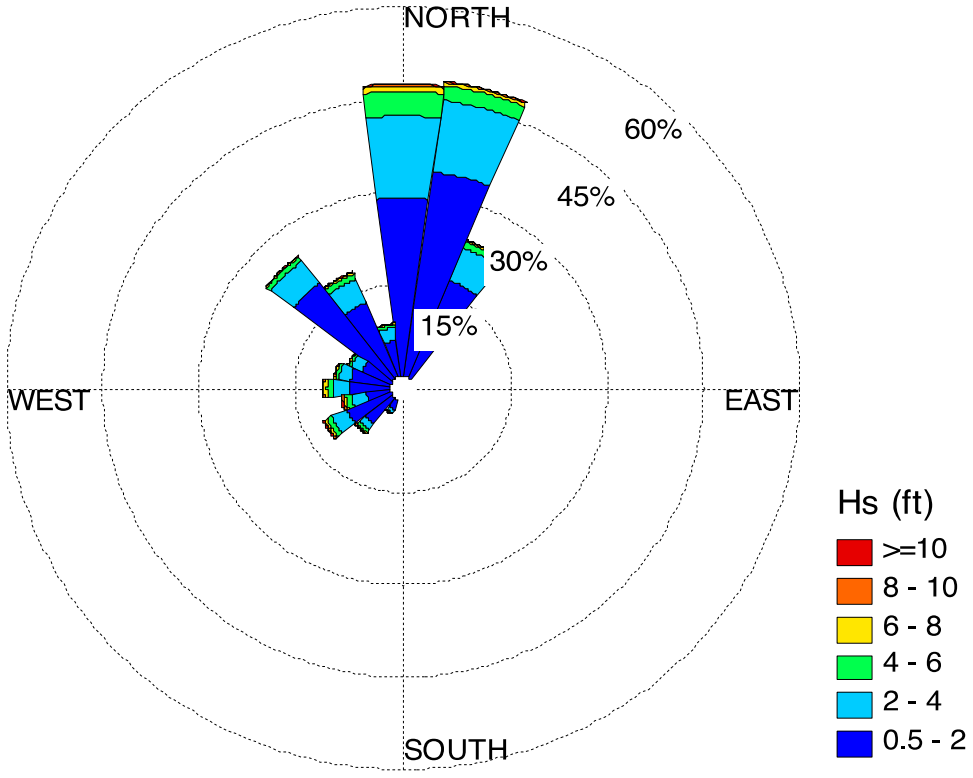

Figure 3-2 Spectral wave height rose plot for NW Tinian

Table 3-1. Frequency of occurrence for spectral wave heights, NW Tinian

Hmo (ft)	0	15	30	210	225	240	255	270	285	300	315	330	345	Total
0.5-1.0	13.41	16.49	7.67	0.86	3.18	3.67	1.49	3.01	3.23	2.56	10.68	6.99	2.92	76.15
1-2	15.56	17.06	9.32	0.84	2.16	3.76	2.28	3.24	3.09	2.48	8.89	6.08	2.94	77.70
2-3	8.59	8.19	4.15	0.40	0.84	1.79	1.50	1.85	1.31	1.38	3.18	2.83	1.43	37.42
3-4	4.75	3.51	1.58	0.18	0.43	0.83	0.95	0.98	0.52	0.50	1.33	1.31	0.69	17.56
4-6	4.02	2.36	0.99	0.13	0.50	0.87	0.88	0.88	0.50	0.38	0.78	0.94	0.54	13.76
6-8	0.91	0.57	0.28	0.07	0.23	0.36	0.39	0.46	0.21	0.14	0.16	0.27	0.13	4.18
8-10	0.24	0.13	0.09	0.04	0.11	0.15	0.17	0.18	0.07	0.02	0.04	0.07	0.04	1.34
10-12	0.10	0.03	0.02	0.02	0.04	0.07	0.14	0.07	0.03	0.00	0.01	0.01	0.01	0.56
12-14	0.01	0.00	0.00	0.01	0.02	0.04	0.06	0.03	0.01	0.00	0.00	0.01	0.00	0.20
14-16	0.00	0.00	0.00	0.01	0.01	0.02	0.03	0.03	0.01	0.00	0.00	0.00	0.00	0.11
16-20	0.00	0.00	0.00	0.00	0.00	0.00	0.00	0.03	0.00	0.00	0.00	0.00	0.00	0.05
20+	0.00	0.00	0.00	0.00	0.00	0.00	0.00	0.00	0.00	0.00	0.00	0.00	0.00	0.00
Total	47.60	48.34	24.10	2.55	7.54	11.56	7.90	10.74	8.97	7.48	25.07	18.51	8.70	229.05
	0	15	30	210	225	240	255	270	285	300	315	330	345	Overall
Mean	2.07	1.76	1.76	2.08	1.97	2.16	2.88	2.40	1.86	1.81	1.51	1.75	1.86	1.90
StDev	1.56	1.30	1.29	2.11	2.05	2.05	2.49	2.25	1.68	1.36	1.12	1.39	1.46	1.59
Min	0.50	0.50	0.50	0.50	0.50	0.50	0.50	0.50	0.50	0.50	0.50	0.50	0.50	0.50
Max	19.15	16.09	19.92	17.31	25.77	26.48	18.56	20.63	18.84	12.38	16.54	18.92	19.09	26.48

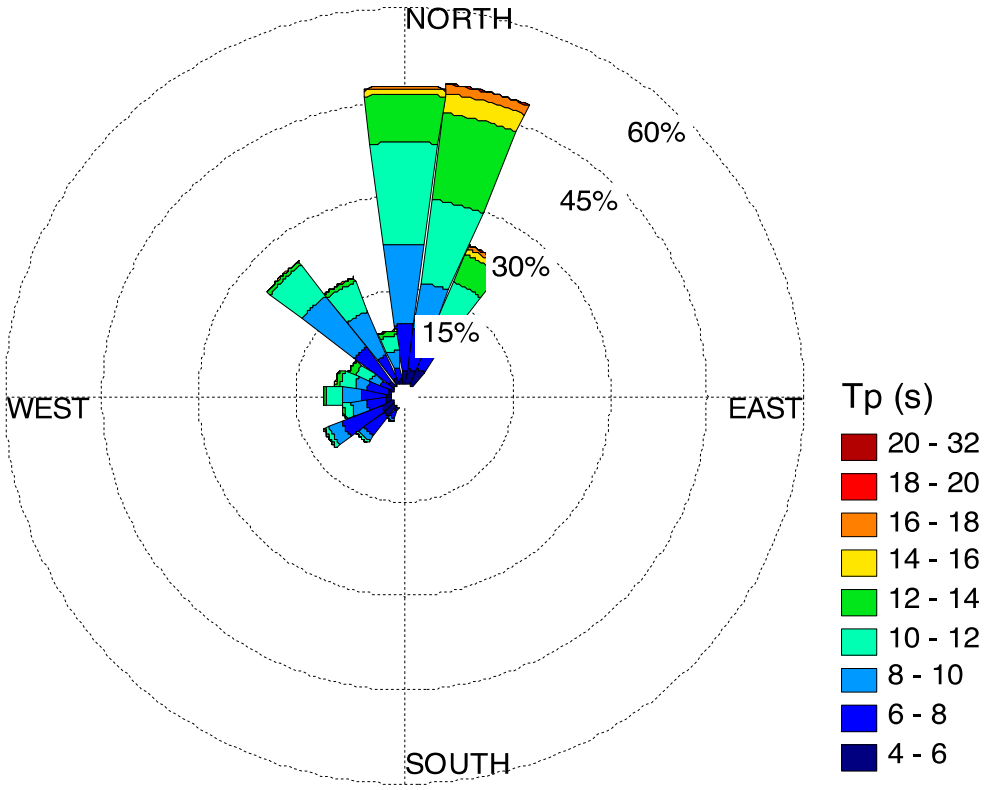

Figure 3-3 Spectral wave period rose plot for NW Tinian

Table 3-2. Frequency of occurrence for spectral wave periods, NW Tinian

Tp (s)	0	15	30	210	225	240	255	270	285	300	315	330	345	Total
4-6	2.16	2.34	2.76	0.71	2.18	1.78	0.84	0.80	0.69	0.48	1.09	0.92	0.67	17.40
6-8	7.27	6.29	3.93	1.24	3.95	6.81	3.12	3.78	3.18	1.63	6.71	4.20	1.94	54.04
8-10	12.80	7.60	4.74	0.45	0.96	2.14	2.36	3.17	1.96	1.72	10.34	7.60	2.72	58.54
10-12	16.41	13.39	6.29	0.14	0.37	0.68	1.31	2.31	2.29	2.45	6.33	5.00	2.50	59.47
12-14	7.65	14.03	4.77	0.01	0.06	0.14	0.26	0.66	0.73	1.12	0.59	0.76	0.78	31.57
14-16	0.91	3.09	0.94	0.00	0.01	0.01	0.01	0.03	0.09	0.06	0.02	0.03	0.06	5.26
16-18	0.39	1.50	0.59	0.00	0.00	0.00	0.00	0.00	0.03	0.02	0.00	0.00	0.04	2.59
18-20	0.01	0.08	0.06	0.00	0.00	0.00	0.00	0.00	0.00	0.00	0.00	0.00	0.00	0.16
20+	0.00	0.01	0.01	0.00	0.00	0.00	0.00	0.00	0.00	0.00	0.00	0.00	0.00	0.03
Total	47.60	48.34	24.10	2.55	7.54	11.56	7.90	10.74	8.97	7.48	25.07	18.51	8.70	229.05
	0	15	30	210	225	240	255	270	285	300	315	330	345	Overall
Mean	9.71	10.62	9.72	6.94	6.77	7.23	8.05	8.46	8.64	9.33	8.62	8.76	8.97	9.26
StDev	2.19	2.73	2.89	1.52	1.54	1.47	1.80	1.90	2.21	2.23	1.57	1.65	2.10	2.46
Min	4.26	4.26	4.26	4.26	4.26	4.26	4.26	4.26	4.26	4.26	4.26	4.26	4.26	4.26
Max	19.53	21.46	23.64	14.66	16.13	14.66	16.13	16.13	17.73	17.73	17.73	16.13	17.73	23.64

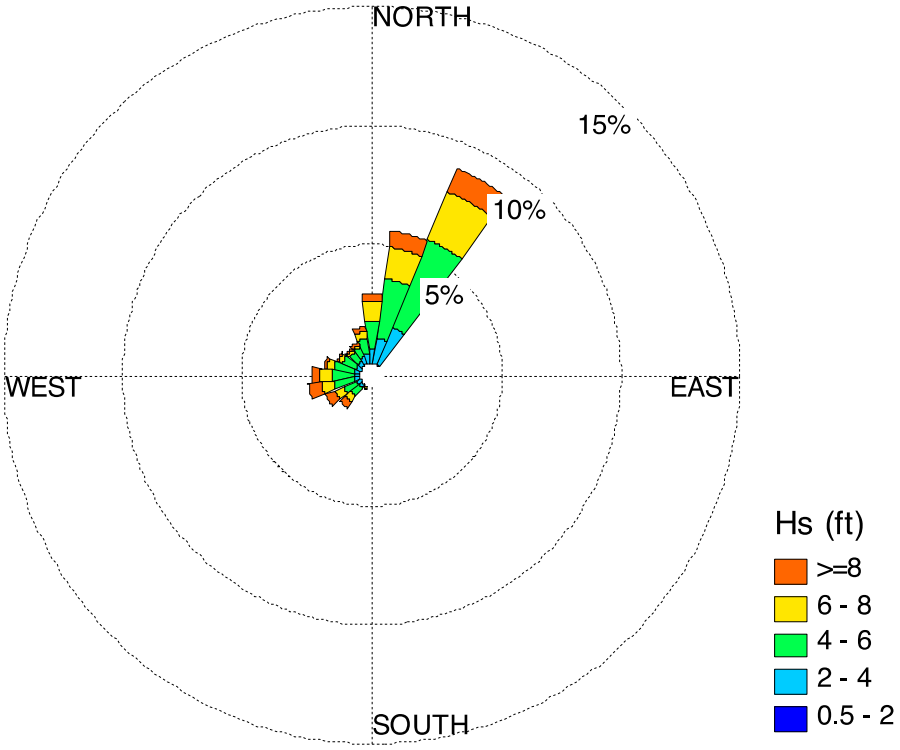

Figure 3-4 Parametric wave height rose plot for NW Tinian

Table 3-3. Frequency of occurrence for parametric wave heights, NW Tinian

Hmo (ft)	0	15	30	210	225	240	255	270	285	300	315	330	345	Total
0.5-1.0	0.00	0.00	0.00	0.00	0.00	0.00	0.00	0.00	0.00	0.00	0.00	0.00	0.00	0.00
1-2	0.00	0.00	0.00	0.00	0.00	0.00	0.00	0.00	0.00	0.00	0.00	0.00	0.00	0.00
2-3	0.11	0.23	0.42	0.00	0.02	0.03	0.02	0.02	0.03	0.01	0.03	0.06	0.11	1.10
3-4	0.47	0.83	1.28	0.01	0.14	0.17	0.24	0.21	0.21	0.21	0.21	0.30	0.34	4.63
4-6	1.22	2.53	3.97	0.05	0.47	0.58	0.88	0.94	0.87	0.61	0.48	0.41	0.61	13.61
6-8	0.79	1.35	2.19	0.02	0.27	0.40	0.51	0.49	0.30	0.18	0.10	0.10	0.31	7.03
8-10	0.27	0.54	0.77	0.02	0.16	0.20	0.25	0.17	0.09	0.04	0.03	0.06	0.14	2.76
10-12	0.06	0.09	0.21	0.01	0.08	0.09	0.15	0.07	0.02	0.02	0.02	0.04	0.05	0.88
12-14	0.01	0.04	0.05	0.00	0.04	0.07	0.08	0.04	0.02	0.00	0.01	0.01	0.01	0.38
14-16	0.00	0.01	0.01	0.00	0.04	0.04	0.03	0.04	0.00	0.00	0.00	0.01	0.00	0.18
16-20	0.01	0.00	0.00	0.00	0.01	0.02	0.03	0.01	0.00	0.00	0.00	0.00	0.01	0.10
20+	0.00	0.00	0.00	0.00	0.00	0.01	0.01	0.00	0.00	0.00	0.00	0.00	0.00	0.03
Total	2.95	5.62	8.90	0.12	1.24	1.61	2.20	2.00	1.54	1.08	0.88	0.99	1.57	30.70

	0	15	30	210	225	240	255	270	285	300	315	330	345	Overall
Mean	5.72	5.65	5.64	6.64	6.82	6.91	6.68	6.26	5.46	5.24	5.15	5.20	5.49	5.82
StDev	2.06	1.96	1.96	2.56	3.05	3.20	2.97	2.59	1.79	1.73	2.03	2.50	2.24	2.30
Min	2.00	2.00	1.77	2.33	2.26	2.26	2.56	2.26	2.59	2.43	2.36	2.26	2.30	1.77
Max	22.24	22.66	23.03	15.61	21.65	26.34	25.81	21.19	18.43	19.09	20.76	23.03	23.58	26.34

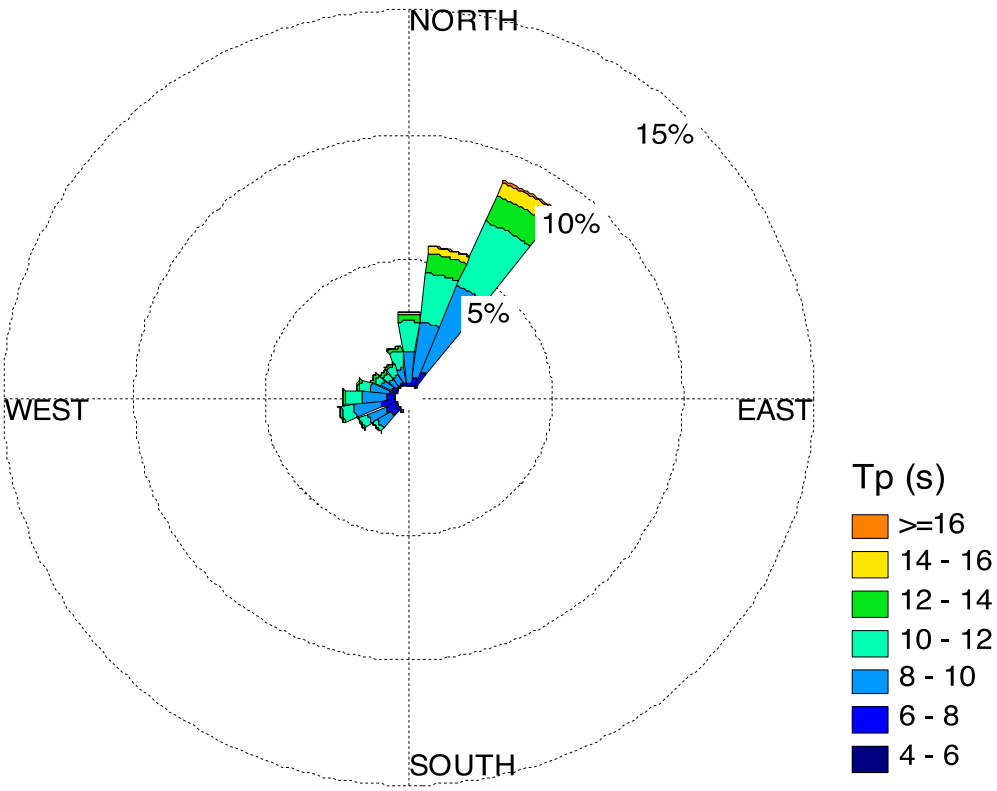

Figure 3-5 Parametric wave period rose plot for NW Tinian

Table 3-4. Frequency of occurrence for parametric wave periods, NW Tinian

Tp (s)	0	15	30	210	225	240	255	270	285	300	315	330	345	Total
4-6	0.01	0.02	0.04	0.01	0.04	0.04	0.07	0.02	0.03	0.02	0.00	0.00	0.01	0.30
6-8	0.11	0.28	0.60	0.03	0.35	0.41	0.51	0.30	0.26	0.16	0.09	0.12	0.11	3.34
8-10	1.19	2.26	3.70	0.06	0.63	0.77	1.05	1.00	0.72	0.47	0.36	0.38	0.59	13.18
10-12	1.25	1.98	2.80	0.02	0.18	0.35	0.47	0.59	0.42	0.27	0.33	0.40	0.71	9.77
12-14	0.25	0.78	1.11	0.00	0.03	0.04	0.09	0.07	0.08	0.13	0.09	0.09	0.13	2.89
14-16	0.13	0.29	0.57	0.00	0.00	0.00	0.00	0.02	0.03	0.02	0.00	0.00	0.02	1.10
16-18	0.01	0.02	0.07	0.00	0.00	0.00	0.00	0.00	0.00	0.00	0.00	0.00	0.00	0.11
18-20	0.00	0.00	0.01	0.00	0.00	0.00	0.00	0.00	0.00	0.00	0.00	0.00	0.00	0.01
20+	0.00	0.00	0.00	0.00	0.00	0.00	0.00	0.00	0.00	0.00	0.00	0.00	0.00	0.00
Total	2.95	5.62	8.90	0.12	1.24	1.61	2.20	2.00	1.54	1.08	0.88	0.99	1.57	30.70
	0	15	30	210	225	240	255	270	285	300	315	330	345	Overall
Mean	10.39	10.49	10.44	8.70	8.72	8.88	9.00	9.46	9.52	9.74	9.98	9.92	10.19	10.01
StDev	1.66	1.85	2.05	1.65	1.52	1.60	1.66	1.55	1.75	1.86	1.65	1.63	1.54	1.90
Min	5.14	4.73	4.65	4.57	4.27	4.61	4.59	4.60	4.65	4.66	4.31	5.17	5.34	4.27
Max	16.54	18.52	20.56	13.60	15.18	15.47	15.34	15.36	15.92	15.76	14.75	14.92	17.11	20.56

3.1.4 Extreme Event Analysis

The hourly records of calculated wave heights were used as the basis for developing return period wave height information using the Gumbel extreme event distribution. The return period, or recurrence interval value is a useful tool for engineering design, as it forms a statistical basis for establishing a level of design criteria.

The Gumbel distribution was applied to the annual maximum wave heights in order to determine return period wave heights. The top annual events are plotted with their calculated return periods in Figure 3-6 and Table 3-5. While the Gumbel distribution is able to generate information on return period wave heights, it cannot predict wave period or direction. The top 10 events on record, listed in the lower half of Figure 3-6, exhibit a relatively constant period but wide range of direction for the top events, suggesting that large wave episodes are generated by passing typhoons known to commonly affect the area – and which can approach from any direction. The U.S. Navy's Joint Typhoon Warning Center best track archive indicates that 32 typhoons and 22 severe tropical storms passed within 60 miles of Tinian between 1950 and 2011. In the figure, Hs and Tp refer to significant wave height and peak period, respectively.

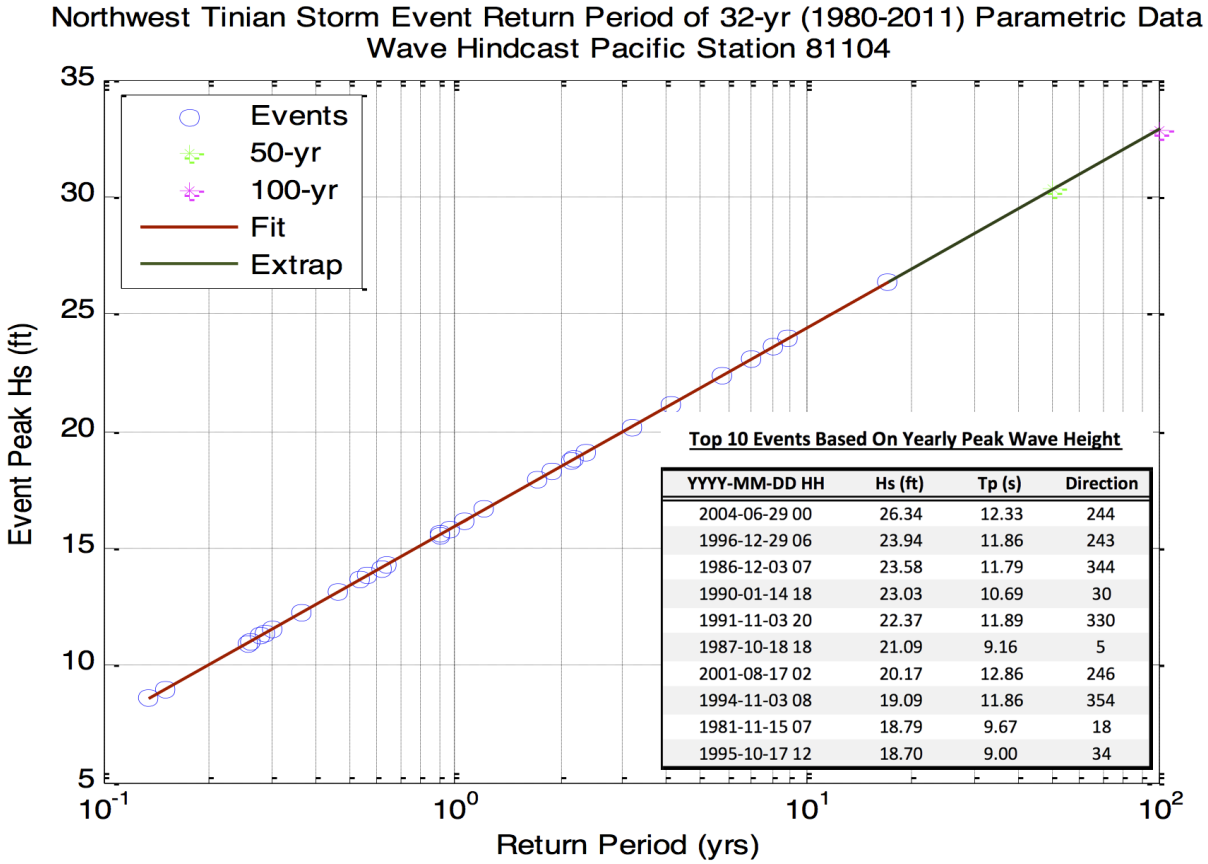

Top 10 Events Based On Yearly Peak Wave Height

YYYY-MM-DD HH	Hs (ft)	Tp (s)	Direction
2004-06-29 00	26.34	12.33	244
1996-12-29 06	23.94	11.86	243
1986-12-03 07	23.58	11.79	344
1990-01-14 18	23.03	10.69	30
1991-11-03 20	22.37	11.89	330
1987-10-18 18	21.09	9.16	5
2001-08-17 02	20.17	12.86	246
1994-11-03 08	19.09	11.86	354
1981-11-15 07	18.79	9.67	18
1995-10-17 12	18.70	9.00	34

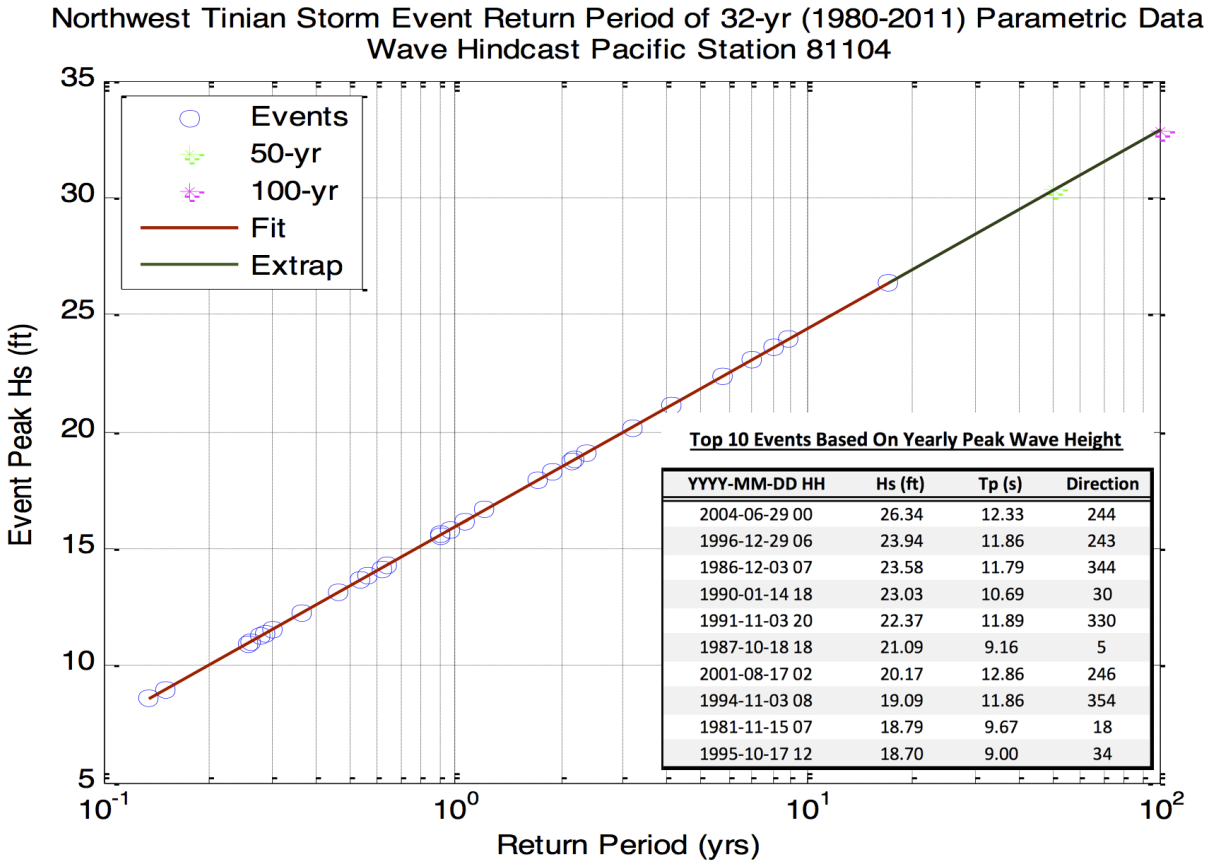

Figure 3-6 Deep water return period wave heights for WIS Station 81104, from U.S. Army Corps of Engineers WIS data

Table 3-5. Return period (recurrence interval) wave heights for WIS Station 81104

Wave Height by Recurrence Interval			Recurrence Interval by Wave Height		
Recurrence (yrs)	Height (m)	Height (ft)	Height (m)	Height (ft)	Recurrence (yrs)
1	5.1	17	4.3	14	0.6
2	6.3	21	4.9	16	0.9
5	7.8	26	5.5	18	1.2
7	8.4	28	6.1	20	1.8
10	9.0	30	6.7	22	2.5
15	9.7	32	7.3	24	3.6
20	10.2	33	7.9	26	5.2
25	10.6	35	8.5	28	7.5
30	10.9	36	9.1	30	10.7
40	11.4	37	9.8	32	15.4
50	11.8	39	10.4	34	22.0
75	12.4	41	11.0	36	31.6
100	12.9	42	11.6	38	45.3
200	14.1	46	12.2	40	64.9
500	15.7	51	12.8	42	93.0
1000	16.8	55	13.4	44	133.2
			14.0	46	190.9
			14.6	48	273.6
			15.2	50	392.0

3.1.5 Deep Water Wave Transformation

Investigating the behavior of waves as they propagate into shallow nearshore waters is critical for an understanding of coastal processes. As deep water waves propagate toward shore they begin to encounter, and be transformed by, the seafloor bathymetry. The 3rd generation spectral wave model SWAN (Simulating WAves Nearshore) developed by Delft Institute of Hydraulics in the Netherlands was used to model the transformation of deep water waves from WIS station 81104 into the shallower waters of coastal NW Tinian. A primary goal of the SWAN modeling is to provide initial conditions to drive high resolution nearshore hydrodynamic wave and circulation models. To accurately and efficiently transform the waves from deep water to the project site a two-grid nested setup was used. A coarse grid of 590 ft (180 m) cell size was used in deep water for ocean-basin scale effects. In shallower water, a finer grid of 200 ft (60 m) cell size was used. An example of the nested grid setup is presented in **Figure** 3-7. The SWAN model calculated wave parameters at a depth of 262 ft (80 m), the results of which were then used to force the nearshore wave modeling presented in CHAPTER 4.

Four wave cases, listed in Table 3-6, were selected for analysis from the deep water WIS station into the northwest Tinian shoreline vicinity. The *high prevailing* case is the most common, or dominant, wave condition in the parametric wave data — 6 ft (1.8 m) occurring 13.6% of the time (see Table 3-3). The high prevailing wave condition was modeled from two directions, 30° and 270°, the two most frequent

directions for waves of this height (see Table 3-3). The 270° direction has the more direct approach to the landing sites, whereas the 30° direction is considered very oblique, and preliminary hydrodynamic model runs suggested that this scenario condition is quickly attenuated before impacting the shoreline. The 270° direction was therefore seen as a representative approach direction for the most common conditions at the site. The 1-year and 50-year return period waves from the Gumbel extreme event analysis were also transformed to the NW Tinian offshore vicinity for use in the landing ramp structural design effort, and are presented here for reference. The transformed nearshore location is in a depth of 640 ft (194 m), directly offshore of the landing sites

Table 3-6. Deep water and transformed wave parameters calculated using SWAN for 4 scenarios

Case	Deep Water Wave			Transformed Nearshore Wave			
	Height	Period	Direction	Depth	Height	Period	Direction
	(m)	(s)	(deg.)	(m)	(m)	(s)	(deg.)
1 Year Wave	4.9	9	315	194	4.9	9.0	311
High Prevailing (North)	1.8	10	30	194	1.4	10.1	26
High Prevailing (West)	1.8	10	270	194	1.8	10.1	266
50 Year Wave	9.1	15	315	194	8.9	14.3	311

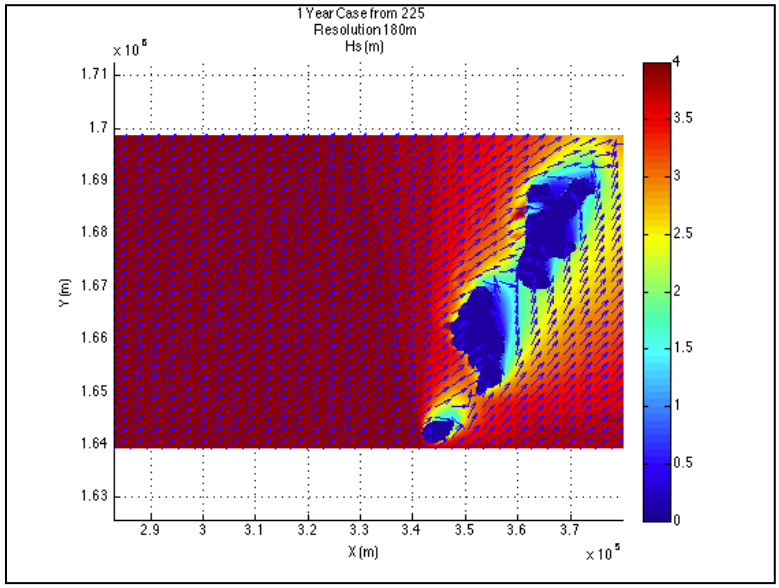

Figure 3-7 Example SWAN results for the 1-year wave case

3.2 TIDES

3.2.1 Astronomical Tide

Tides in the Marianas are a combination of diurnal and semi-diurnal regimes, which is referred to as a mixed semi-diurnal tide. Water level data was recorded continuously at Tanapag Harbor, (in the Port of Saipan, CNMI) by a tide station located on Delta Dock operated by National Oceanic and Atmospheric Administration's (NOAA) Center for Operational Oceanographic Products and Services, between the dates of August 24, 2000 and March 19, 2001. This is the closest tide station to the project location with recorded data.

The diurnal range for Tanapag has been calculated to be 2.2 ft (0.67 m), which is a measure of the vertical distance between mean lower low water (MLLW) and mean higher high water (MHHW). As measured from mean sea level (MSL), MLLW is -1.2 ft (-0.37 m), and MHHW is +0.9 ft (+0.27 m), based on the latest Epoch of 1983-2001. A diagram of commonly used local tidal datums and their reference elevations for the Saipan tide station is illustrated in Figure 3-8. The current published diurnal range for Tinian Island, based on Guam's tide station, is 1.8 ft (0.55 m).

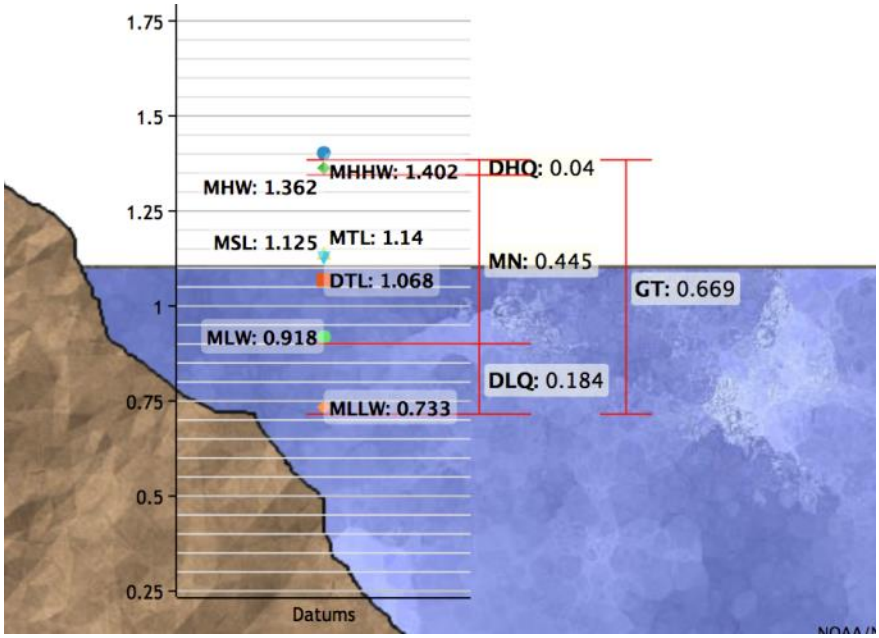

Figure 3-8 Local tidal datums calculated for the Tanapag Harbor tide station, Saipan

Source: NOAA 2001

3.2.2 Tidal Currents

In a 2007 study completed for the U.S. Army Corps of Engineers and the CNMI of potential environmental impacts to the nearby coastal waters from a proposed new sewage outfall located north of Puntan Atgidon on Tinian's western shoreline, a series of oceanographic deployments collected continuous current data over a period of 1 year. Acoustic Doppler current profilers were used to collect vertical current profiles from a deployment depth of approximately 80 ft (24 m) at 1-hour intervals. Analysis of the data showed that surface currents were typically 0.5 ft/s (0.15 m/s) in the summer and 0.3 ft/s (0.09 m/s) in the winter. Currents exceeded 1.6 ft/s (0.5 m/s) 5% of the time during the summer months, and 2 to 3% in the winter months. Current directions were shore-parallel, reciprocating north to south in response to tidal phase. In general, current velocity was shown to attenuate gradually with depth.

The 2007 deployment location was approximately 4 miles (6.4 kilometers) to the southwest of the AAV landings project site along the west shoreline, and possesses a similar exposure and bottom type. Currents at the Atgidon location are therefore likely representative for the Unai Babui and Unai Chulu landing sites.

3.3 SEA LEVEL RISE

Due to the heat-trapping effects of greenhouse gases, climate scientists project that if greenhouse gases emissions continue to accelerate at current output trends, the average global temperature will likely increase by 3 to 7 degrees Fahrenheit (1.7 to 3.9 degrees Celsius) by the year 2100 (Climate Change 2007). These figures were derived from a number of global climate models, which were based on various scenarios of changes in the concentrations of greenhouse gases in the Earth's atmosphere. As the Earth's atmosphere warms, so do the oceans, and as seawater warms up it expands, increasing the total volume of the oceans and producing *thermosteric* sea level rise. Global average thermal expansion can be calculated directly from simulated changes in ocean temperature. Other major components to sea level rise which have been identified by scientists are: glacier and ice cap melting; Greenland Ice Sheet; Antarctic Ice Sheet; Land Ice Sum; and, Scaled-up Ice Sheet Discharge. All components are additive and are directly related to global warming. Latest study results from the Intergovernmental Panel on Climate Change given in their 2007 report on sea levels titled, *Fourth Assessment Report,* or AR4, predicts a range of sea level rise of 0.6 to 2.0 ft (0.2 to 0.6 m) by the year 2100.

According to U.S. Army Corps of Engineers Circular No. 1165-2-212, which currently applies to all U.S. Army Corps of Engineers Civil Works responsibilities, potential relative sea level change must be considered in every U.S. Army Corps of Engineers coastal activity as far inland as the extent of estimated tidal influence. All planning, engineering, designing, operating, and maintaining for sea level change must consider how sensitive and adaptable: (1) natural and managed ecosystems; and (2) human and engineered systems are to climate change and other related global changes. Guidance provided in EC 1165-2-212 gives the planner or engineer specific instructions to account for changes in MSL for U.S. Army Corps of Engineers civil works projects in order to satisfy Federal requirements.

Specifically, for the island of Tinian, U.S. Army Corps of Engineers methods estimate future for the year 2070 to be 0.27 ft (0.08 m), using their projection for an intermediate rate of rise. A plot of sea level rise calculated for Tinian is provided in Figure 3-9. The small rate of sea level rise compared to many other parts of the world is in part attributed to the local sea floor rising (along with the rest of the Mariana Islands) as the Pacific plate is subducted under the Philippine plate, partially offsetting the rise in sea level.

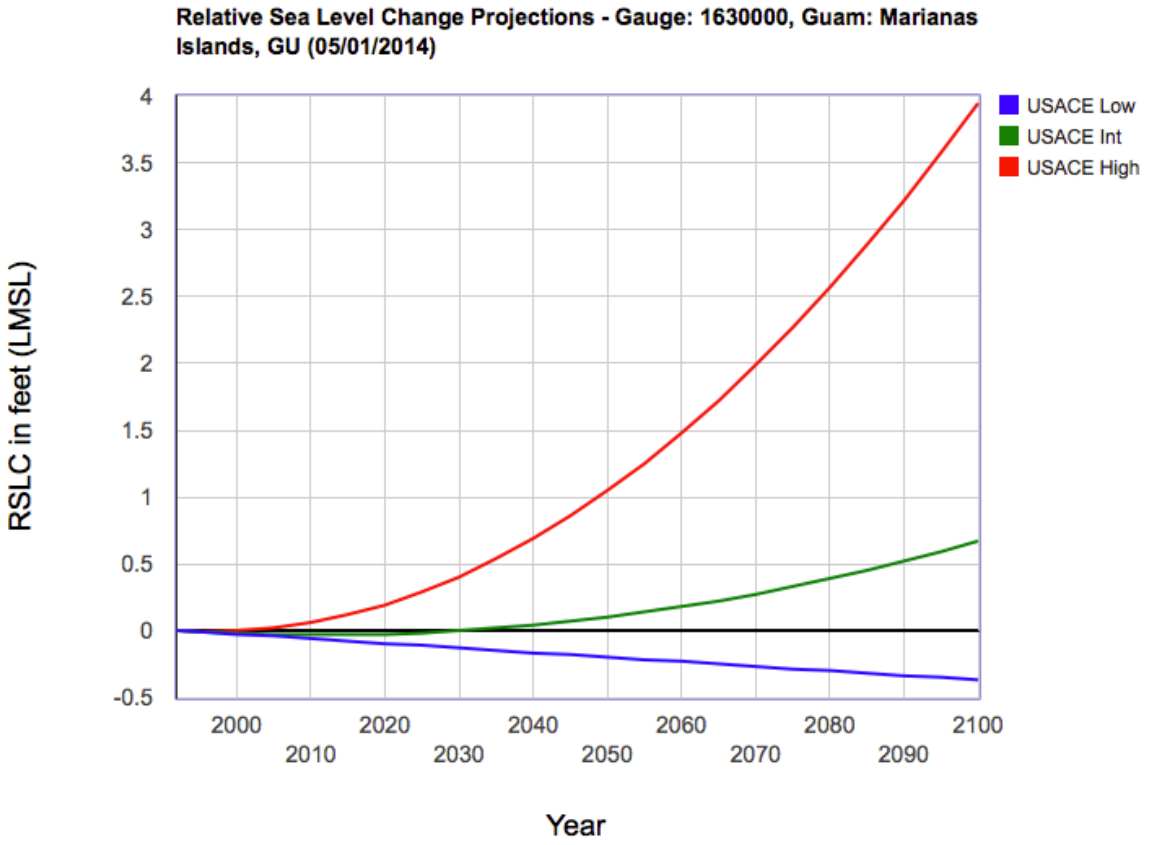

Figure 3-9 Sea level rise, as calculated by U.S. Army Corps of Engineers methods

Source: http://www.corpsclimate.us/ccaceslcurves.cfm

This page intentionally left blank.

CHAPTER 4
NEARSHORE WAVE MODELING

The numerical model SWAN was utilized to transform wave heights from the deep water WIS virtual buoy location to the nearshore vicinity of the harbor, as discussed in Section 3.1.5. Wave transformation results from SWAN were then used as the input for a higher resolution hydrodynamic model of currents and waves in the vicinity of the landing sites. Nearshore wave heights and wave generated currents were analyzed computationally using the coupled Coastal Modeling System (CMS)-Wave and CMS-Flow models.

The hydrodynamic circulation model CMS-Flow is a component of the Coastal Modeling System developed by the U.S. Army Corps of Engineers Coastal and Hydraulics Laboratory. CMS-Flow is a two-dimensional, finite-difference numerical approximation of the depth-integrated continuity and momentum equations. The model simulates currents, water level, sediment transport, and morphology in the dynamic coastal zone. CMS-Wave, also a component of the Coastal Modeling System, is a two-dimensional wave spectral transformation model that employs a 'forward-marching', finite-difference method to solve the wave action conservation equation. It is a phase-averaged model, which neglects changes in the wave phase in calculating wave and other near shore processes. CMS-Wave utilizes theoretically developed approximations for both wave diffraction and reflection and is, therefore, suitable for conducting wave simulations over complex morphology such as the variegated reefs of Tinian's northwest shoreline.

Wave conditions affect currents, and the currents they produce may then affect the waves themselves; therefore, the strength of the CMS models for this project is their capability for inline steering (coupling) of results from one model to the other. This interaction means that for every time step (or iteration) in the simulation, the wave model will pass calculated wave height and other parameters to the flow model for its calculations, which in turn will pass back wave-induced current data to the wave model, enabling a direct solution for a seemingly difficult iterative process.

In addition to the CMS-Wave and circulation models, further analysis was completed utilizing the phase-resolving Boussinesq (BOUSS-2D) model, also developed by the U.S. Army Corps of Engineers Coastal and Hydraulics Laboratory. BOUSS-2D employs shallow water assumptions in solving the BOUSS-2D type governing equations, and can simulate most wave-related phenomena of interest occurring in the nearshore zone. Graphical results of the model effectively simulate the actual appearance of the sea surface, clearly illustrating the refractive and diffractive behavior of shoaling waves, which subsequently allows assessment of sand transport and shoreline processes.

Four physical model configurations were developed for the numerical modeling process, including the existing condition at each of the landing sites, and a modified condition representing the dredged ramp configuration at each site. Complete results of the wave and circulation modeling are presented in Section 4.4.

4.1 MODEL FORCING

Wave conditions selected to force the nearshore model cases were chosen based on data gathered from the WIS virtual buoy at Station Number 81104 (refer to Section 3, Wave Climate). Table 4-1 below summarizes the wave conditions considered for this study, along with a designation for each wave condition which is referred to in the modeling results discussion. The table presents the transformed deep water wave conditions from the WIS station into the transitional depth of the offshore boundary of the wave/circulation model at approximately 640 ft (194 m) depth. The 1-year and 50-year wave conditions are presented here for reference, and were calculated for use in the *engineering study*, a separate but related effort that includes a force analysis and structural design of landing ramp alternatives at the proposed landing sites.

This *coastal processes assessment* aims to identify and quantify as much as possible, the existing nearshore oceanographic and shoreline conditions on an average day, and investigate how these conditions may be altered by the proposed landing ramp alternatives at the Unai Babui and Unai Chulu sites. Because they are more commonly occurring conditions that are of interest in this analysis, the 1-year and the high prevailing conditions were selected to drive the nearshore modeling. Furthermore, it was determined early on in the initial modeling effort that the northern high prevailing condition was largely attenuated by refractive and diffractive processes at the project location so it was dropped from continued analysis, leaving only the high prevailing condition from the west.

The water level used for all model runs was MHHW. Tidal currents were assumed to be negligible on the reef top and not included as a model forcing constituent.

Table 4-1. Wave parameters used at CMS-Wave model offshore boundary, developed from SWAN

Designation	CMS-Wave Spectra ID	Deep Water Dir. (deg)	Height (m)	Period (s)	Direction (deg)
1 Year Wave (force analysis)	Spec 1	315	4.9	9.0	311
High Prevailing (North)	Spec 2	30	1.4	10.1	26
High Prevailing (West)	Spec 3	270	1.8	10.1	266
50 Year Wave (force analysis)	Spec 4	315	8.9	14.3	311

4.2 NEARSHORE WAVE AND HYDRODYNAMIC MODELING (CMS-WAVE/CMS-FLOW)

4.2.1 Unai Babui

Graphical results of the wave and circulation modeling for Unai Babui are presented in Figure 4-1, which shows the bathymetry, wave height distribution, and current velocity distribution for both the existing condition (left side) and for the proposed ramp (right side). Arrows indicate direction for both wave propagation and currents. The approximate location of the ramp is indicated on the figure with a black outline, representing the dredge cut extents.

A.

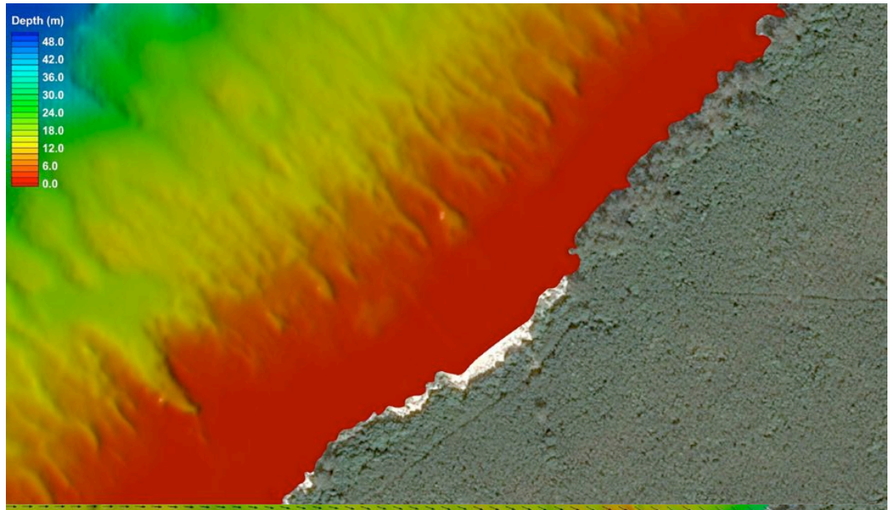

B.

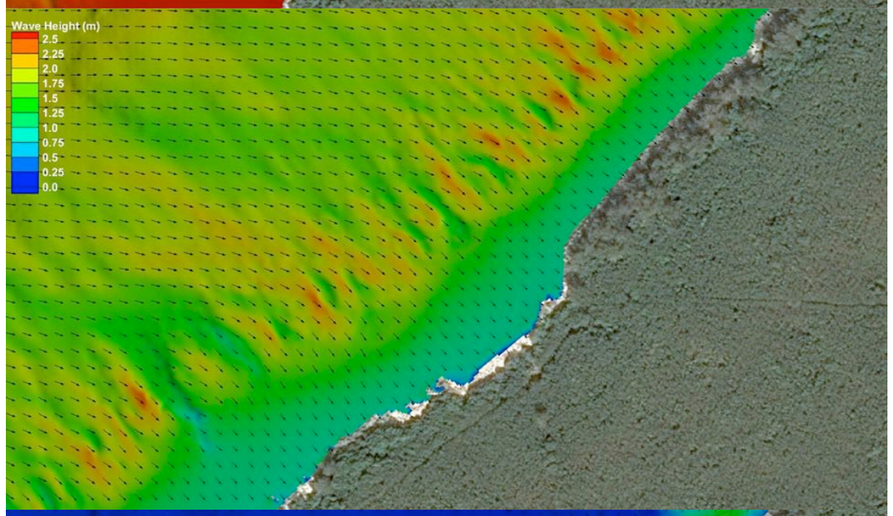

C.

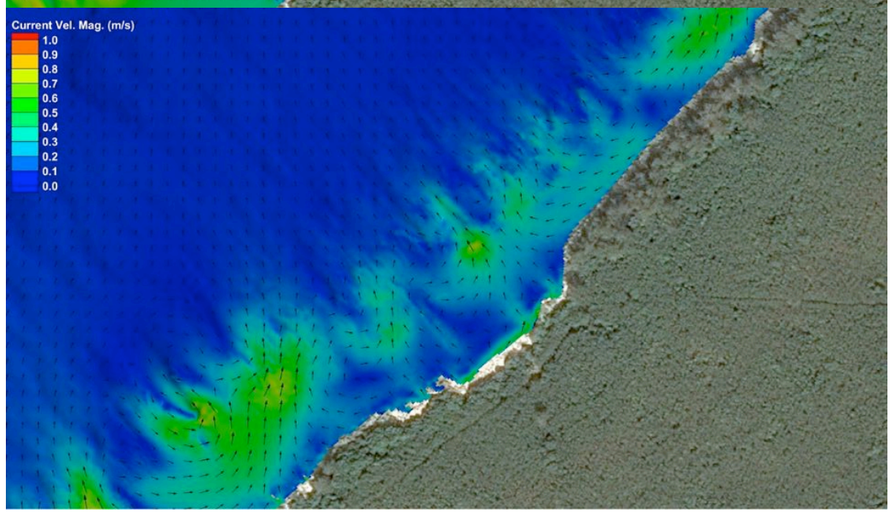

D.

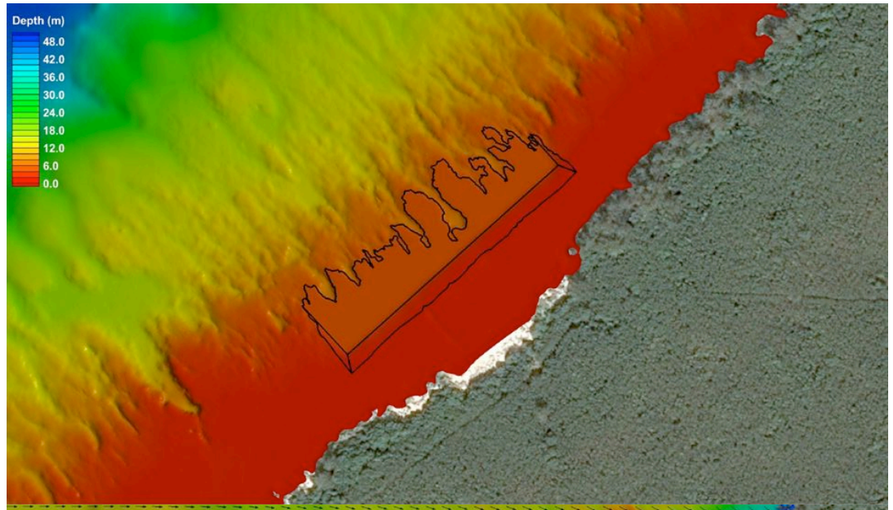

E.

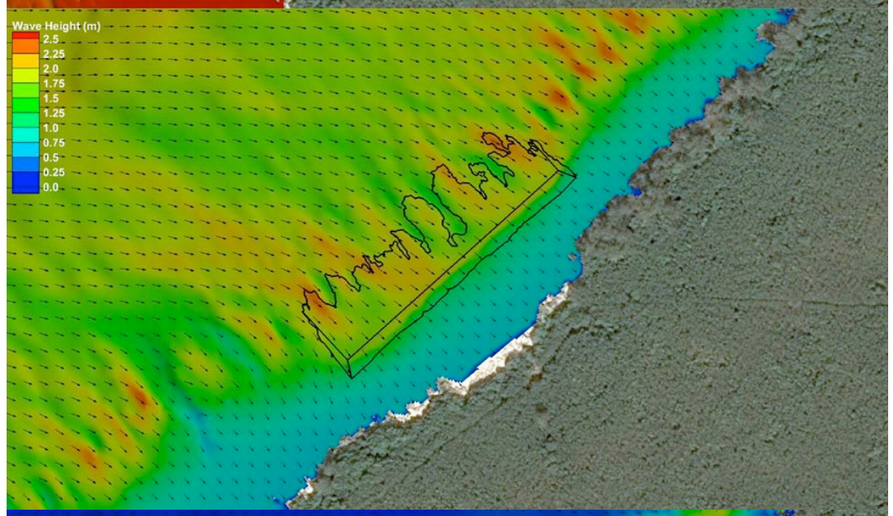

F.

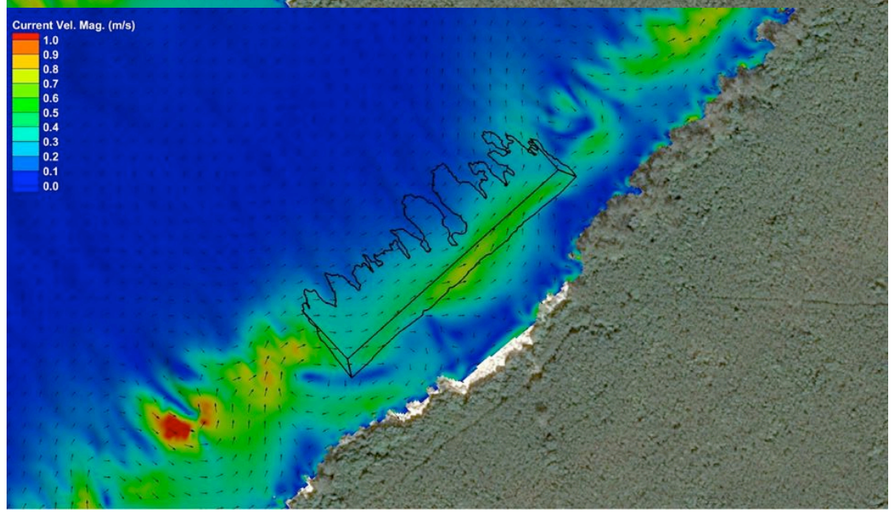

Sea Engineering, Inc.
MAKAI RESEARCH PIER
WAIMANALO, HI 96795
PH 808.259.7966
FAX 808.259.8143

NOTES:

CMS-Wave & Flow Model Results

High Prevailing Wave Conditions at Unai Babui:

A. Existing bathymetry
B. Wave heights for existing
C. Current pattern for existing
D. Ramp modified bathymetry
E. Wave heights for ramp mod.
F. Current pattern for ramp mod.

Figure 4-1.
Hydrodynamic Model Results at Unai Babui

Tinian AAV Landing Sites Investigation

Project: 25445
November 2014
Scale Varies

C-7

This page intentionally left blank.

Figure 4-1, Panels B and E (wave height), show that wave propagation direction along the shoreline in the vicinity of Babui is essentially shore-orthogonal (wave crests would be shore-parallel), meaning the shallow reef has effectively straightened the waves as they reach the shoreline. At the slight shoreline embayment where the beach is located, this results in wave crest alignment with respect to the shoreline that induces currents and sand transport toward the beach. In this case, wave model results suggest relatively low currents along the shoreline, and more importantly, no significant change at the beach between the existing condition and ramp construction. Areas where maximum wave height (≥ 8.2 ft [2.5 m]) quickly reduces to less than 4.1 ft (1.25 m), indicate the breaker zone, which is where wave energy is rapidly dissipated by breaking. This zone generally follows the breaker depth, which is roughly approximated by $0.78(H_b)$, where H_b is the breaking wave height. The dredged ramp does appear to modify the breaker zone location. However, wave heights inshore and near the beach are, unexpectedly, slightly smaller than for the existing condition. This is potentially explainable by the shape of the ramp, which might be forcing waves to break more energetically, thus removing more energy and subsequently further reducing wave height inshore.

Panels C and F (current velocity) indicate that wave-driven current velocities along the beach are relatively low, at 1.6 ft/s (0.5 m/s) or less. The circulation pattern within the breaker zone appears to differ somewhat between the existing and dredged conditions; however, as with wave heights the current speeds inshore of the breaker zone near the beach appear very consistent between the two, and even slightly slower for the dredged ramp condition.

4.2.2 Unai Chulu

Graphical results of the wave and circulation modeling for Unai Chulu are presented in Figure 4-2, which shows the bathymetry, wave height distribution, and current velocity distribution for both the existing condition (left side) and for the proposed ramp (right side). Arrows indicate direction for both wave propagation and currents. The approximate location of the ramp is indicated on the figures with a black outline, representing the dredge cut extents.

In general, results for Unai Chulu closely mirrored those of Unai Babui, although with some minor differences. Again, wave heights shown in Panels B (existing conditions) and E (proposed ramp) were largely unchanged near the shoreline, with some wave energy focusing on the ramp face, as at Babui. Inshore of the ramp, wave heights appear identical between the two conditions.

Current and wave model results for Unai Chulu (Panels C and F) clearly illustrate the convergent alongshore transport mechanism that is responsible for the accretion of beach material at this location, and which was previously hypothesized from field observations in Section 2.2. This phenomenon can be seen in the form of current vectors (arrows) along the southern half of Unai Chulu pointing northwards, and those along the northern half pointing southward, converging near the midpoint of Unai Chulu. In reality, the point of convergence likely wobbles to the north and south of center over time in response to extreme swell directions, temporarily redistributing more sand at one end of the beach relative to the other. This is consistent with the varied beach widths seen in Figure 2-16 (and similarly Figure 2-15 at Babui), which were created from the historic shoreline analysis in Section 2.2.3.

This page intentionally left blank.

A.

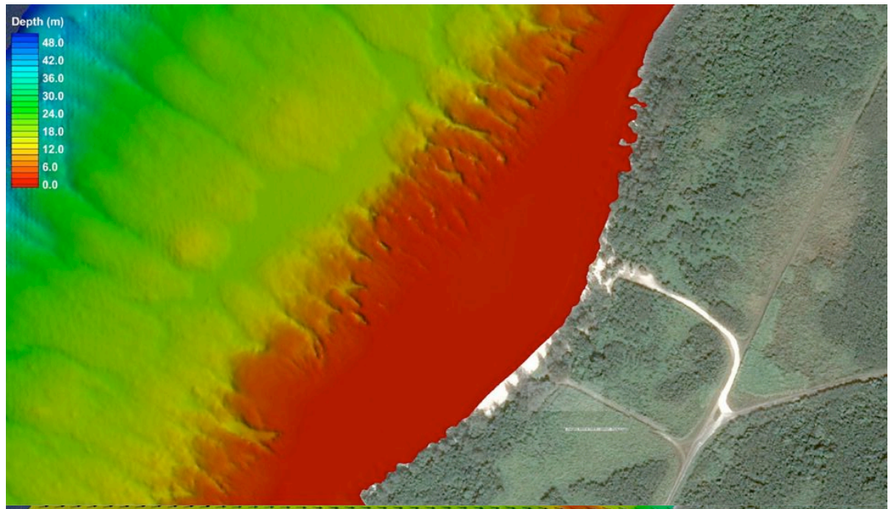

B.

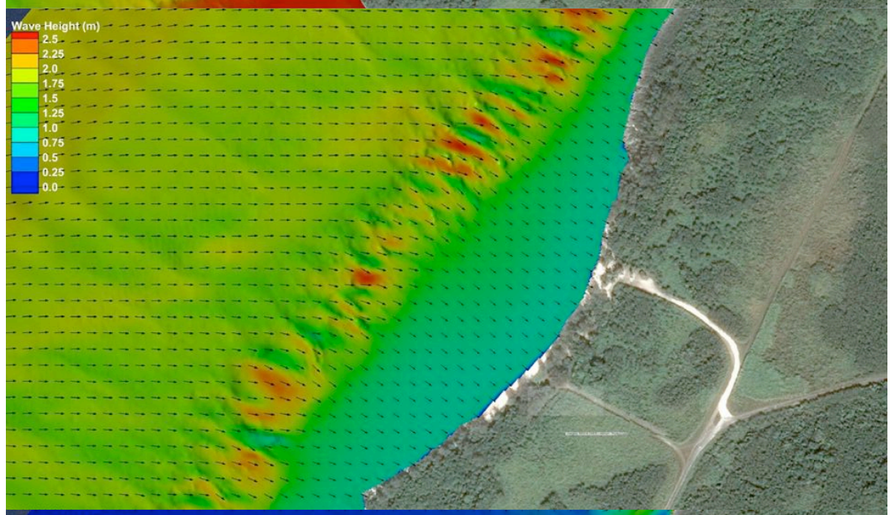

C.

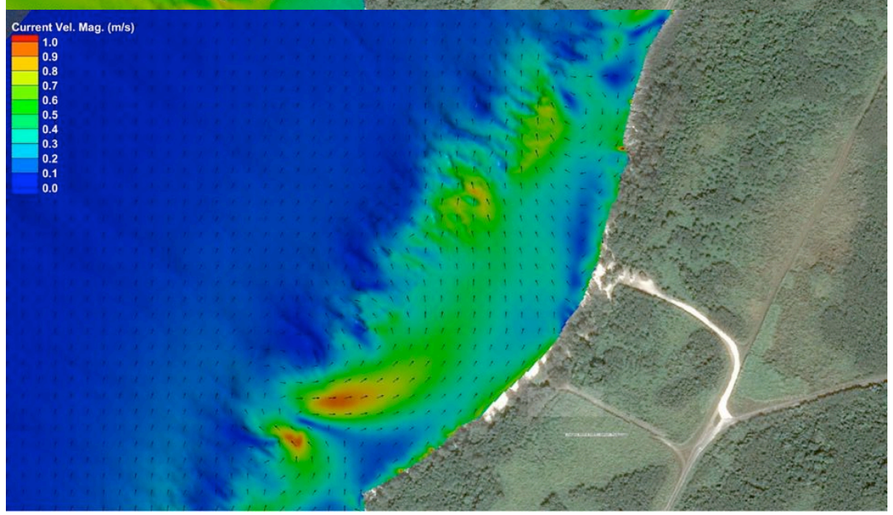

D.

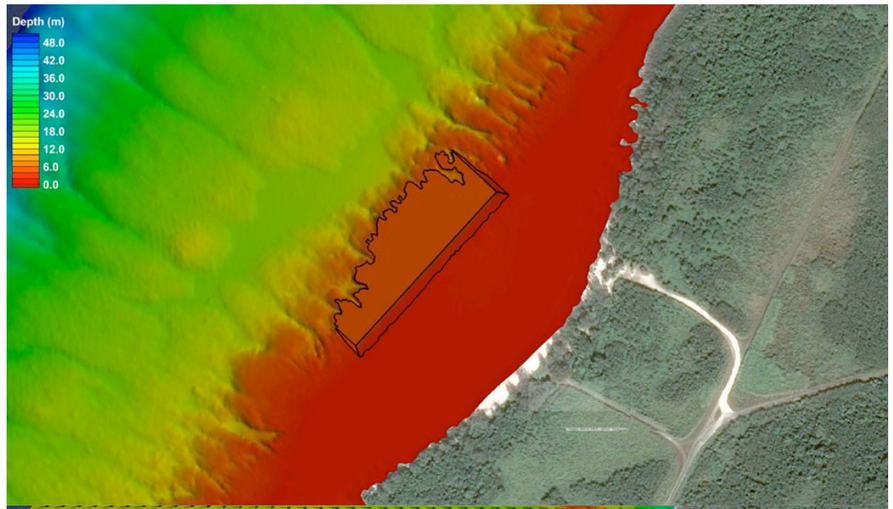

E.

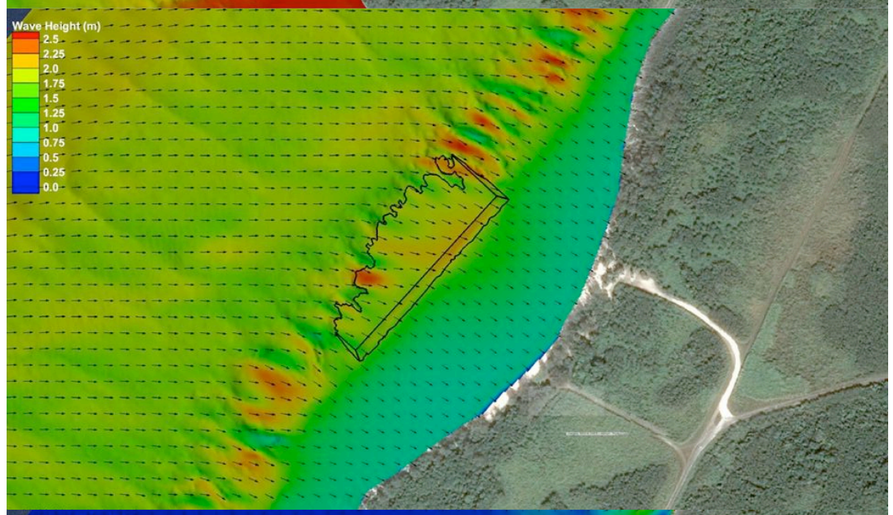

F.

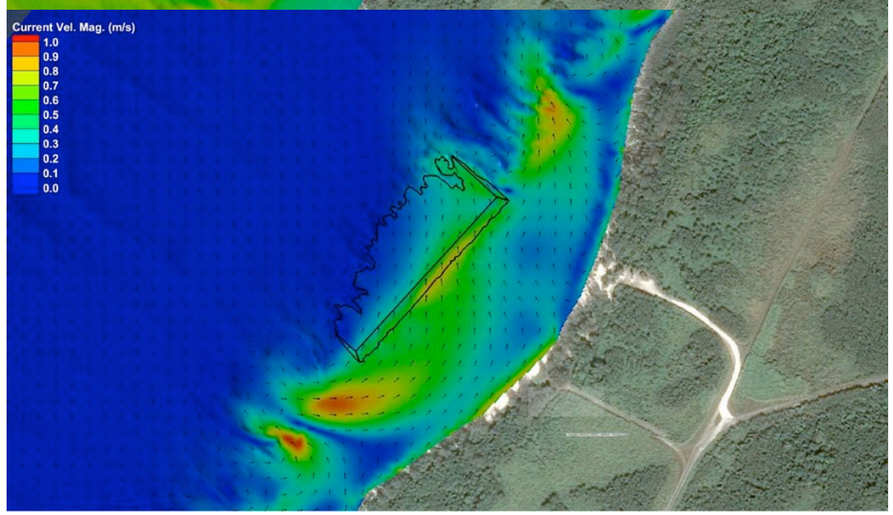

Sea Engineering, Inc.
MAKAI RESEARCH PIER
WAIMANALO, HI 96795
PH 808.259.7966
FAX 808.259.8143

NOTES:

CMS-Wave & Flow Model Results

High Prevailing Wave Conditions at Unai Chulu:

A. Existing bathymetry
B. Wave heights for existing
C. Current pattern for existing
D. Ramp modified bathymetry
E. Wave heights for ramp mod.
F. Current pattern for ramp mod.

Figure 4-2.
Hydrodynamic Model Results at Unai Chulu

Tinian AAV Landing Sites Investigation

Project: 25445
November 2014
Scale Varies

C-8

This page intentionally left blank.

4.2.3 Results Comparison

Representative data transects through the approximate ramp center were used to numerically compare the differences between the existing and dredged ramp condition at each site for prevailing conditions. Composite plots were then developed to make direct comparisons of the data at each site, displaying overlain profiles for current magnitude (dashed line), wave height (thin line), and water depth (thick line), where depth and wave height are read from the left axis and current magnitude is read from the right axis. Grey shading represents the modeled water level of MHHW. The x-axis origin lies approximately on the beach waterline.

The representative transect location for Unai Babui is shown in Figure 4-3, which was roughly centered on both the ramp and beach. Extracted model data plotted along this transect for the existing condition is presented in Figure 4-4, and then for the proposed ramp configuration in Figure 4-5.

Comparison of these figures suggest that wave energy is absorbed more rapidly by breaking on the relatively steep dredged ramp face, which reduces wave height by 50% over a distance of less than 33 ft (10 m), while the existing profile requires 3 to 4 times that distance for the same reduction in wave height. Wave heights at the beach/shoreline are very similar, with the ramp configuration showing a slightly smaller wave height, likely due to the energetic wave breaking on the ramp. The breaker intensity on the ramp is also corroborated by the surge in current velocity at this location, which more than doubles the corresponding existing condition current speed. The phenomenon rapidly attenuates towards shore however, where currents at the beach are very comparable between the two, with no significant difference.

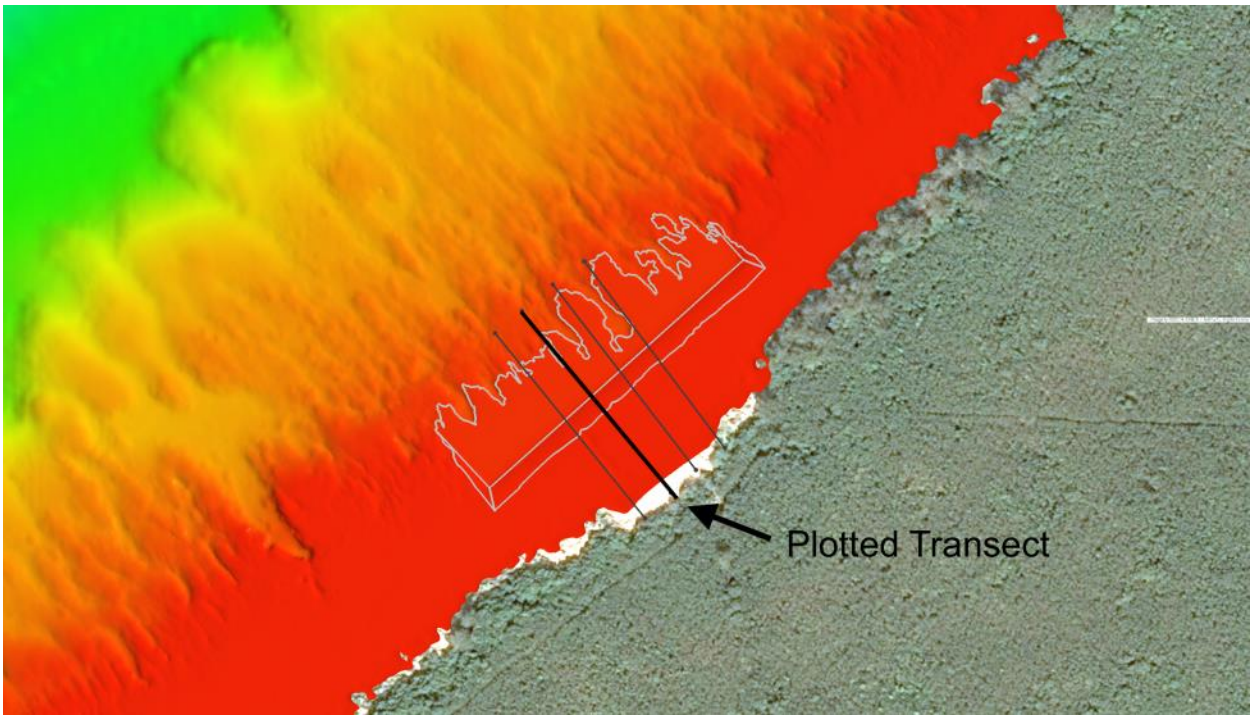

Figure 4-3 Profile transect location—Unai Babui

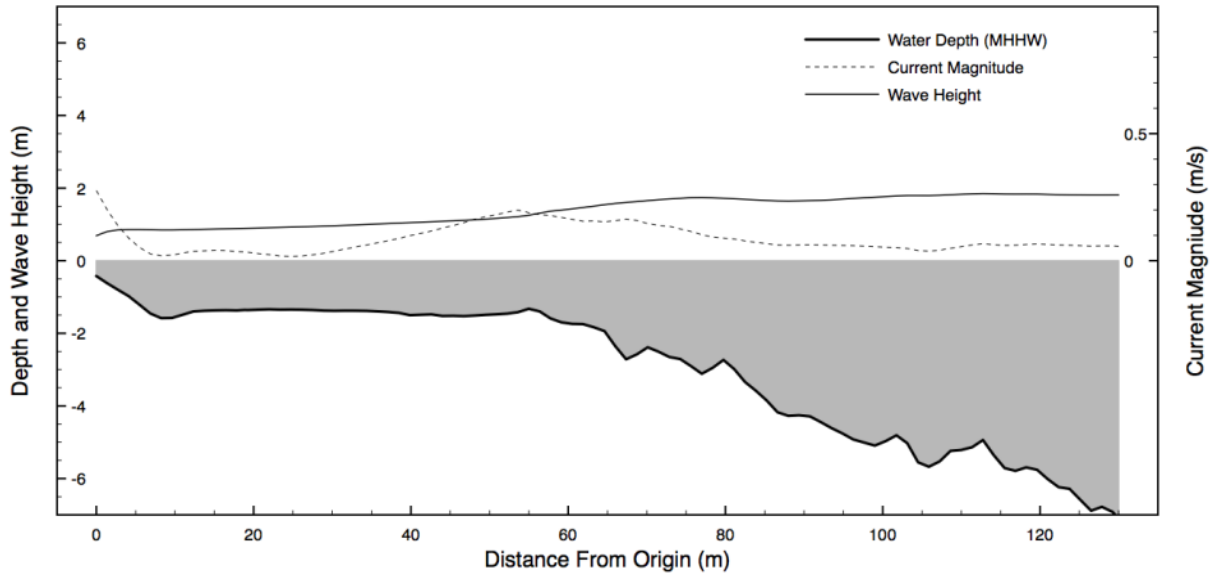

Figure 4-4 Wave height and current magnitude profile—Unai Babui, existing condition

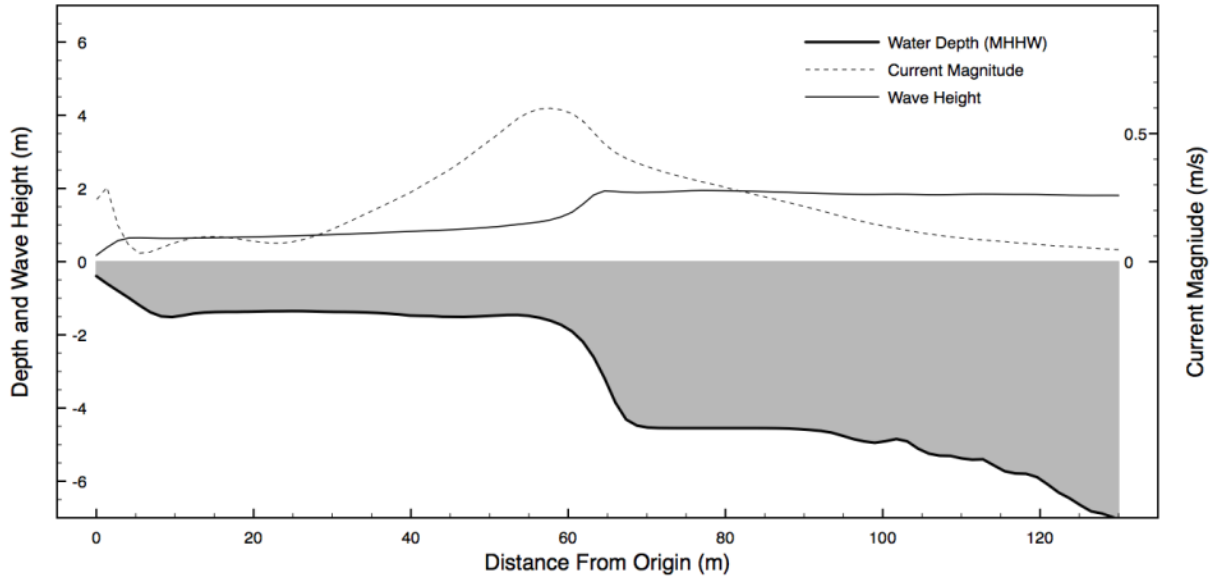

Figure 4-5 Wave height and current magnitude profile—Unai Babui, dredged ramp condition

The representative transect location for Unai Chulu is presented in Figure 4-6, which was roughly centered on both the ramp and beach. Extracted model data plotted along this transect for the existing condition are presented in Figure 4-7 and Figure 4-9, and then for the proposed ramp configuration in Figure 4-8 and Figure 4-10 for the high prevailing and 1-year waves, respectively.

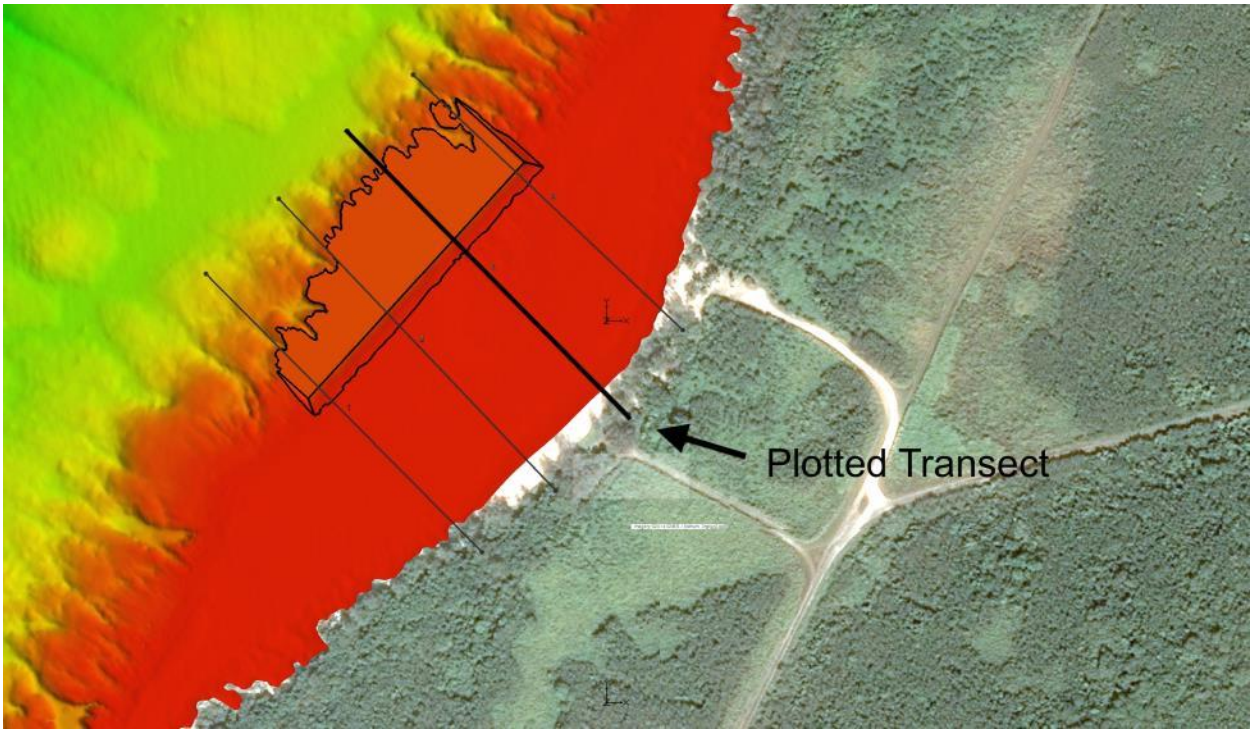

Figure 4-6 Profile transect location—Unai Chulu

The plots in Figure 4-7 and Figure 4-8 show that prevailing wave height is again reduced more rapidly by vigorous breakers on the ramp as compared to the existing condition; however, the effect is not as pronounced as that found for Unai Babui. Wave heights on the inner reef and at the beach appear nearly identical between the two configurations. Current velocities again show a surge in speed at the ramp due to wave breaking, but later become very comparable along the inner reef. One difference is a slight increase in current magnitude at the beach for the ramp configuration. Elsewhere, the currents and wave height profiles are nearly identical between the two configurations.

The 1-year return period wave height and current plots exhibit a very similar effect to that seen with the high prevailing condition results, with wave heights reduced rapidly by the ramp and current speeds and wave heights on the inner reef and near the shoreline being very comparable between the existing and dredged configurations. The double-stepped profile of wave height for the ramp indicates that the waves would break first on the initial dredge cut, and reform and break again on the ramp, with energy being absorbed at each stage. This suggests that the ramp may have less effect on nearshore processes as wave height increases, with more energy being attenuated offshore.

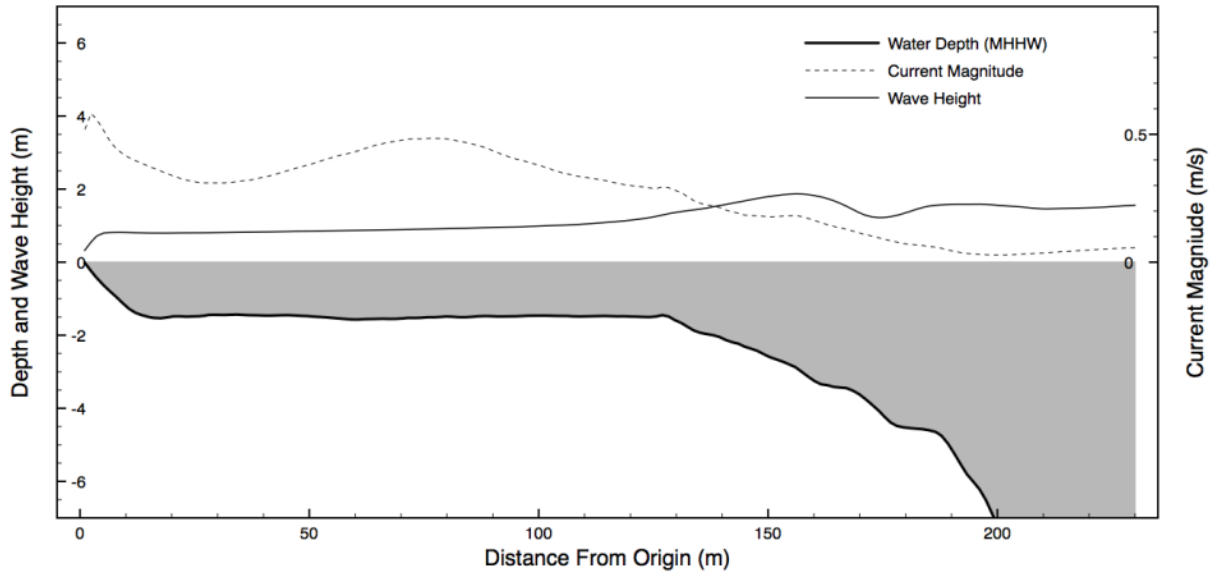

Figure 4-7 Wave height and current magnitude profile—Unai Chulu, existing condition

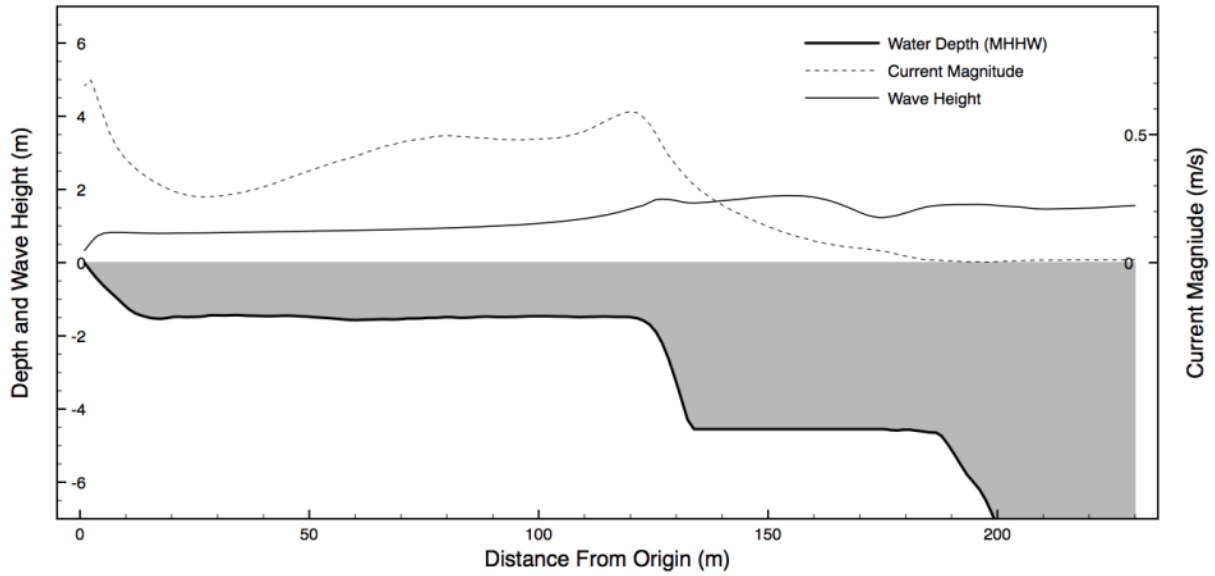

Figure 4-8 Wave height and current magnitude profile—Unai Chulu, dredged ramp condition

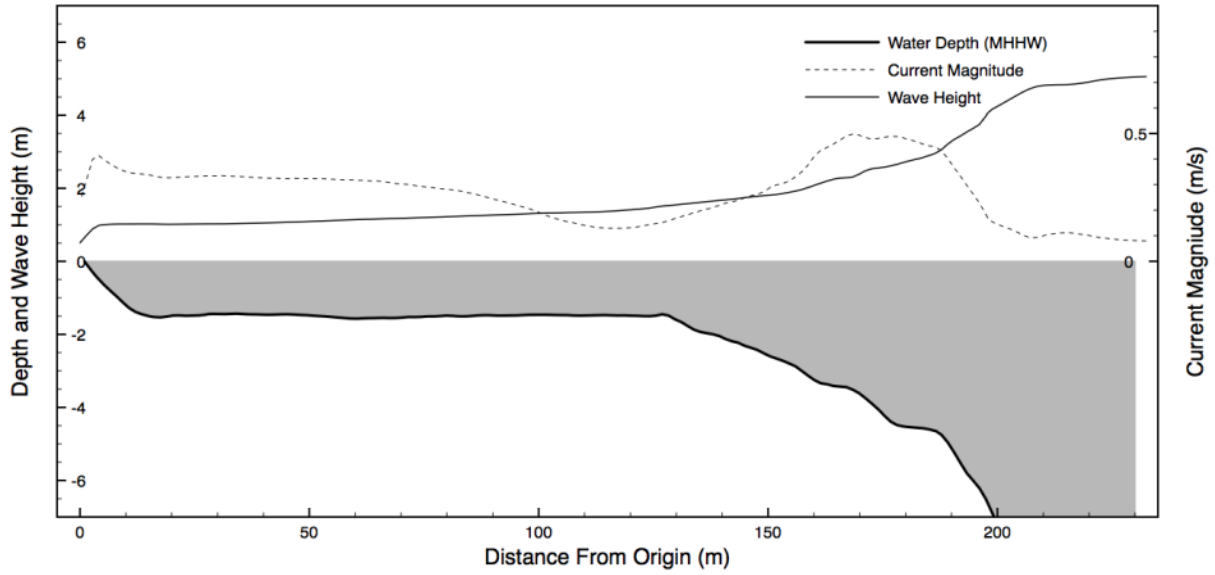

Figure 4-9 1-yr Wave height and current magnitude profile—Unai Chulu, existing condition

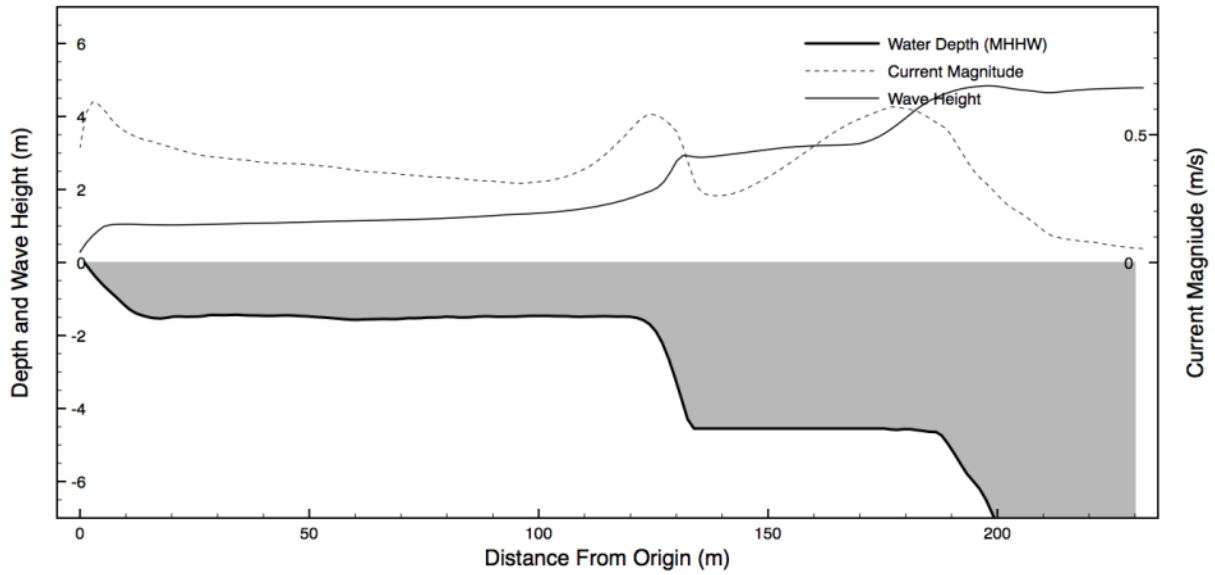

Figure 4-10 1-yr Wave height and current magnitude profile—Unai Chulu, dredged ramp condition

4.3 PHASE-RESOLVING WAVE MODEL (BOUSS-2D)

The BOUSS-2D model functions by numerically generating a spectral distribution of waves and propagating them through the model over time. The result is a realistic approximation of wave patterns, similar to what one would see from an aerial perspective. It requires accurate bathymetric data to be incorporated into the model, and assignment of specific boundary conditions which are enforced on the limits of the model domain. BOUSS-2D employs a numerical wave generator along the offshore boundary of the domain, and propagates a non-uniform (spectral) wave train over the bathymetry. The model is driven by user input wave conditions such as wave height, period, and direction, and for the simulations in this study, input wave conditions were the same as for the CMS models in Section 4.2, which consisted of the high prevailing condition from the west (see Table 4-1).

4.3.1 Unai Babui

Results of the BOUSS-2D modeling for Unai Babui are presented in Figure 4-11 (existing condition) and Figure 4-12 (dredged ramp). The figures are a numerical visualization of the sea surface calculated by the model, where the underlying bathymetry is color shaded by depth, and sea surface elevation is sun-shaded with a translucent white to emulate the appearance of real water. Wave patterns are clearly identifiable by the shadowed troughs and highlighted crests. The ramp position is overlain in thin linework for reference where applicable.

Most noticeably in the figures, a complicated refractive pattern is seen to the south of Unai Babui, which marks the location of a significant underwater feature that consists of a deep cut into the reef adjacent to a large prominence at the reef edge. The actual feature is more visible in Figure 4-13, which shows the underlying model bathymetry. Generally, the results indicate that waves are essentially shore-parallel (propagation direction orthogonal to shoreline) by the time they reach the inner reef. Comparison of the existing and ramp configurations indicates that the dredged area does alter the wave patterns, but not dramatically, and the effect appears to be limited to the immediate vicinity of the ramp.

Wave crest alignments inshore of the ramp location appear essentially identical. In both cases, alongshore wave alignment at the beach exhibits a significant angle to the shoreline at either end of the beach. This angle to the shoreline is the mechanism which drives swash zone currents and sediment transport along the beach face, with the inferred direction of transport indicated on the figures by black arrows. Where the wave crests become roughly parallel to the beach near its midpoint, transport would slow or stop. Typically, greater angles induce greater sediment transport rates, and conversely, smaller angles yield smaller transport rates.

Figure 4-13 presents a snapshot image of actual wave angles at northern Babui, showing an agreeable correlation with the modeled results. It is clear in this figure that the waves form a sufficient angle with the north end of the beach to provide the potential for sediment transport. Likewise, at the south end, waves approach the embayed shoreline at an angle, forming a convergent area roughly mid-beach. The convergent process is what has allowed the beach to accrete in this location, and importantly, the modeled results suggest that this process does not appear to be altered significantly by the addition of the dredged ramp offshore at Unai Babui.

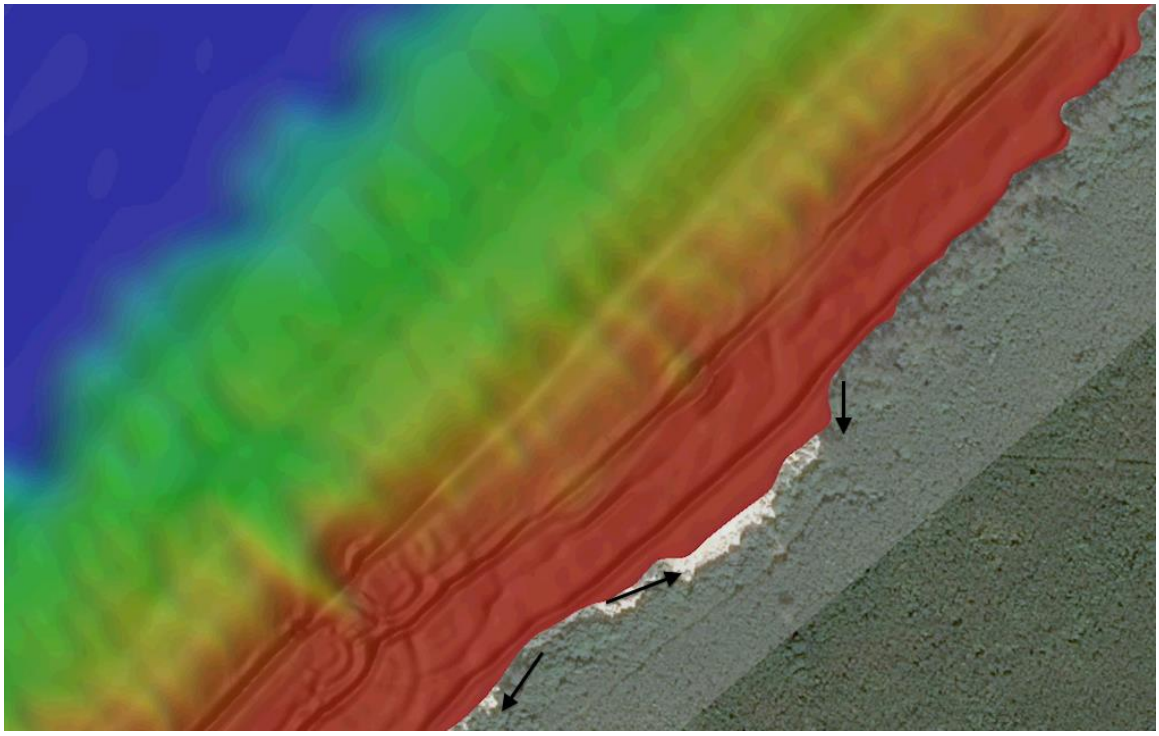

Figure 4-11 Wave crest alignment (refraction/diffraction) patterns —Unai Babui, existing condition

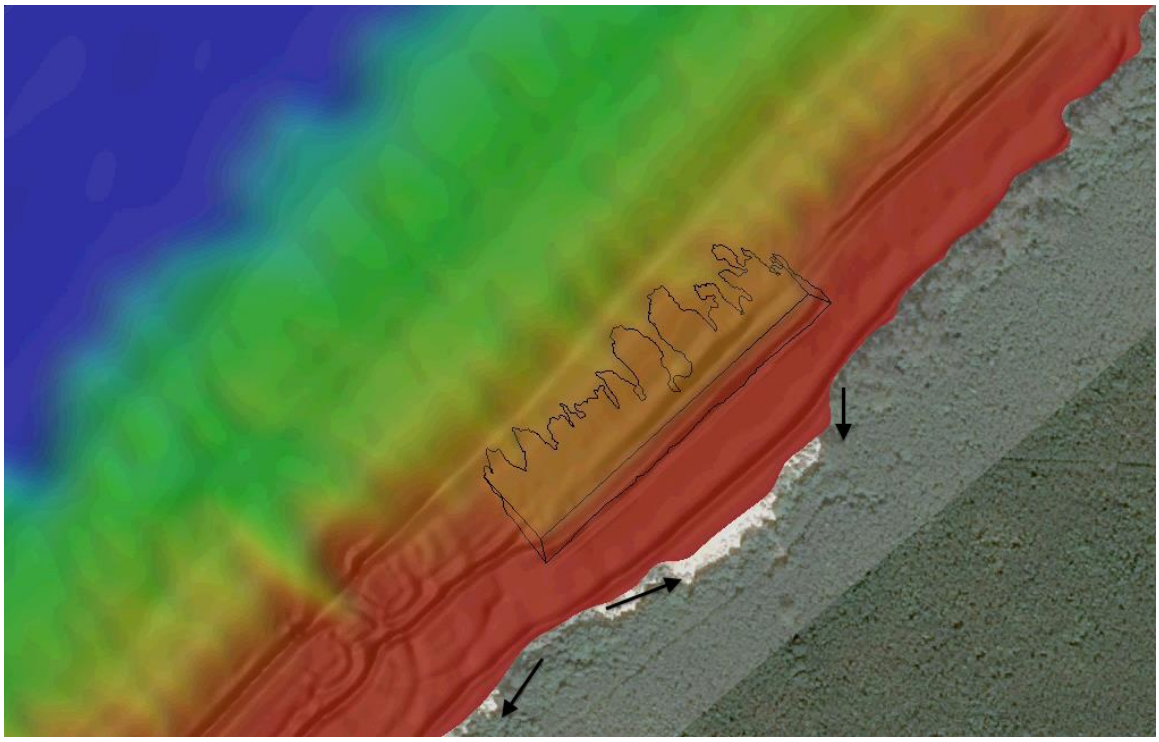

Figure 4-12 Wave crest alignment (refraction/diffraction) patterns—Unai Babui, dredged ramp condition

Figure 4-13 Actual wave crest alignment for Unai Babui

4.3.2 Unai Chulu

BOUSS-2D model results for Unai Chulu are presented in Figure 4-14 (existing condition) and Figure 4-15 (dredged ramp). In general, Chulu model results are similar to those discussed for Babui in Section 4.2.1; however, the convergence effect appears even more accentuated here due to the more exaggerated indentation of the shoreline and prominence of the outer reef. Wave angles at the north and south end of Unai Chulu are pronounced at the shoreline and propagating towards mid-beach, forming a well-defined area of convergence and sediment accretion. This effect is corroborated by visual observations and aerial photographs, a snapshot of which is illustrated in Figure 4-16.

Comparison of the two figures with and without the ramp yields minimal differences in wave patterns between the two. A slight change in wave alignment is found in the footprint of the ramp, were the dredged area has removed a prominent high spot. The existing condition in Figure 4-14 shows a distinct wave peak at this location, and formation of the a slight seaward inflection in wave crests inside the reef, while the ramp configuration indicates a straightening of wave crests aligning with the ramp face. Importantly however, wave angles at the shoreline are nearly identical between the two cases, meaning sediment transport patterns will likely not be significantly altered.

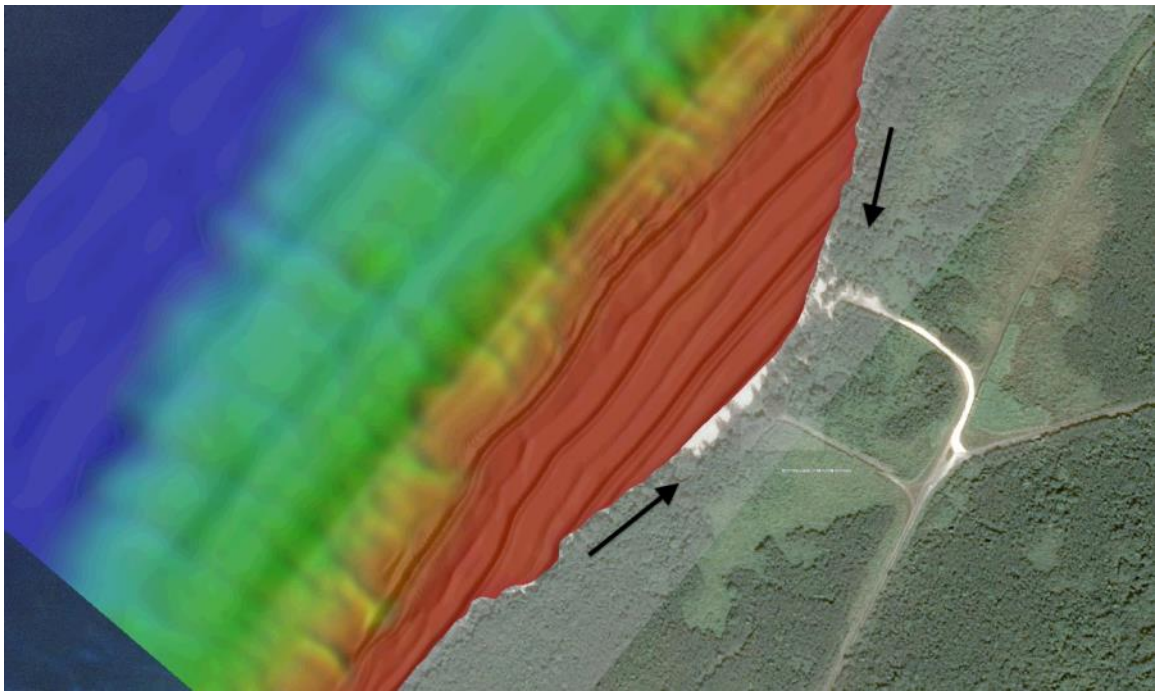

Figure 4-14 Wave crest alignment (refraction/diffraction) patterns —Unai Chulu, existing condition

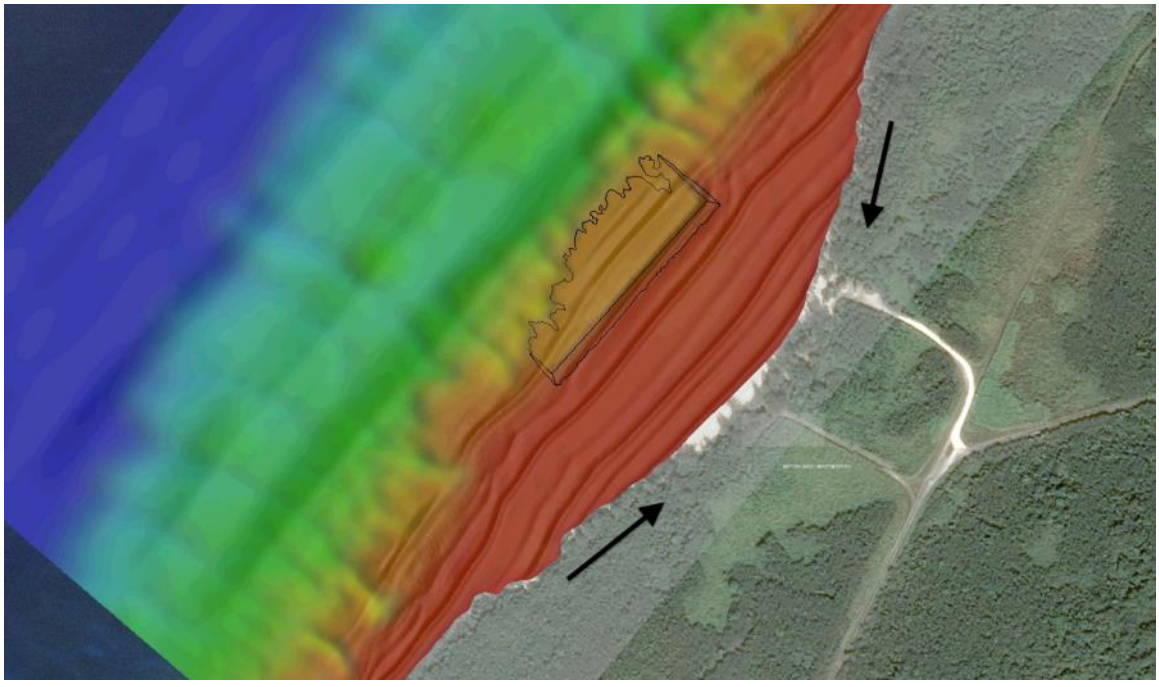

Figure 4-15 Wave crest alignment (refraction/diffraction) patterns —Unai Chulu, dredged ramp condition

Figure 4-16 Actual wave crest alignment for Unai Chulu

CHAPTER 5
COASTAL IMPACTS ASSESSMENT

5.1 ALTERATION OF WAVE CONDITIONS AND NEARSHORE CIRCULATION

Data from model runs conducted in this investigation suggest that there will be some effects to the existing wave refraction/diffraction patterns and circulation patterns, however, the results also suggest that these changes are localized to the immediate vicinity of the dredged ramp. The CMS-Wave and hydrodynamic models indicate that minimal changes in nearshore and along-beach current velocity and wave height would occur with the dredged ramp in place at either Unai Babui or Unai Chulu. BOUSS-2D simulation results demonstrate that wave approach angles at the shoreline and beach do not change significantly between the existing condition and the proposed ramp configuration, essentially leaving intact the existing sediment transport regimes which naturally trap sand at both beach locations.

A caveat is that the present investigation uses a small selection of representative wave conditions for the numerical modeling. The modeling utilized a site-specific high-prevailing wave condition, which is a good representation of typical conditions. The 1-year wave condition modeled for Unai Chulu suggests that larger waves would exhibit a similar response compared to the smaller high-prevailing conditions. It is reasonable to infer that even much larger wave conditions, such as typhoon waves, would shift the energetic breaker zone into deeper water, offshore of the dredged areas, and the ramps would subsequently have less relative influence on the wave patterns and currents under that scenario.

5.2 EFFECTS TO BEACH STABILITY

In the tropical Pacific, calcareous sand is produced on the reef top through biological and mechanical breakdown of the reef material and hard shells of marine organisms, and accumulates in veins and patches throughout the reef. At Unai Babui and Unai Chulu, sand was found in small deposits within channels, depressions, and fissures dispersed across the inner reef. Typically, small waves act to gradually transport sand shoreward from the shallow reef top towards the shoreline, where it is deposited and redistributed by currents acting along the shoreline and wave swash zone. If the shoreline happens to be excessively energetic such as along the rocky bluffs north and south of the landing sites, the entrained sand particles will remain suspended and be transported elsewhere, eventually accreting in a lower energy environment.

The sandy beach at Unai Chulu exists because of a unique configuration of the shoreline at that particular location. The rocky, vertical shoreline typical of northwest Tinian takes a gentle curve landward, forming an embayment with respect to the surrounding shoreline orientation. Offshore, and in line with this indented feature, the fringing reef bulges seaward, forming a roughly elliptical-shaped broad and shallow reef terrace between the surf zone and the shoreline. The combined effect of this configuration is that wave crests are oriented at an angle to the shoreline to the north and south, driving swash zone currents and sand transport toward the beach. This allows sand accretion and the formation of a beach at this location. The convergent along-shore currents revealed during the numerical modeling act as the lateral restorative forces that keep the beach in equilibrium.

Similar processes are also responsible for the existence of the beach at Unai Babui, with the difference that the configuration of the shoreline is not as pronounced when compared to Unai Chulu. At Babui, the shoreline indentation is less prominent and the reef line does not form a significant extension or bulge

seaward, and therefore the shoreline is less sheltered than Unai Chulu, and as seen from the modeling, the convergent along-shore currents are less well defined. As a result, Unai Babui is not as effective at accruing and trapping sand, which is consistent with its present and historical condition.

The numerical modeling results presented in CHAPTER 4 imply that existing sediment transport mechanisms remain relatively unchanged following ramp dredging; therefore, it is probable that beach stability would be minimally affected. Although it was found that current speed along the beach at Chulu increased slightly with the ramp in place, the convergent shoreline current pattern was shown to remain unchanged. Episodic storm or large wave events could have unpredicted effects on the beach, yet the effects would likely be relatively short-lived. The active convergent zones of these two beaches would likely act over time to re-deposit beach material that was temporarily lost from highly energetic conditions. It is known that this must have occurred at least once in the past (likely many times over), at each location, as shown by the photographs in Figure 2-20 and Figure 2-21 which were taken in 1944. These images show both beaches nearly devoid of sand at that time, a condition which is in contrast to the beaches today.

5.3 CONCLUSIONS

The results of the numerical modeling analysis suggest that the alteration of the nearshore bathymetry by dredging the AAV approach and ramp should not significantly alter shoreline coastal processes and cause erosion of the beach.

The site investigation at Unai Babui and Unai Chulu revealed that these beaches are small, narrow and shallow with limited sand volume. There are numerous rock outcroppings, particularly at Unai Babui, and both beaches are underlain by reef rock ledges at an elevation of approximately -3.3 ft (-1 m). The historical shoreline analysis indicated that the beaches are dynamic, varying in width and orientation during the analysis period of 2003 to 2014. World War II era photographs show periods where both sites had little sand beach.

The limited spatial extent and volume of sand at Babui and Chulu suggests that the beaches are vulnerable to either natural or man-made perturbations. Episodic large waves could nearly completely strip the beaches of sand. As discussed above, the prevailing wave and current dynamics of both sites would act to rebuild the beaches over time, although it is not known how quickly or to what degree. The beach has reformed since World War II, when photographs indicate there was little sand beach.

CHAPTER 6
REFERENCES

Climate Change. 2007. *Climate Change 2007: Synthesis Report*; *An Assessment of the Intergovernmental Panel on Climate Change (IPCC).* Valencia, Spain, November.

Farrell, Don. A. 2012. *Tinian: A Brief History*, Pacific Historic Parks.

Hoffman, Maj. Carl W. (U.S. Marine Corps). 1951. *The Seizure of Tinian*, The Battery Press, Inc.

NOAA. 2001. http://tidesandcurrents.noaa.gov/datums.html?id=1633227. Accessed November 2014.

This page intentionally left blank.